

Distribution Agreement

In presenting this thesis or dissertation as a partial fulfillment of the requirements for an advanced degree from Emory University, I hereby grant to Emory University and its agents the non-exclusive license to archive, make accessible, and display my thesis or dissertation in whole or in part in all forms of media, now or hereafter known, including display on the world wide web. I understand that I may select some access restrictions as part of the online submission of this thesis or dissertation. I retain all ownership rights to the copyright of the thesis or dissertation. I also retain the right to use in future works (such as articles or books) all or part of this thesis or dissertation.

Signature:

Nicholas Harbin

Date

RGS14 protects against seizure-induced mitochondrial oxidative stress and pathology in the hippocampus

By

Nicholas Harbin

Doctor of Philosophy

Graduate Division of Biological and Biomedical Sciences
Molecular and Systems Pharmacology

John Hepler, Ph.D.
Advisor

Andrew Escayg, Ph.D.
Committee Member

Steve Traynelis, Ph.D.
Committee Member

David Weinshenker, Ph.D.
Committee Member

Accepted:

Kimberly Jacob Arriola, Ph.D., MPH

Dean of the James T. Laney School of Graduate Studies

Date

RGS14 protects against seizure-induced mitochondrial oxidative stress and pathology in the hippocampus

By

Nicholas Harbin

B.S., Auburn University, 2017

Advisor: John Hepler, Ph.D.

An abstract of

A dissertation submitted to the Faculty of the James T. Laney School of Graduate Studies of
Emory University

in partial fulfillment of the requirements for the degree of

Doctor of Philosophy in Graduate Division of Biological and Biomedical Sciences Molecular and
Systems Pharmacology

2023

Abstract

RGS14 protects against seizure-induced mitochondrial oxidative stress and pathology in the hippocampus

By Nicholas Harbin

RGS14 is a multifunctional scaffolding protein that is highly enriched within pyramidal cells (PCs) of hippocampal area CA2. In these neurons, RGS14 suppresses glutamate-induced calcium influx and related G protein and ERK signaling in dendritic spines to restrain postsynaptic signaling and plasticity. Previous findings show that, CA2 PCs are resistant to degeneration (unlike CA1 and CA3 PCs), modulate hippocampal excitability, generate epileptiform activity, and promote hippocampal pathology in animal models and patients with temporal lobe epilepsy (TLE). While RGS14 is protective against peripheral injury, similar roles for RGS14 during pathological injury in hippocampus remain unexplored. Because RGS14 suppresses CA2 excitability and signaling, we hypothesized that RGS14 would moderate seizure behavior and hippocampal pathology following seizure activity, possibly affording protection to CA2 PCs. Using kainic acid (KA) to induce status epilepticus (KA-SE) in mice, we show that the loss of RGS14 (RGS14 KO) accelerated onset of limbic motor seizures and mortality compared to wild type (WT) mice, and that KA-SE upregulated RGS14 protein expression in CA2 and CA1 PCs of WT. Our proteomics data show that the loss of RGS14 impacted the expression of a number of proteins at baseline and after KA-SE, many of which associated unexpectedly with mitochondrial function and oxidative stress. RGS14 was shown to localize to the mitochondria in CA2 PCs of mice and reduce mitochondrial respiration *in vitro*. As a readout of oxidative stress, we found that RGS14 KO dramatically increased 3-nitrotyrosine levels in CA2 PCs, which was greatly exacerbated following KA-SE and correlated with a lack of superoxide dismutase 2 (SOD2) induction. Assessing for hallmarks of seizure pathology in RGS14 KO, we unexpectedly found no differences in neuronal injury in CA2 PCs. However, we observed a striking and unexpected lack of gliosis in CA1 and CA2 compared to WT. Together, our data demonstrate a newly appreciated role for RGS14 in protecting against intense seizure activity and pathology in hippocampus. Our findings are consistent with a model where RGS14 limits seizure onset and mortality and, after seizure, is upregulated to support mitochondrial function, prevent oxidative stress in CA2 PCs, and promote glial activation in hippocampus.

RGS14 protects against seizure-induced mitochondrial oxidative stress and pathology in the hippocampus

By

Nicholas Harbin

B.S., Auburn University, 2017

Advisor: John Hepler, Ph.D.

A dissertation submitted to the Faculty of the James T. Laney School of Graduate Studies of
Emory University

in partial fulfillment of the requirements for the degree of

Doctor of Philosophy in Graduate Division of Biological and Biomedical Sciences Molecular and
Systems Pharmacology

2023

Acknowledgements

I would like to acknowledge: Dr. Asheebo Rojas for being a valuable intellectual resource during development and execution of experiments and creating a stimulating space for academic discussion on epilepsy; Dr. Nicholas Varvel for assistance with behavioral seizure scoring; Dr. Thomas Shiu for preliminary seizure induction studies; my mentor Dr. John Hepler for his patience, understanding, and trust in me to develop my own project; my friend and colleague Dr. Daniel Lustberg for helping me become the scientist I am today and assisting in the development of the project that would have never had happened if not for the fortuitous partnership between us; my family for the immense support, constant encouragement, and pushing me to endure until the end; my friends for providing respite and reminders that there is a life beyond graduate school through the beauty and evolution of music and friendship; the craggy buttresses and boulders that have captivated my imagination throughout my dissertation work, forever existing to challenge me in every conceivable way, and providing peace and mediation through the power of demanding ascents; and finally my dog Kaia for her endearing and undying love and support, her beauty and emotional gaze that melts away the days, and her nagging reminders that there is more to life than being inside, ruminating about RGS14 like basking in the sun, long walks through the woods, gnawing on a good stick, and the never-ending pursuit of squirrels.

Table of Contents

Chapter 1: Introduction

1.1. Overview of dissertation.....	1
1.2. Synaptic transmission and neuronal signaling	2
1.3. G-protein signaling in neurons	7
1.4. Regulation of G-protein signaling by RGS	14
1.5. RGS14 expression and regulation of cell signaling	18
1.6. Roles of RGS14 in neuronal function and behavior	23
1.7. Excitability, epilepsy, and temporal lobe epilepsy (TLE)	29
1.8. Animal models of TLE and hippocampal pathology	32
1.9. Area CA2 function, emerging role in TLE, and implications for RGS14	38
1.10. Research focus of the dissertation project.....	43

Chapter 2: Materials and Methods

46

Chapter 3: Results and Findings of Dissertation

3.1. Loss of RGS14 increases susceptibility to KA-induced seizures by expediting entry into SE and mortality	59
3.2. RGS14 protein expression is upregulated following status epilepticus	62
3.3. Metabolic and mitochondrial proteins are differentially expressed between WT and RGS14 KO mice 1 day after KA-SE	67
3.4. WGCNA Analysis reveals significant alterations of protein modules related to cellular/lipid metabolism and astrocytes in RGS14 KO hippocampi	76
3.5. RGS14 localizes to mitochondria in CA2 PCs and reduces mitochondrial respiration in vitro	82
3.6. RGS14 is necessary for SOD2 induction in area CA2 and prevents 3-nitrotyrosine accumulation	85
3.7. Loss of RGS14 does not alter early hippocampal neuronal injury in areas CA2 or CA1 after KA-SE	90
3.8. RGS14 is required for glial response to KA-SE	93

Chapter 4: Discussion of Dissertation Findings and Future Directions

4.1. Summary of findings	103
4.2. Neuronal mechanisms by which loss of RGS14 primes the hippocampus and the brain to seizure sensitivity caused by KA	104

4.3. Factors that may influence susceptibility to seizures and pathology based on hippocampal proteomics	111
4.4. Mechanisms by which RGS14 regulates mitochondrial function and oxidative stress	119
4.5. Mechanisms that RGS14 may regulate to promote glial response	126
4.6. Possible protective roles of RGS14 in CA2 hippocampus and hippocampal TLE pathogenesis	130
4.7. Future directions.....	134
4.7.1. In vitro measurement of epileptiform activity in acute hippocampal slices.....	135
4.7.2. In vivo EEG measurements of epileptiform activity and physiological monitoring of respiratory and cardiac function.....	136
4.7.3. Evaluation of RGS14's effects on neuronal mitochondria.....	138
4.7.4. Characterizing RGS14's role in glial response.....	139
4.7.5. Monitoring the development of TLE and associated pathology after SE.....	141
4.8. Conclusions and working model of CA2 regulation by RGS14	142

List of Tables and Figures

Tables

Table 1. Modified Racine scale to evaluate behavioral seizure progression in mice	47
Table 2. Comprehensive list of differentially expressed proteins (DEPs) between WT and RGS14 KO after SAL or KA treatment	70
Table 3. Comprehensive list of differentially expressed proteins (DEPs) one day after KA-SE in WT or RGS14 KO hippocampi	75

Figures

Figure 1. Overview of synaptic transmission between neurons.....	3
Figure 2. Overview of G-protein coupled receptor (GPCR) and G-protein signaling.....	10
Figure 3. Regulator of G-protein signaling (RGS) family of proteins.....	15
Figure 4. RGS domain structure and interacting partners.....	19
Figure 5. Regions of RGS14 expression in rodent and primate brain.....	25
Figure 6. Basic circuitry and plasticity of the hippocampus.....	26
Figure 7. Common pathological hallmarks of TLE.....	34
Figure 8. The kainic acid model of status epilepticus induction (KA-SE) used to evaluate the effects of RGS14 on hippocampal seizure activity and pathology.....	44
Figure 9. Loss of RGS14 increases susceptibility to KA-induced seizure by expediting mortality and entry into SE	60
Figure 10. Behavioral sensitivity to KA-SE in RGS14 KO mice is not affected by sex	63
Figure 11. Hippocampal RGS14 protein expression is upregulated following KA-SE	64
Figure 12. Differential expression analysis of the hippocampal proteome reveals altered mitochondrial and metabolic protein expression in RGS14 KO versus WT mice	68
Figure 13. Comparison of WT and RGS14 KO hippocampal proteome after KA-SE suggests oxidative stress as a potential consequence of RGS14 KO	73
Figure 14. WGCNA uncovers modules of hippocampal proteins that exhibit different expression patterns between WT and RGS14 KO	77
Figure 15. Gene ontology of WGCNA further demonstrates altered metabolic processes altered in RGS14 KO mice	80
Figure 16. RGS14 localizes to mitochondria in CA2 PCs and reduces mitochondrial respiration in vitro	83

Figure 17. RGS14 is necessary for SOD2 induction in area CA2 and prevents 3-nitrotyrosine accumulation	86
Figure 18. SOD2 is upregulated in area CA1 of RGS14 KO mice one day after KA-SE	89
Figure 19. Loss of RGS14 does not alter early hippocampal neuronal injury in areas CA2 or CA1 after KA-SE	91
Figure 20. RGS14 is required for microglial recruitment and activation in hippocampal areas CA1 and CA2	94
Figure 21. Reduction in microglial density persists 7 days after KA-SE in RGS14 KO mice	98
Figure 22. Loss of RGS14 causes deficits in astrocyte reactivity following KA-SE	100
Figure 23. Proposed working model for RGS14 regulation of CA2 pyramidal neurons following seizure	143

List of Abbreviations

Calcium (Ca^{2+}); Voltage-gated calcium channel (VGCC); γ -aminobutyric acid (GABA); sodium (Na^+); G-protein coupled receptors (GPCRs); guanosine diphosphate (GDP); guanine nucleotide exchange factor (GEF); guanosine triphosphate (GTP); receptor tyrosine kinases (RTKs); adenylyl cyclase (AC); cyclic adenosine monophosphate (cAMP); phospholipase C (PLC); 1,4,5-trisphosphate (IP_3); diacylglycerol (DAG); G-protein inward rectifying potassium (GIRK); protein kinase A (PKA); endoplasmic reticulum (ER); protein kinase C (PKC); N-methyl D-aspartate (NMDA); α -amino-3-hydroxy-5-methyl-4-isoxazolepropionic acid (AMPA); cAMP response element binding protein (CREB); GTPase-activating proteins (GAPs); regulators of G-protein signaling (RGS); mitogen activated protein kinase (MAPK); long-term potentiation (LTP); long-term depression (LTD); extracellular response kinase (ERK); calcium/calmodulin ($\text{Ca}^{2+}/\text{CaM}$); $\text{Ca}^{2+}/\text{CaM}$ -dependent kinase II (CaMKII); nuclear export sequence (NES); nuclear localization sequence (NLS); pyramidal cells (PCs); entorhinal cortex (EC); dentate gyrus (DG); knockout (KO); brain-derived neurotrophic factor (BDNF); excitation/inhibition balance (E/I balance); kainate receptors (KARs); electroencephalogram (EEG); interictal epileptiform spikes (IESs); high-frequency oscillations (HFOs); anti-seizure drugs (ASDs); temporal lobe epilepsy (TLE); kainic acid (KA); pilocarpine (PILO); pentylenetetrazol (PTZ); ionized calcium binding adaptor molecule 1 (IBA1); Glial fibrillary acidic protein (GFAP); blood brain barrier (BBB); electron transport chain (ETC); reactive oxygen species (ROS); superoxide (O_2^-); hydrogen peroxide (H_2O_2); nitric oxide (NO); superoxide dismutase (SOD); mitochondrial manganese SOD (MnSOD or SOD2); NADPH oxidase (NOX); perineuronal nets (PNNs); sharp wave ripples (SPW-Rs); adenosine 1 receptor (A1R); kainic acid induction of status epilepticus (KA-SE); wild-type (WT); immunohistochemistry (IHC); stratum radiatum (SR); stratum pyramidale (SP); stratum oriens (SO); label-free quantification (LFQ); weighted gene correlation network analysis (WGCNA); Gene ontology (GO); FluoroJade B (FJB); NO synthase (NOS); differentially expressed proteins

(DEPs); prostaglandin E2 (PGE2); citric acid cycle (TCA); Cyclooxygenase 2 (COX-2); oxygen consumption rate (OCR); 3-nitrotyrosine (3-NT); A-kinase anchor protein (AKAP); mitochondrial Ca²⁺ uniporter (MCU); mitochondrial targeting sequence (MTS); optic atrophy 1 (OPA1); prostaglandin reductase 2 (Ptgr2); tumor necrosis factor alpha (TNF- α); artificial cerebrospinal fluid (ACSF); 4-amino-5-methylamino-2',7'-difluorofluorescein diacetate (DAF-FM); lipopolysaccharide (LPS); real-time polymerase chain reaction (RT-PCR);

1. Introduction

1.1. Overview of dissertation

The central nervous system, consisting of the brain and spinal cord, is arguably the most important system for vertebrate organisms and in particular mammalian species. The brain is essential for sustaining the life of an organism and mediating animal behavior for adaptation and survival. As such, the mammalian brain has evolved to become very specialized and utilizes mechanisms distinct from other organ systems to prompt behavioral responses. However, these processes that are essential for adaptation can go awry when not properly regulated in a diseased brain and contribute to brain injury and pathology. In this dissertation, I will demonstrate how a single component of the brain that is crucial for certain functions and animal behaviors also acts in a protective capacity when an animal is challenged with an injury, likely acting on similar mechanisms during both physiological and pathological processes.

First, I will overview fundamental processes of communication between neurons (i.e., how neurons transmit, receive, and interpret these signals) and components that regulate certain aspects of signal integration, detailing one very interesting and important component that is the subject of this dissertation (i.e., RGS14). After overviewing what is known about the function of RGS14, I will describe a common consequence of dysregulated neuronal signaling (i.e., seizures and epilepsy), a major brain structure (i.e., the hippocampus) where dysregulated signaling promotes seizure activity, the pathological consequences of dysregulation in the hippocampus, and how RGS14 and the hippocampal subregion where RGS14 is primarily expressed (i.e., area CA2) may be involved with seizure disorders and epileptic pathology. I will then focus on the findings of this dissertation, where I evaluate RGS14's role in protecting against seizures and seizure-related pathology in the hippocampus and the exacerbated pathological effects observed when RGS14 is deleted. Lastly, I will thoroughly discuss how the data here support and relate to other recent findings in the epilepsy field, the implications of RGS14 in epileptic disorders, future

directions that stem from these findings, and overarching conclusions that can be drawn from this dissertation.

1.2. Synaptic transmission and neuronal signaling

Neurons, consists of branching dendrites that receive signals from other neurons, a cell body (or soma) that integrates signals from various dendritic compartments, and axons that propagate the signal away from the cell body and towards connected neurons to form a synapse. Typically, the synapse consists of the terminal end of the axon (axon bouton) with the dendritic spine of another neuron and a small space between the axon bouton of the presynaptic neuron and dendritic spine of the postsynaptic neuron known as the synaptic cleft. The principle means of cell-to-cell communication between neurons in the central nervous system is synaptic transmission (summarized in Figure 1), where the synaptic cleft acts as a medium for biological signal transfer to occur via neurotransmitters and other biomolecules. Neurons are excitable cells that rely on ion flux through membrane channels to cause depolarization of the cell (i.e. a net increase of positive charge), and with sufficient depolarization, neurons surpass a threshold and fire an action potential: a rapid depolarization that propagates from the cell body down the axon causing neurotransmitter release at synapses. Presynaptic neurotransmitter release from the axon bouton of a firing neuron into the synaptic cleft results in activation of receptors, changes in ion flux across the plasma membrane, activation of intracellular signaling proteins that amplify the neurotransmitter signal, and structural, transcriptional, and translational modifications in the dendrites of the postsynaptic neuron. The sum of these perturbations on the postsynaptic neuron influences the probability of firing in the postsynaptic neuron and perpetuating the signal to other neurons connected in the circuit (Purves, 2008).

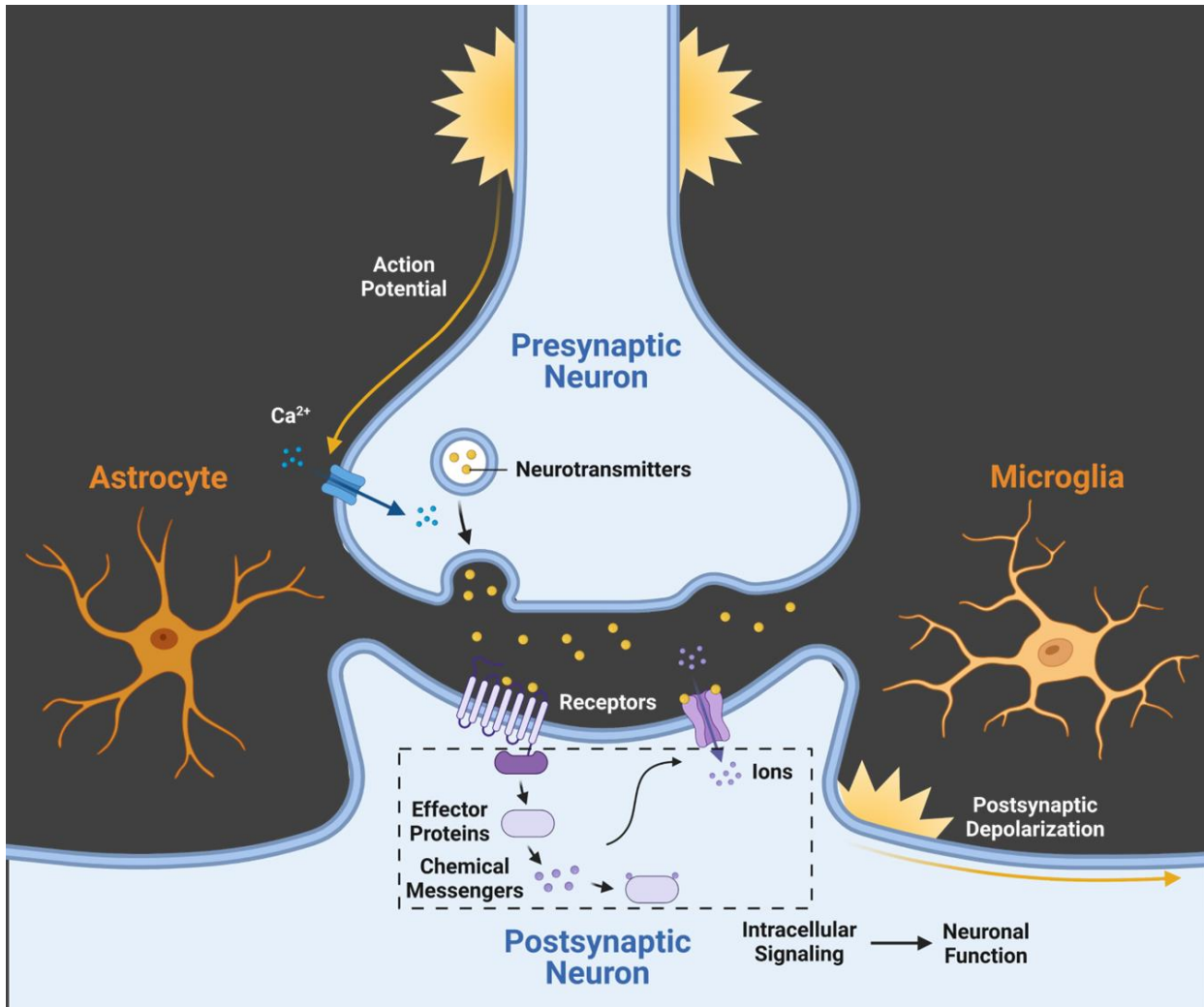


Figure 1. Overview of synaptic transmission between neurons. The firing of an action potential by the presynaptic neuron propagates a wave of depolarization, which causes the activation and opening of voltage gated calcium channels (VGCCs) and increasing intracellular calcium into the presynaptic neuron. Sufficient levels of calcium prompt the release of neurotransmitters from packaged vesicles into the synaptic cleft. Neurotransmitters bind and activate receptors on the postsynaptic neuron, which transduce the signal from the extracellular space of the synaptic cleft to the intracellular space of the postsynaptic neuron. Activation of ionotropic receptors permits the flow of ions through the receptor channel, which positively or negatively affects the postsynaptic depolarization. Activation of metabotropic receptors tunes the response (positively or negatively) of the ionotropic receptors through activation of effector

proteins and synthesis of chemical messenger inside the postsynaptic neuron. The sum of receptor activation and signaling influences the amount of postsynaptic depolarization and likelihood of action potential firing at the postsynaptic neuron, and the intracellular response by receptors and downstream signaling in the postsynaptic neuron is critical for neuronal function. Glial cells (astrocytes and microglia) support synaptic transmission and neuronal function. Generally, astrocytes form contacts with synapses to regulate the level of neurotransmitters in the synaptic cleft and provide nutrients and other factors needed for neuronal function, while microglia monitor the synaptic environment for neuron injury, cell death, and pathogens that would impair brain function in pathological conditions while also influencing synapse development and strength in physiological conditions. Created in BioRender.

In the presynaptic neuron, neurotransmitters are packaged into membrane-bound vesicles that localize to the axon bouton awaiting fusion with the plasma membrane and release into the synaptic vesicle upon neuron firing. When the presynaptic neuron fires an action potential, rapid depolarization activates a number of voltage-gated calcium (Ca^{2+}) channels (VGCCs) that allow entry of calcium into the axon and axon bouton. Calcium influx is a necessary step for neurotransmitter release as a number of presynaptic proteins require calcium for their activation, which prompt vesicular fusion to the plasma membrane and the emptying of vesicle-contained neurotransmitters into the extracellular space in a process known as exocytosis. The rate of neuron firing is proportional to the amount of neurotransmitter release from the presynaptic neuron, and proper regulation neuronal firing and neurotransmitter release is critical for proper neuronal signaling and function. The majority of neurons in the brain release glutamate, the principal excitatory neurotransmitter that depolarizes and increases the likelihood of neuronal excitation at the postsynaptic neuron. Balancing glutamatergic excitation is γ -aminobutyric acid (GABA), the principal inhibitory neurotransmitter that is released by a smaller but significant proportion of neurons and functions to decrease the likelihood of action potential firing by increasing the amount of negative charge entering into the postsynaptic neuron. While glutamate excites and GABA inhibits the postsynaptic neuron, monoamine neurotransmitters such as dopamine, serotonin, and norepinephrine are released from a subset of neurons and modulate the excitatory and inhibitory signals released from glutamatergic and GABAergic neurons, respectively. In addition to these canonical neurotransmitters, there is a growing diversity of molecules that mediate communication between neurons including neuropeptides and membrane-permeable molecules like nitric oxide and endocannabinoids. Together, these molecules transmit signals between the presynaptic and postsynaptic neurons to enable proper brain function (Purves, 2008).

The postsynaptic neuron receives the neurotransmitter signal through a wide array of cell surface receptors embedded within the plasma membrane of dendrites (in addition to other neuronal compartments). Neurotransmitters act as ligands, which bind to protein domains located outside of the cell and cause conformational changes in the receptor that activate it. Receptors are critical for transducing the extracellular signal into an intracellular signal and act as a primary means for neuronal communication. Receptors are broadly classified based on the events following their activation. Ionotropic receptors are membrane channels that permit ion flux upon their activation, which can cause an increase or decrease of membrane potential on the postsynaptic neuron and directly affect the likelihood of an action potential firing. For example, glutamate activates a number of glutamate receptors that can depolarize the postsynaptic neuron via influx of sodium (Na^+) and calcium and increase probability of action potential firing, while GABA activates GABA_A receptors that result in chloride influx that polarizes the cell (net negative effect on membrane potential) and decreases the probability of action potential firing. Metabotropic receptors transduce neuronal signals through intracellular mechanisms involving intermediate molecules. These receptors are crucial for signal amplification and diversification, and the mechanisms and consequences of their activation will be discussed in greater detail in the next section. Importantly, ionotropic receptors mediate fast neuronal communication on the order of milliseconds, while metabotropic receptors are slower and transmit signals on the order of seconds and minutes. Both types of receptors are essential for neuron communication and signal integration, and their dysfunction is implicated in a wide array of brain disorders (Purves, 2008).

Critically, neurons are supported by glial cells (notably astrocytes and microglia), which outnumber neurons, do not fire action potentials, and instead sense and modulate the synaptic environment to maintain neuronal communication. Astrocytes are distributed throughout the brain and extend processes that terminate at synapses, forming what is known as the tripartite synapse

along with the presynaptic and postsynaptic neuron. Here, astrocytes regulate the amount of neurotransmitters like glutamate in the synaptic cleft via excitatory uptake transporters. In return, astrocytes can facilitate or inhibit presynaptic neurotransmitter release and synchronize neuronal firing and communication via direct or indirect signaling with neurons. Importantly, astrocytes also regulate cerebral blood flow to the brain and help connect metabolic changes to neuronal function and signaling (Volterra and Meldolesi, 2005). Microglia on the other hand are the primary immune cells of the brain that regulate synaptic development and transmission while also mediating inflammatory responses to injury during disease. Microglia actively survey the neuronal environment to prune and modulate the strength of synapses depending on synaptic activity and the release of chemoattractive and inflammatory factors by neurons and astrocytes during development and brain injury (Wu et al., 2015). Therefore, neurons rely heavily on glia to establish proper synaptic connections with other neurons and regulate synaptic activity during physiological and pathological states.

1.3. G-protein signaling in neurons

Intracellular signaling is a complex, intertwined ballet of spatial and temporal coordination, empowered by a spectrum of signals generated outside and within the cell, and supported by a plethora of molecules that create the finely tuned physiological responses that are essential for life. This dizzying dance of biomolecular bravado has quested the biologist onto a long, complicated, and ever-expanding tale of explanation. In the brain, intracellular signaling in neurons represents a black box between endogenous and exogenous stimulatory input and the physiological, behavioral, and cognitive output that supports life, action, and inquisition: How does the most minute sound disturb sleep? Why does a small dose of a drug provoke deep changes in behavior and thought? And why does a single experience cause debilitating mental health issues in one individual but is unremarkable for another? These stimuli trigger enigmatic machinations within the cell, causing propagation to connected cells, and coalescing to

measurable outputs from a change in a cell's membrane potential to remembering a lost loved one.

At the nexus of input are receptors, and the largest and most diverse class of receptors are G-protein coupled receptors (GPCRs) (Lagerstrom and Schioth, 2008). GPCRs are seven transmembrane, metabotropic receptors that are abundant on all types of cells and tissues, especially within the brain. Activation by their endogenous or exogenous agonists initiates a cascade of molecular changes inside the cell. This cascade is known as signal amplification and is a fundamental property of GPCRs, where activation by relatively little quantities of agonist can trigger activation of many downstream effector proteins and generate large amounts of biological messengers that transduce the signal throughout the cell. Virtually all neurotransmitters in the brain serve as agonists (or occasionally antagonists that prevent receptor activation by agonists) for a wide array of GPCRs that affect neuronal properties like synaptic transmission, neuronal depolarization, action potential firing, and modulation of synaptic strength (Betke et al., 2012). Because GPCRs affect nearly every aspect of neuronal function, their dysfunction is thought to contribute to many neurological and psychiatric diseases. Due to this and the availability of agonist-binding domains in the extracellular space of the synaptic cleft (i.e. drugs need not enter the cell to be active), GPCRs represents a major therapeutic target for drug development, and the mechanisms by which they initiate intracellular signaling cascades is critical for the fundamental understanding of neuronal communication (Stewart and Fisher, 2015).

When agonist binds to a GPCR, the receptor undergoes a conformational switch that allows for activation of nearby G-proteins inside of the cell via interaction with the cytoplasmic face of the receptor. When agonist is not bound to the receptor, G-proteins are bound to guanosine diphosphate (GDP) and are inactive. Upon agonist stimulation, GPCRs act as a guanine nucleotide exchange factor (GEF) by causing the dissociation of GDP from the G-protein, allowing for the binding of guanosine triphosphate (GTP) and subsequent activation of G-proteins.

A single GPCR can activate many G-proteins and amplifying the extracellular signal from agonist. Activated G-proteins interact with a wide array of effector molecules downstream of receptor activation, which not only amplify the signal but diversify it as well (Oldham and Hamm, 2008). There are two types of G-proteins: monomeric and heterotrimeric. Monomeric G-proteins (e.g. Rho and Ras family proteins) are small single proteins that are typically activated downstream of receptor tyrosine kinases (RTKs). RTK activation results in autophosphorylation of tyrosine residues on the receptor and tyrosine phosphorylation of adaptor proteins (e.g. Raf kinase) that can act as GEFs for the small monomeric G-proteins. GPCRs can also indirectly or directly activate monomeric G-proteins, allowing for cross talk between the two receptor families. Monomeric G-proteins play numerous roles in cellular function by transducing signals to cytoskeletal components, vesicles, nuclei, and more (Bos et al., 2007). Heterotrimeric G-proteins consist of three subunits ($G\alpha$, $G\beta$, $G\gamma$) that form a complex near GPCRs awaiting receptor activation, where $G\alpha$ is in the inactive, GDP-bound states and $G\beta$ and $G\gamma$ are bound together forming $G\beta\gamma$. When GPCRs are agonized, $G\alpha$ switches GDP for GTP and adopts an active conformation that promotes the dissociation of $G\alpha$ from $G\beta\gamma$. Now activated $G\alpha$ and $G\beta\gamma$ subunits interact with and activate a number of effector proteins (e.g. membrane channels and enzymes) that can generate chemical second messengers, which amplify and perpetuate signal transduction throughout the cell (Oldham and Hamm, 2008) (G-protein signaling summarized in Figure 2).

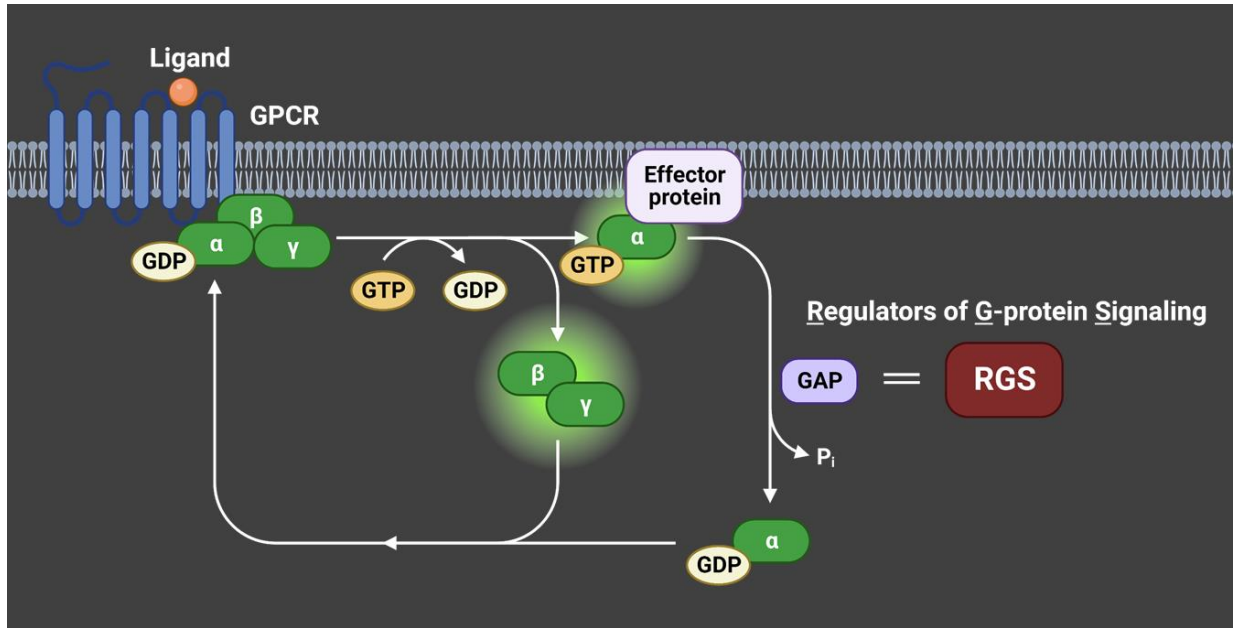


Figure 2. Overview of G-protein coupled receptor (GPCR) and G-protein signaling. At rest, GPCRs are bound to the heterotrimeric G-protein complex (G α , G β , G γ), which are inactive via the binding of guanosine diphosphate (GDP) to the G α subunit. Ligands (such as neurotransmitters) activate GPCRs on the cell membrane, which prompts a conformational shift of the receptor, prompting the exchange of GDP for guanosine triphosphate (GTP) on G α , and activating G α . GTP-bound G α dissociates from G $\beta\gamma$ to interact with effector proteins that promote the formation of chemical, secondary messengers, whereas G $\beta\gamma$ also interacts with a number of effector proteins to alter their activity. To terminate G-protein signaling, GTPase activating proteins (GAPs), which include the family of regulators of G-protein signaling (RGS) proteins, bind to G α to accelerate the hydrolysis of GTP to GDP and thereby inactivating G α . GDP-bound G α can then reassociate with G $\beta\gamma$ and reform the inactive complex with a GPCR. Created in BioRender.

There are 16 G α isoforms classified into four main families based on their effector protein binding and second messenger generation caused by their activation: G α_s that bind to and increase the activity of the membrane-tethered adenylyl cyclase (AC), which promotes the formation of the second messenger cyclic adenosine monophosphate (cAMP); G $\alpha_{i/o}$ that also bind to AC but inhibit the enzyme and the formation of cAMP; G $\alpha_{q/11}$ that bind to phospholipase C (PLC) and catalyze membrane lipid hydrolysis to form second messengers inositol 1,4,5-trisphosphate (IP₃) and diacylglycerol (DAG); and G $\alpha_{12/13}$ that bind to effector RhoGEFs, which can then activate small, monomeric G-proteins of the Rho family and enable crosstalk between GPCR and RTK pathways (Betke et al., 2012; Suzuki et al., 2009). Additionally, 5 G β and 12 G γ isoforms associate together in a variety of ways to differentially interact and regulate the activity of distinct and overlapping effector proteins compared to G α , including AC, PLC, G-protein inward rectifying potassium (GIRK) channels, and VGCCs (Khan et al., 2013). Regulation of these effectors by G-proteins is essential for conveying the signals detected by GPCRs, and the dizzying number of permutations that may exist for the G $\alpha\beta\gamma$ heterotrimer guarantees a diverse means of signaling within the cell. Second messengers generated from effector enzymes bind to and alter the activity of their target enzymes. cAMP activates its primary target protein kinase A (PKA), promotes the phosphorylation of many intracellular proteins, and causes alterations in cell structure, signaling, and gene expression. Additionally, cAMP can regulate the activity of cAMP-gated ion channels and intracellular GEFs. IP₃ activates IP₃ receptors in intracellular compartments like the endoplasmic reticulum (ER) and increases calcium release into the cytosol from these organelles. Calcium is a second messenger itself and modulates the function of a staggering number of cellular effectors, especially in neurons. DAG binds to protein kinase C (PKC) and along with calcium can activate the kinase, promoting translocation of PKC to the membrane and phosphorylation of its substrates. Together with other nucleotide, lipid, and ionic second messengers, these molecules generated by G-protein activation regulate cellular function at all levels and thus requiring tight regulation to prevent cellular dysfunction (Newton et al., 2016).

In the presynaptic neuron, GPCRs can regulate synaptic transmission by affecting the likelihood of neurotransmitter release via G-protein activation. An important feedback mechanism of synaptic transmission is the presence and activation of GPCRs near the active zones of neurotransmitter release. When stimulated, these GPCRs can inhibit ($G\alpha_{i/o}$ -coupled GPCRs) or facilitate ($G\alpha_s$ - or $G\alpha_q$ -coupled GPCRs) subsequent neurotransmitter release depending on the GPCR and the type of G-proteins that it couples. $G\alpha_{i/o}$ -coupled GPCRs inhibit synaptic transmission primarily through the $G\beta\gamma$ subunits. $G\beta\gamma$ can inhibit VGCCs, which decreases the amount of calcium influx at the axon bouton and limit calcium-dependent exocytosis of neurotransmitters, activate GIRK channels, which can repolarize the cell via potassium efflux from the neuron and inhibit action potential firing and subsequent neurotransmitter release, and interact with proteins involved with exocytosis, which can inhibit vesicle fusion with membrane and preventing the release of packaged neurotransmitters. In contrast with $G\alpha_{i/o}$, GPCRs coupled to $G\alpha_s$ and $G\alpha_q$ can facilitate successive release of neurotransmitters by acting through $G\alpha$ subunit and second messenger signaling. Phosphorylation of VGCCs by PKA and PKC can enhance calcium influx into the axon terminal and increase neurotransmission via $G\alpha_s$ and $G\alpha_{q/11}$ -dependent activation, respectively. Additionally, these two kinases can phosphorylate exocytotic machinery and influence vesicle release independent of calcium channels. cAMP and DAG can also facilitate neurotransmission by binding and activating presynaptic effectors other than PKA or PKC (Brown and Sihra, 2008).

While GPCRs in the presynaptic neuron largely influence action potential firing and vesicular neurotransmitter release, GPCRs and G-protein signaling at the postsynaptic neuron is capable of modulating a variety of cellular effects including neuronal depolarization and excitability, synaptic plasticity, cytoskeletal structure, transcriptional and translational activation, receptor recycling, and neuronal metabolism. At the membrane, G-protein signaling functions to support the quick ion flux caused by ionotropic receptor activation from glutamatergic and

GABAergic receptor activation by creating slower but longer lasting changes and promoting amplification of the signal released by the presynaptic neuron. Like the presynaptic neuron, both $G\alpha$ and $G\beta\gamma$ modulate the activity of their effector proteins following neurotransmission and GPCR activation, where $G\beta\gamma$ is also capable of directly activating GIRK channels to antagonize depolarization of the postsynaptic neuron. $G\alpha$ signaling can indirectly modulate ion flux through glutamate-activated N-methyl D-aspartate (NMDA) and α -amino-3-hydroxy-5-methyl-4-isoxazolepropionic acid (AMPA) receptors via second messenger activation of kinases like PKA and PKC, which phosphorylate either the receptor or scaffold proteins that modulate NMDA and AMPA receptor activity and postsynaptic depolarization. GPCR modulation of ionotropic NMDA and AMPA receptors is a critical regulatory mechanism at excitatory synapses not only due to the effects on postsynaptic depolarization but also because both NMDARs and AMPARs are responsible for calcium influx from the extracellular space (Rojas and Dingledine, 2013). Calcium is a major second messenger in dendrites and is essential for the strengthening and weakening of a synapses (i.e. synaptic plasticity) in addition to major signaling events resulting in a number of cellular consequences (Higley and Sabatini, 2012; Lisman et al., 2012). Because GPCR activation can also cause calcium influx from intracellular stores via $G\alpha_q$ signaling and alter extracellular calcium transients via modulation of VGCCs, the levels of intracellular calcium and calcium-dependent signaling can be tightly regulated by GPCR and G-protein activation in the postsynaptic neuron, similar to what is seen in the presynaptic neuron (Higley and Sabatini, 2012; Zamponi and Currie, 2013). Transduction of membrane signals towards the cell body is essential for proper neuronal function, as neurons often span across long distances to transmit neuronal signals from one brain region to another (Johanson et al., 1996). G-proteins, their effectors, and second messengers mediate signal transduction to various cellular compartments within the neuron, including the nucleus (Goetzl, 2007). For example, $G\alpha_s$ -cAMP activation of PKA can promote activation of cAMP response element binding protein (CREB) in the nucleus, where it functions as a transcription factor of genes containing a cAMP response element (CRE). These

gene products are needed for long-term stabilization of synaptic plasticity, which is essential for memory formation in the brain (Alberini, 2009). Therefore, by adjusting ion flux and membrane depolarization at the membrane or transducing signals intracellularly, G-proteins mediate changes that influence the postsynaptic neuron's ability to communicate within and between neurons.

1.4. Regulation of G-protein signaling by RGS

Signaling by G-proteins must be tightly controlled by mechanisms that restrict the duration of activation of G-proteins to prevent aberrant signaling to its downstream effectors. G-proteins have intrinsic GTPase activity, which allow for hydrolysis of GTP to GDP, reassociation of the $G\alpha\beta\gamma$ heterotrimer, and thus terminating G-protein signaling. However, GTPase activity is inherently slow and requires enhancement by GTPase-activating proteins (GAPs), which accelerate GTP hydrolysis and deactivation of G-proteins. Over three decades of investigation have led to the identification and characterization of GAPs that endogenously terminate G-protein signaling. GAPs that negatively regulate $G\alpha$ activation are known as regulators of G-protein signaling (RGS), of which there are 20 canonical RGS proteins (Squires et al., 2018b) (Figure 3). All canonical RGS proteins contain an RGS domain, a ~120 amino acid sequence that is necessary for its ability as a GAP, which interacts with and stabilizes the switch regions of $G\alpha$ subunits to accelerate G-protein deactivation (Tesmer et al., 1997). The RGS protein family is grouped into four main subfamilies based on sequence similarity: R4 (RGS1, 2, 3, 4, 5, 8, 13, 16, 18, 21), R7 (RGS6, 7, 9, 11), R12 (RGS10, 12, 14), and Rz (RGS17, 19, 20). Additionally, RGS proteins in the R7 and R12 (all but RGS10) subfamilies contain other domains that enable it to bind and affect the function of other proteins beyond its potentiation of GTPase activity (Squires et al., 2018b).

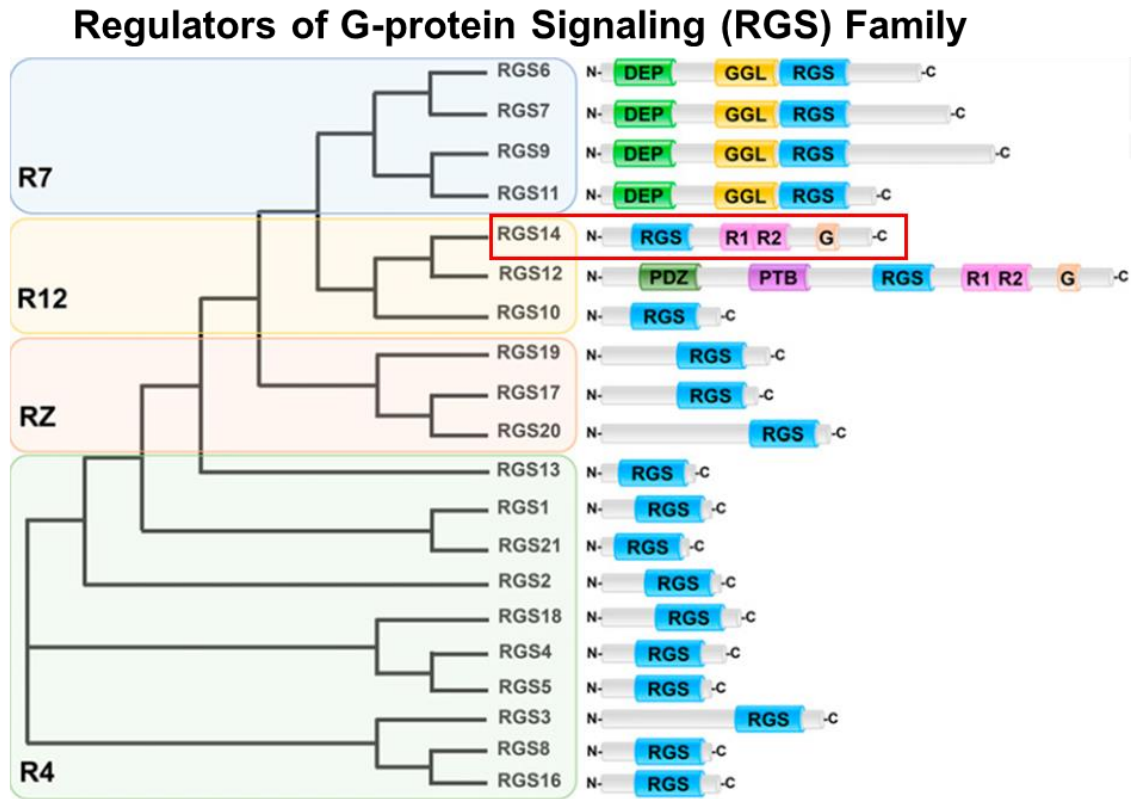


Figure 3. Regulator of G-protein signaling (RGS) family of proteins. (modified from Squires et al., 2018b) The twenty proteins of the RGS family are divided into four subfamilies based on sequence homology: R7, R12, RZ, and R4. All RGS proteins are characterized by a RGS domain, which is necessary for its GAP activity towards G α subunits and termination of G-protein signaling. RGS14, the RGS protein of interest for this dissertation, is highlighted with a red box.

RGS proteins are highly important for termination of heterotrimeric G-protein signaling after activation of $G\alpha_{i/o}$ - and $G\alpha_{q/11}$ -coupled GPCRs but not for GPCRs coupled to $G\alpha_s$ or $G\alpha_{12/13}$, as these $G\alpha$ subtypes contain residues in the switch I region that occlude RGS binding (Masuho et al., 2020). However, it should be noted that RGS-like proteins (similar but distinct from canonical RGS proteins) exist that can act as both effectors and GAPs of $G\alpha_{12/13}$ isoforms, which allow for tight regulation of $G\alpha_{12/13}$ signaling (Suzuki et al., 2009). Critical to their function, RGS proteins do not broadly deactivate all $G\alpha_{i/o}$ - and $G\alpha_{q/11}$ subunits but rather exhibit subtype selectivity based on RGS sequence. Generally, R7 and R12 members are selective for $G\alpha_{i/o}$ subunits, R4 are selective for most $G\alpha_{i/o}$ and $G\alpha_{q/11}$ subunits, and members of the Rz are selective for $G\alpha_z$ (a member of the $G\alpha_{i/o}$ subfamily). RGS proteins are unique in their affinity towards $G\alpha$ isoforms with varying selectivity (even within the same $G\alpha$ family) depending on the specific RGS subtype, allowing for preferential regulation of GPCRs depending on their $G\alpha$ coupling (Masuho et al., 2020). Defying convention, recent investigations have demonstrated non-canonical signaling roles for RGS proteins through non-RGS domains or other motifs in the protein that influence cell signaling pathways (e.g., mitogen activated protein kinase (MAPK) signaling) independent of their effect on heterotrimeric G-protein signaling (Sethakorn et al., 2010). Further exploration of RGS function is therefore warranted to unravel their complex effects on the intracellular response.

Importantly, RGS proteins are discretely and selectively expressed based on tissue and cell-type, providing further specialization of RGS function. RGS proteins are expressed in the brain, heart, spleen, and lungs among other tissues and within those tissues have varying degrees of expression based on the cell-type and subtype, especially in the brain (Squires et al., 2018b). Their expression in the cell is regulated at multiple levels including epigenetic, transcriptional, and post-transcriptional regulation. Protein stabilization and binding to obligate partners also modulates RGS function, while their subcellular localization can affect the ability of RGS to

perform their regulatory duties. Being negative regulators of G-protein signaling, a common feedback mechanism of G-protein signaling is modification of RGS expression following agonist stimulation of GPCRs and other cell surface receptors, which can function to increase or decrease the brake on cell signaling. For example, some RGS genes contain CRE sites, and agonist-induced increases of intracellular cAMP lead to activation of CREB, which can alter transcription of these RGS genes. mRNA stability is also emerging as a means of regulating RGS protein, where micro RNAs (miRNAs) and RNA-binding proteins can influence the stability and translation of RGS14 mRNA transcripts. Post-transcriptional modifications of RGS proteins, such as phosphorylation, ubiquitination, and oxidation, and interaction with binding partners, such as G β 5 for R7 RGS family members, can influence protein stability, activity, and subcellular localization and are well characterized for many RGS proteins. Altered expression of RGS proteins is associated with pathology in cardiovascular disease, immune system diseases, and disorders of the central nervous system, and the effects of RGS expression and function in disease modification is a blossoming field in G-protein research (Alqinyah and Hooks, 2018).

Most RGS proteins have some degree of expression in the brain, where many are selectively and dynamically expressed in distinct brain regions to affect synaptic transmission, neuronal excitability, synaptic plasticity, and neuronal differentiation and survival with consequences on behavior (e.g. cognitive function, emotional regulation, movement) and neurological and psychiatric disease (e.g. epilepsy and depression) (Gerber et al., 2016; Gold et al., 1997; Larminie et al., 2004). RGS proteins localize to pre- and postsynaptic neurons of glutamatergic, GABAergic, and monoaminergic neuron types, where they can antagonize GPCR signaling by accelerating the recoupling of G α to G $\beta\gamma$ and terminating both heterotrimeric signaling arms. RGS proteins with activity towards G $\alpha_{i/o}$ (e.g. RGS2) have been shown to facilitate neurotransmitter release by decreasing G $\beta\gamma$ -mediated inhibition of presynaptic VGCCs (Chen and Lambert, 2000). Likewise, RGS2 also negatively regulates G $\beta\gamma$ -dependent inhibition of

postsynaptic GIRK channels after GABA activation of metabotropic GABA receptors ($G\alpha_{i/o}$ -coupled $GABA_B$ R), which reduces the inhibitory effect of GABA (Labouebe et al., 2007). Regulation of $G\alpha_{q/11}$ signaling by RGS is also important in synaptic transmission. For example, RGS4 negatively modulates $G\alpha_q$ -coupled metabotropic glutamate receptors (mGluRs), which limits mGluR activation (Saugstad et al., 1998). Postsynaptic mGluRs can mediate retrograde release of neuromodulators like endocannabinoids and opioids, which act on presynaptic GPCRs to tune neurotransmitter release, and RGS4 actions here regulate this response (Kreitzer and Malenka, 2005). Especially important is RGS's effects on synaptic plasticity, where several RGS proteins are essential for proper regulation of stable potentiation of the synapse (long-term potentiation, LTP) or depotentiation of the synapse (long-term depression, LTD). Through effects on GPCR and G-protein signaling, RGS proteins from multiple subfamilies have been shown to regulate G-protein dependent effects on LTP and LTD by acting pre- and postsynaptically. Although the exact mechanisms of RGS regulation of synaptic plasticity are still under investigation, mounting evidence shows RGS proteins modulate synaptic strength by altering presynaptic neurotransmitter release and/or interacting with G-protein- and NMDAR-dependent pathways to regulate postsynaptic potentiation or depotentiation. Increased or decreased expression of these RGS proteins can have detrimental consequences on neurobehavioral processes that rely on LTP and LTD, including learning and memory, coordinated movement, and drug-seeking behaviors (Gerber et al., 2016).

1.5. RGS14 expression and regulation of cell signaling

RGS14, a member of the R10 family of RGS proteins, is a particularly interesting and unusual RGS protein as it is rather large (~58 kDa in rodent, ~63 kDa in primates), contains additional domains outside of its RGS domain, and binds to a number of G-proteins, kinases, and cytoskeletal proteins that allow it to function as a large scaffolding molecule (Figure 4). As a canonical RGS protein, RGS14 acts as GAP for $G\alpha_{i/o}$ isoforms (except $G\alpha_z$) following their

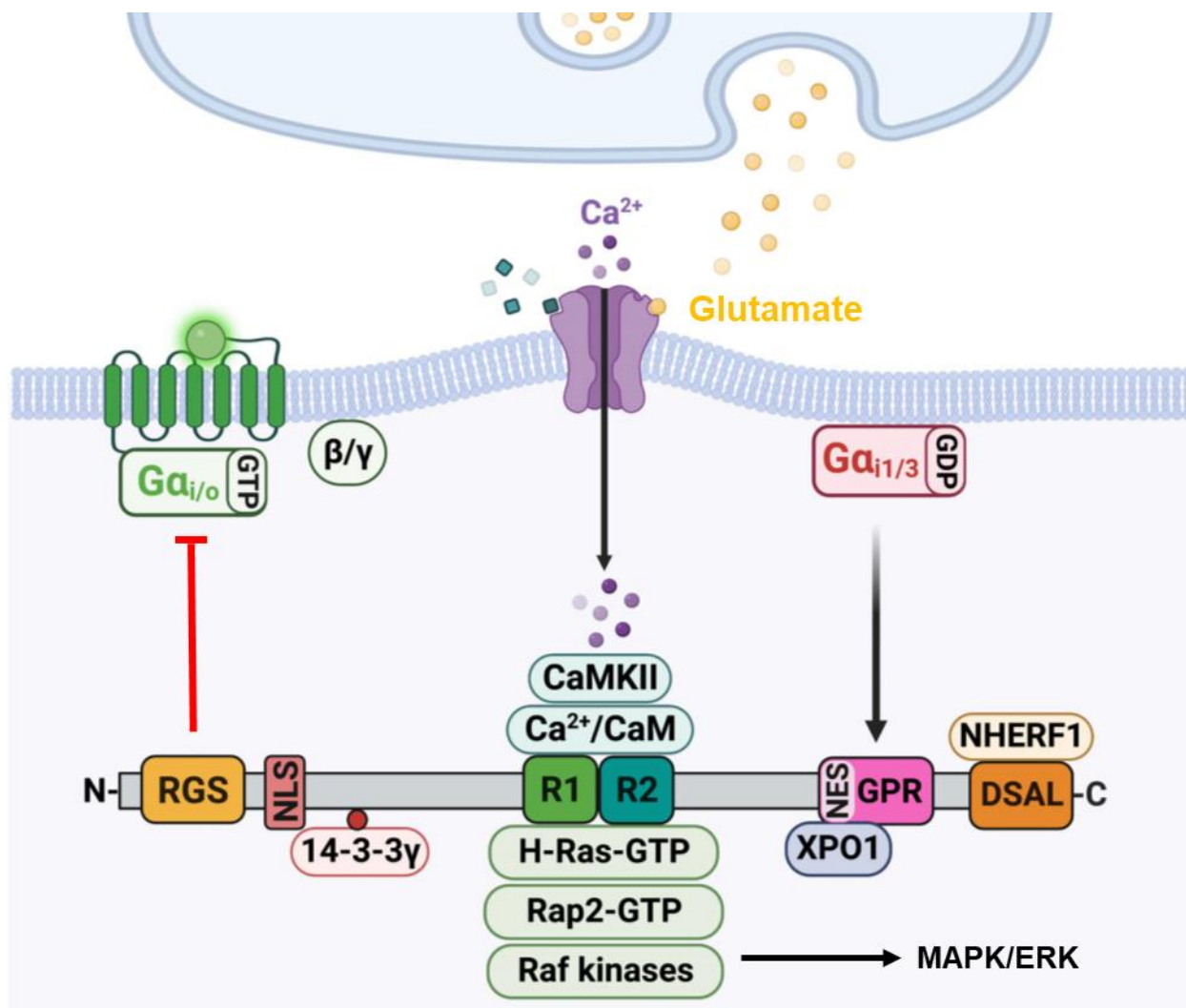


Figure 4. RGS domain structure and interacting partners. (modified from Montanez-Miranda et al., 2022) Human RGS14 is 566 amino acids (534 amino acids in rodents) and contains several domains that mediate interaction between a number of interacting partners. The RGS domain binds to activated, GTP-bound $G\alpha_{i/o}$ isoforms to accelerate inactivation. The Ras/Rap tandem binding domain (R1/R2) is necessary for the binding of activated, monomeric G-proteins H-Ras and Rap2 and upstream Raf kinases, which mediate RGS14's effects on downstream mitogen activated protein kinase/extracellular response kinase (MAPK/ERK) signaling. The R1/R2 domain is also necessary for RGS14 interaction with calcium calmodulin (Ca^{2+}/CaM) and Ca^{2+}/CaM kinase II (CaMKII) that are activated by calcium entry. The G-protein regulatory (GPR) motif promotes the association of RGS14 with inactive, GDP-bound $G\alpha_{i1/3}$

isoforms. RGS14 contains a nuclear localization sequence (NLS) in the linker region between the RGS and R1/R2 domains and a nuclear export sequence in the GPR motif, which mediate the import and export of RGS14 in and out of the nucleus, respectively. While binding to exportin 1 (XPO1) promotes nuclear export of RGS14, binding to 14-3-3 γ prevents nuclear import and localization of RGS14. Last, primate RGS14 (but not rodent) contains a PDZ recognition motif that permits binding of RGS14 to PDZ domain-containing proteins like Na⁺/H⁺ Exchange Regulatory Factor 1 (NHERF1).

activation by GPCRs or non-receptor GEFs to terminate their signaling. Strikingly, RGS14 is able to traverse throughout the cell and distribute to multiple subcellular compartments including the plasma membrane, cytosol, and nucleus, where its localization is controlled (at least partially) by its interacting partners. mRNA and protein of RGS14 has been detected in various regions of the rodent and primate brain, the heart, liver, and immune system (spleen, thymus, immune cells) in rodents, and, most recently, the proximal and distal tubule of human kidneys among other regions where its function is unknown (Harbin et al., 2021).

Much of what is known about RGS14 function comes from cellular studies that have uncovered the wide range of binding partners of RGS14 and how they influence RGS14 subcellular localization and RGS14 function. Through its N-terminal RGS domain, RGS14 interacts with GTP-bound $G\alpha_{i/o}$ proteins following $G\alpha_{i/o}$ -coupled GPCRs (e.g. α_2 -adrenergic receptor) or non-receptor GEFs (e.g. Ric-8a) (Vellano et al., 2013; Vellano et al., 2011). Activation of $G\alpha_{i/o}$ recruits RGS14 from the cytosol to the plasma membrane, where it accelerates the inactivation of $G\alpha_{i/o}$ (Hollinger et al., 2001; Traver et al., 2000; Vellano et al., 2011). Additionally, RGS14 is capable of binding with inactive, GDP-bound $G\alpha_{i1}$ and $G\alpha_{i3}$ subunits, through its C-terminal G-protein Regulatory (GPR) motif (also known as a GoLoco domain), and this interaction also localizes RGS14 to the plasma membrane (Shu et al., 2007; Traver et al., 2004). Here, RGS14 is hypothesized to act as a guanine nucleotide dissociation inhibitor (GDI), preventing GDP dissociation and activation of $G\alpha_{i1/3}$, and/or form a local signaling nexus where RGS14 can scaffold and regulate $G\alpha_{i/o}$ activation and other membrane signaling molecules (Harbin et al., 2021). Between the RGS domain and GPR motif is a Ras/Rap tandem-binding domain (R1/R2), which is essential for binding of RGS14 to activated monomeric G-proteins like H-Ras and Rap2 and provides a scaffold for Raf kinases that activate H-Ras (Shu et al., 2010; Traver et al., 2000; Vellano et al., 2013; Willard et al., 2009). Little is known about how RGS14 influences Rap2 function and vice versa, although this binding does not appear to alter interactions with active or

inactive $G\alpha_{i/o}$ subunits (Mittal and Linder, 2006). Contrary to Rap2, RGS14 binding to H-Ras promotes RGS14 distribution to the plasma membrane, and this binding inhibits receptor-dependent MAPK/extracellular response kinase (ERK) signaling (Shu et al., 2010; Vellano et al., 2013; Willard et al., 2009). RGS14 interactions with inactive $G\alpha_{i/3}$ increase its affinity towards H-Ras (Shu et al., 2010), and H-Ras binding enhances RGS14 GAP activity (Zhao et al., 2013). How RGS14 inhibits H-Ras dependent MAPK/ERK activation is unknown but may do so by regulating H-Ras interaction with downstream effectors. Our recent report investigated the primate/human-type RGS14, which contains an additional 22 amino acid sequence at the protein C-terminus and ends in a PDZ recognition motif. In kidney cells, primate/human RGS14 can bind to one of the PDZ domains of Na⁺/H⁺ Exchange Regulatory Factor 1 (NHERF1) via its PDZ motif, allowing RGS14 to disinhibit phosphate uptake into the cell following agonist stimulation (Friedman et al., 2022). The identification of PDZ interactions between RGS14 and PDZ-containing proteins represents another, largely unexplored mechanism of RGS14 scaffolding, especially in the brain where PDZ interactions are vital for membrane scaffolding and signaling at the postsynaptic neuron (Dunn and Ferguson, 2015).

Recently, our lab characterized the RGS14 interactome in mouse brain, which identified a number of novel interacting partners (Evans et al., 2018a). Interestingly, we identified calcium/calmodulin (Ca^{2+}/CaM) and Ca^{2+}/CaM -dependent kinase II (CaMKII) in the mouse brain, which was confirmed *in vivo* and *in vitro*. Both Ca^{2+}/CaM and CaMKII are highly expressed throughout, notably in the brain where they regulate phosphorylation and activity of hundreds of their downstream effectors to control many aspects of neuronal function, including synaptic plasticity (Lisman et al., 2012; Xia and Storm, 2005). While it is unclear to what purpose RGS14 binds to Ca^{2+}/CaM and CaMKII, the interaction between RGS14 and these calcium-dependent proteins is likely of high importance regarding RGS14's function in the brain. The interactome also revealed a number of dendritic spine proteins that may complex with RGS14 including actin

binding proteins (e.g. dreberin), proteins that regulate AMPA receptor trafficking (e.g. myosin VI), and postsynaptic density (PSD) scaffold proteins (e.g. Homer1) (Evans et al., 2018a). Follow-up studies demonstrated that RGS14 binds the scaffold 14-3-3 γ (identified in the interactome) in a phosphorylation-dependent and independent manner, which decreases RGS14 GAP activity and regulates RGS14 subcellular localization, respectively (Gerber et al., 2018). Interestingly, RGS14 contains a nuclear export sequence (NES) within the GPR motif and a nuclear localization sequence (NLS) in the linker region between the RGS and R1/R2 domains (Squires et al., 2021). RGS14 shuttles between the plasma membrane, cytosol, and nucleus, where it utilizes its NLS and NES to be imported into and exported out of the nucleus, respectively (Branch and Hepler, 2017; Cho et al., 2005; Squires et al., 2021). Similar to subcellular control via G α i/o and H-Ras binding, RGS14 engages with 14-3-3 γ to prevent nuclear import (Gerber et al., 2018). Although the role of RGS14 in the nucleus is unknown, we have shown that mutations in the NES of RGS14 that restricts it to the nucleus interferes with its ability to function at the membrane (Squires et al., 2021). Taken together, it is clear that RGS14 is uniquely positioned and well-equipped to regulate cell signaling, especially in neurons, by forming diverse signaling complexes with a number of interacting partners.

1.6. Roles of RGS14 in neuronal function and behavior

In the mouse brain, RGS14 is developmentally expressed, where it generally increases starting at P7 and stabilizing at P21 but varies depending on the region. In the adult mouse, it is highly expressed throughout the hippocampus in the glutamatergic pyramidal cells (PCs) of the hippocampal area CA2, in the stratum oriens layer of CA1 (where CA2 axons connect to basal dendrites of CA1 PCs), and sparsely in CA1 pyramidal cells (Evans et al., 2014; Lee et al., 2010). In CA2 pyramidal cells, RGS14 developmental expression is under the control of the mineralocorticoid receptor along with other CA2-specific genes (McCann et al., 2021). Interestingly, RGS14 mRNA is very high in the dendrites and cell bodies of CA2 in adult mice,

suggesting RGS14 protein expression is controlled in part by local translation (Farris et al., 2019). Expression is also detected in the olfactory areas like the olfactory nucleus, orbital, entorhinal, and piriform cortices, the central amygdala, and the nucleus accumbens of the ventral striatum (Evans et al., 2014; Foster et al., 2021; Squires et al., 2021). In primate and human tissue, additional expression is found in postsynaptic and nuclear compartments of inhibitory medium spiny neurons of the dorsal striatum and in presynaptic axons and terminals in the globus pallidus and substantia nigra (Squires et al., 2018a) (RGS14 expression in rodent and primate brain summarized in Figure 5).

As noted earlier, synaptic plasticity is the functional and structural alterations of a synapse that result in their strengthening or weakening. In the hippocampus, the entorhinal cortex (EC) provides cortical, excitatory input onto glutamatergic granule cells of the dentate gyrus (DG) that project to glutamatergic PCs of area CA3, which terminate their axons in area CA1 (Figure 6). This is the classical tri-synaptic pathway of the hippocampus (EC>DG>CA3>CA1), and synaptic plasticity (LTP and LTD) in this pathway underlies memory formation in the hippocampus. CA3>CA1 synapses can be robustly strengthened via LTP or weakened via LTD, which can be maintained over longer periods of time by alterations in the dendritic spine structure (known as structural plasticity) (Basu and Siegelbaum, 2015). LTP and LTD require NMDAR activation and calcium influx through NMDARs and VGCCs, where calcium influx activates Ca^{2+}/CaM and its downstream effectors (Xia and Storm, 2005). It is thought that LTP and LTD expression is dependent on the amount of calcium influx into the postsynaptic neuron, where high calcium influx causes LTP and low or modest calcium influx causes LTD. During LTP, Ca^{2+}/CaM activates CaMKII, which promotes the insertion of AMPARs into the PSD via phosphorylation of AMPAR and other targets and increases potentiation in subsequent synaptic transmission events (Herring and Nicoll, 2016).

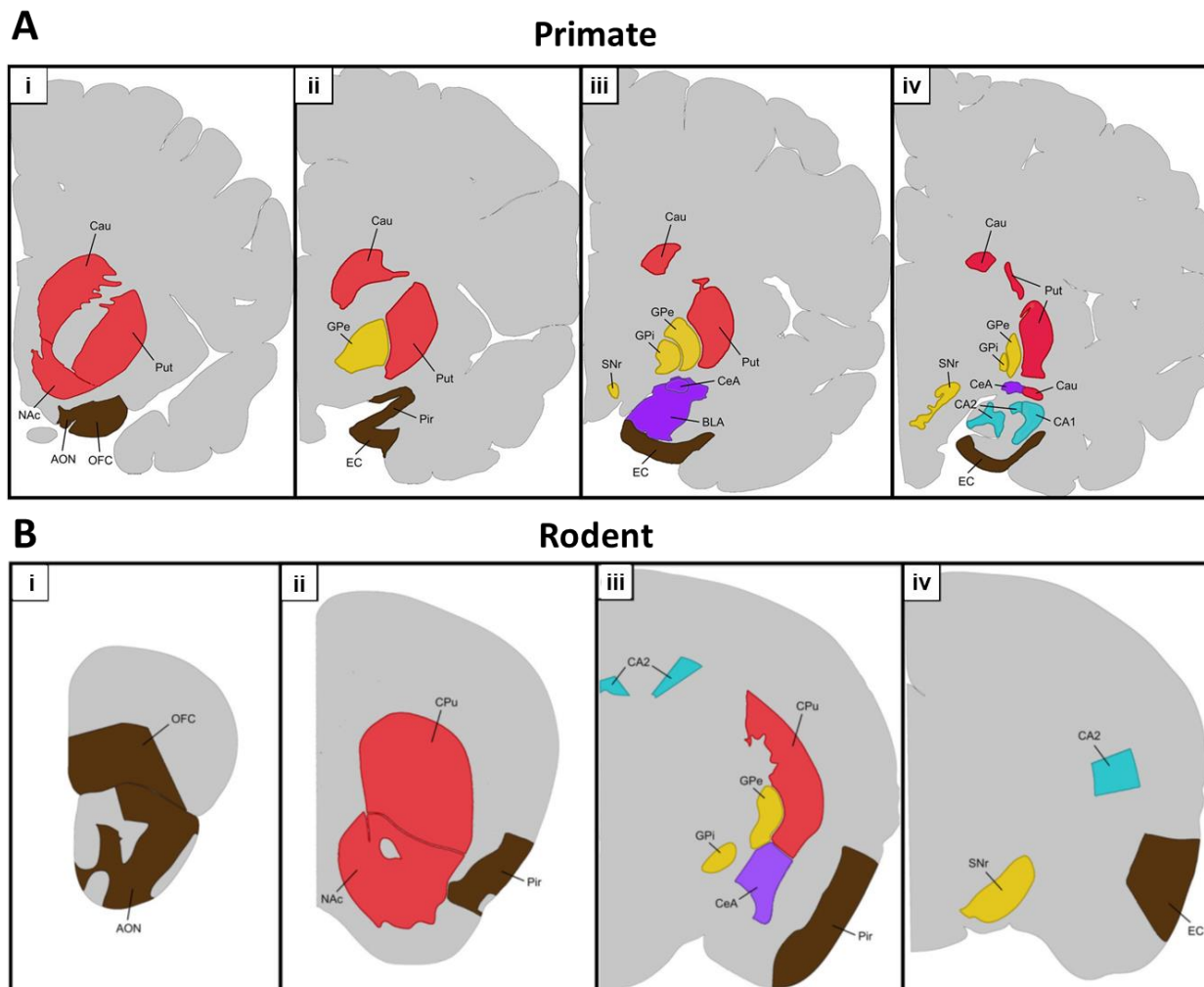


Figure 5. Regions of RGS14 expression in rodent and primate brain. (modified from Montanez-Miranda et al., 2022) Overview of RGS14 expression in the primate (A) and rodent (B) brain from the most rostral (i) to most caudal (iv) regions of expression. Region abbreviations: Caudate (Cau), putamen (Put), nucleus accumbens (NAc), anterior olfactory nucleus (AON), orbital frontal cortex (OFC), external segment of the globus pallidus (GPe), entorhinal cortex (EC), piriform cortex (Pir), internal segment of the globus pallidus (GPi), substantia nigra (SNr), central nucleus of the amygdala (CeA), basolateral nucleus of the amygdala (BLA), hippocampal areas CA1 and CA2, caudoputamen (CPu).

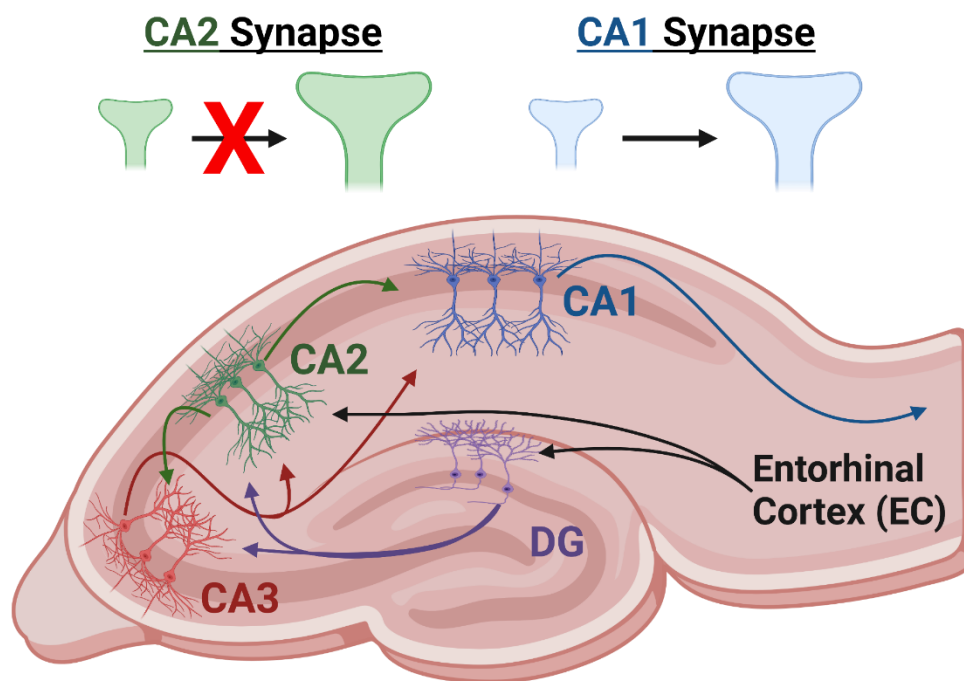


Figure 6. Basic circuitry and plasticity of the hippocampus. In the classical trisynaptic pathway, the hippocampus receives cortical input from the entorhinal cortex (EC), which provides input to the granule cells of the dentate gyrus (DG). Mossy fibers from the DG synapse onto pyramidal cells of areas CA3, which transmit information to pyramidal cells of area CA1. As an alternative means of information flow, area CA2 receives strong excitatory input from the EC and projects to area CA1. Additionally, area CA2 receives input from both the DG and CA3 and projects back to CA3 and forward to CA1. While excitatory synapses of CA3>CA1 connections are robustly strengthened during stimuli that promote synaptic plasticity of the circuit (i.e., memory formation), the excitatory synapses of CA3>CA2 are resistant to such plasticity under physiological conditions. Created in BioRender.

During LTD, weak calcium influx promotes Ca^{2+} /CaM binding and effects on phosphatases (e.g., calcineurin), which generally dephosphorylates substrates to causes depotentiation (Xia and Storm, 2005). Additionally, G-protein related events like cAMP/PKA, PKC, and MAPK/ERK activation play critical roles in modulating LTP, LTD, and memory formation (Gerber et al., 2016).

Like CA1, CA2 PCs, where RGS14 is highly expressed, also receives input from CA3, but these synapses are notoriously resistant to LTP in adolescent or older WT mice (Zhao et al., 2007) (Figure 6). Global knockout of RGS14 (RGS14 KO) in mice permits LTP in a MAPK/ERK-dependent manner at CA3>CA2 synapses (Lee et al., 2010). Additionally, the same study demonstrated that loss of RGS14 increased excitability of CA2 PCs without affecting normal synaptic transmission at CA3>CA2 synapses, suggesting RGS14 also influences intrinsic properties of CA2 PCs firing. A follow-up study showed that RGS14 suppresses glutamate-induced calcium transients in CA2 PCs (and CA1 PCs when ectopically expressed) to inhibit LTP and structural enlargement of dendritic spines, and suppression of LTP here was shown to be dependent on NMDAR, CaMKII, and PKA inhibition (Evans et al., 2018b). A recent report demonstrated that a functional mutation in the GPR motif (preventing RGS14 localization to the plasma membrane) restored LTP in a similar manner as RGS14 KO, whereas mutations in the RGS or R1/R2 domains had no effect on LTP inhibition by RGS14 (Squires et al., 2021). Therefore, RGS14 in area CA2 (and CA1 when expressed in sufficient quantity) modulates CA2 PC function by suppressing calcium influx and synaptic plasticity likely through upstream mechanisms at the plasma membrane that inhibit NMDAR, CaMKII, PKA, and MAPK/ERK signaling, where RGS14 also affects the intrinsic excitability of CA2 PCs through unknown mechanisms. Coincident with the unmasking of LTP at CA3>CA2 synapses, RGS14 KO mice exhibit enhanced spatial memory in Morris water maze and novel object recognition tasks, which is thought to be due to the enhanced LTP in CA2 (Lee et al., 2010). Interestingly, a mutation in the RGS14 NES (RGS14 L504R) that sequesters RGS14 to the nucleus prevents its association

with $G\alpha_{i1/3}$ at the plasma membrane. However, RGS14 L504R mice have normal spatial memory, suggesting RGS14 in the nucleus may be sufficient for its effects on learning and memory and independent of its ability to suppress LTP at the plasma membrane (Squires et al., 2021).

Contrary to LTP, CA2 pyramidal cells can express LTD at CA3>CA2 synapses, including LTD derived from GABAergic, inhibitory neurons (iLTD) and mGluR-mediated LTD (Piskorowski and Chevaleyre, 2013; Samadi et al., 2023). Recently, it was demonstrated that RGS14 KO mice lack mGluR-dependent LTD relative to WT, which robustly express this form of LTD. This effect was dependent on protein synthesis, as inhibition of translation rescued LTD in RGS14 KO mice, but not CaMKII signaling. Interestingly, RGS14 KO mice had an impairment in social memory, where KO mice spent similar amounts of time investigating a novel mouse compared to a familiar mouse. However, RGS14 KO mice had no impairment in sociability, suggesting RGS14 is important for recognition of a novel mouse (Samadi et al., 2023). This finding in particular is exciting as it has been repeatedly demonstrated that proper CA2 functioning is critical for social memory, and mouse models that result in social impairment display altered CA2 function. Whether RGS14's effect on social memory is dependent on its modulation of LTP, LTD, or another property of CA2 remains to be seen. A last finding of hippocampal RGS14 comes from the viral expression of an RGS14 transcript that omits the RGS domain and part of the linker region between RGS and R1/R2 but includes the C-terminal PDZ motif (RGS14₄₁₄). Overexpression of this RGS14₄₁₄ in CA1 PCs has been reported to enhance spatial memory, neurite formation, and brain-derived neurotrophic factor (BDNF) production associated with increased plasticity in CA1 PCs (Masmudi-Martin et al., 2019). Although this data conflicts with reports that RGS14 suppresses memory and LTP and promotes LTD in CA2, it demonstrates RGS14's complexity in the cell, where each domain and motif of the protein can greatly influence its effect in cell signaling and behavior.

Aside from hippocampal plasticity, RGS14 KO mice were shown to have enhanced anxiety-like behavior in a novel environment. RGS14 KO mice locomote less than their WT littermates overall, an effect that is driven by increased avoidance of the center of the environment relative to the periphery. In the same report, RGS14 KO mice were shown to be more sensitive to the behavioral effects of cocaine, which causes RGS14 KO mice to locomote preferentially in the periphery of the environment relative to the center, an effect that is potentiated when the environment is novel. This effect correlated with increased neuronal activation in area CA1, CA2, and the central amygdala of RGS14 KO mice, which suggests RGS14 in these areas regulates postsynaptic receptor activation of dopaminergic and glutamatergic stimuli caused by novelty-induced stress and cocaine to dampen locomotor behavior (Foster et al., 2021). Likewise, RGS14 KO in females enhances retention of cued fear, which may be attributable to RGS14's actions in the central amygdala, an area fundamental to cued fear response (Alexander et al., 2019). Therefore, RGS14 within or outside the hippocampus may be involved with drug response and response to stressful stimuli like novel environments.

1.7. Excitability, epilepsy, and temporal lobe epilepsy (TLE)

The vast majority of neurons in the brain are either excitatory, glutamatergic neurons or inhibitory, GABAergic neurons (also known as interneurons). Balance between excitation and inhibition (E/I balance) is fundamental for proper behavioral response to stimuli, and dysregulation of E/I balance is thought to underly a variety of neuropathological states. In the hippocampus, the principal neurons (pyramidal cells of the CA regions and granule cells of the DG) are glutamatergic, and as mentioned in the previous section, are essential for proper memory formation and spatial learning. Glutamate transmission activates ionotropic NMDAR, AMPARs, and kainate receptors (KARs) to cause depotentiation of the postsynaptic neuron as well as metabotropic mGluRs that can modulate postsynaptic excitability (Niswender and Conn, 2010; Traynelis et al., 2010). Their activity is regulated by a smaller number but highly interconnected

network of inhibitory neurons, which release GABA to activate ionotropic GABA_A receptors that oppose glutamate-induced depolarization or metabotropic GABA_B receptors that can modulate presynaptic glutamate release or postsynaptic responses to tune inhibition (Gassmann and Bettler, 2012; Sigel and Steinmann, 2012).

Epilepsy is characterized by the development of spontaneous seizures that originate from a focal point in the brain (focal seizures) or generalized with multiple, undefined foci spread across the brain (generalized seizures). Epilepsy can develop from neurotrauma (e.g. traumatic brain injury or long, uncontrolled seizure activity known as status epilepticus), genetic mutations, infectious diseases, or immune disorders. Epileptogenesis is the period prior to the occurrence of spontaneous seizures, where numerous pathological alterations in the brain lower the threshold for seizure activity and increasing the propensity for seizure occurrence. Behavioral seizures can manifest as a loss of consciousness, confusion, convulsions involving dystonic posturing, involuntary muscle twitching (myoclonic seizure), muscle spasms (tonic seizure), muscle jerking (clonic seizure), or hallucinations of sensory stimuli among other clinical presentations. The main seizure period is known as the ictal period, and the time between seizure events is known as the interictal period, which consist of electrical hallmarks that can be detected using electroencephalogram (EEG) and aid in the diagnosis of epileptic disorders (Devinsky et al., 2018)

The most basic theory of seizure generation is an imbalance of E/I in brain regions of seizures occurrence, where principal excitatory neurons become more excitable and aberrant neuronal activity is uncontrolled through typical inhibitory mechanisms. However, enhanced inhibitory tone is also thought to play an important role in seizure generation in some cases. Period of intense seizure activity during ictal periods consists of abnormal firing of excitatory neurons, which fire in a rapidly hyperexcitable and/or synchronous manner and can spread to connected neurons in the network. Interictal epileptiform discharges may present as interictal epileptiform spikes (IESs), which originate from hypersynchronous activity from excitatory neurons, and/or low

voltage, fast spiking high-frequency oscillations (HFOs), which are dependent on hypersynchronous inhibitory network activity and is the type of activity thought to propagate to other structures in the case of focal seizures. Importantly, glial factors and changes in the extracellular environments are thought to sustain this type of interictal activity and possibly precipitate this to ictal activity/behavioral seizures. Anti-seizure drugs (ASDs) are the primary pharmacological treatment for epilepsy, which prevent or reduce seizure frequency in those who respond to treatment. ASDs mostly act by inhibiting voltage-gated sodium channels (e.g. carbamazepine and phenytoin) or VGCCs (ethosuximide) to reduce action potential firing of glutamatergic neurons or enhancing inhibition of GABA transmission (e.g. benzodiazepines like diazepam). Seizures can also be mitigated with neurostimulation (e.g. vagal nerve stimulation), dietary changes (e.g. ketogenic diet), or surgical resection of seizurogenic tissue, especially for those who do not respond to ASDs. However, all current treatments target seizure activity to reduce seizure frequency and severity rather than the mechanisms that promote the development of spontaneous recurrent seizures (i.e. epileptogenesis) (Devinsky et al., 2018; Engel, 2001; Tatum, 2012).

Temporal lobe epilepsy (TLE) refers to spontaneous seizures that originate from limbic and cortical areas of the temporal lobe (e.g. hippocampus, amygdala, EC, and associated neocortical areas). TLE is the most common type of focal epilepsy and the hardest to treat, where approximately 30% of TLE patients are unable to control seizures with ASDs (Tellez-Zenteno and Hernandez-Ronquillo, 2012). TLE seizures are often preceded by auras with sensory hallucinations and gastrointestinal symptoms, and loss of consciousness, amnesia, absent gazing, and automatisms are common with TLE seizures. Clinical symptoms during a seizure can reflect the foci of seizure generation and the temporal spread of epileptiform activity to regions associated with those symptoms including the hippocampus, parahippocampal structures like the EC, or frontotemporal cortices. Motor symptoms are less common in TLE but are reflective of

seizure propagation to the motor cortex. EEG signatures can be monitored with dural, subdural, or depth electrodes in conjunction with clinical presentation prior to, during, and after seizure activity, which is important for defining the source of seizure generation (Tatum, 2012). Aside from seizure activity, TLE patients may also have cognitive, learning and memory, and language impairments, comorbidities like depression or anxiety, or other reductions in quality of life caused by disease progression or side effects of treatment (Devinsky et al., 2018; Novak et al., 2022). Understanding the epileptogenic process by investigating fundamental mechanisms that contribute clinical symptoms and pathology is an active area of epilepsy research.

1.8. Animal models of TLE and hippocampal pathology

TLE is commonly modeled in rodents (rats and mice) with the use of genetic models, electrical stimulation models, and induction of status epilepticus (SE) using chemoconvulsants (Kandratavicius et al., 2014). To model TLE in animals, there must be a precipitating injury, a latent period following injury of which epileptogenesis occurs, the development of spontaneous recurrent seizures, and typical pathology associated with TLE (discussed in more detail below). Genetic models utilize loss- or gain-of-function genetic mutations, gene knockout or knockin, or the development of rodent strains that are seizure susceptible (e.g. audiogenic seizure susceptible strains of rats and mice) to assess epileptogenesis and associated pathology. Electrical shock of the entire brain, selective stimulation of seizurogenic areas (e.g. hippocampus), or progressive enhancement of epileptic seizures via electrical kindling of known seizurogenic circuits (e.g. amygdala) can reliably induce spontaneous seizures and is widely used to investigate underlying mechanisms of epileptogenesis. Chemoconvulsants like the glutamate analog and receptor agonist kainic acid (KA), muscarinic receptor agonist pilocarpine (PILo), and GABA_A receptor antagonist pentylenetetrazol (PTZ) are commonly administered systemically or intracerebrally to induce SE (a precipitating injury), which promotes typical TLE pathology and the formation of spontaneous seizures (Kandratavicius et al., 2014). Additionally, SE can be used as

a model of acute seizure-induced injury regardless of epileptogenesis, as SE causes pronounced neuronal death and related pathology (Wang et al., 2005). KA is especially useful to target the hippocampus, as there is a high abundance of KARs in the hippocampus, activation of KARs by KA causes hippocampal-generated seizure activity, and KA administration causes seizure-induced damage and pathology in the hippocampus similar to what is seen in TLE patients (Ben-Ari and Cossart, 2000).

In many cases, the hippocampus is the major focus of TLE seizures and is highly susceptible to injury primarily due to the highly excitable nature of the hippocampus and its excitatory synaptic connections to cortical and amygdala regions (Engel, 2001). Several pathological hallmarks are common in the hippocampi of TLE patients and animal models of TLE, particularly in the KA model of SE induction (Rusina et al., 2021) (summarized in Figure 7). Pathology is attributed to the effects of seizure activity as well as fundamental mechanisms underlying epileptogenesis (Devinsky et al., 2018). Hippocampal sclerosis (i.e. atrophy and neuronal loss in hippocampal tissue) is the most common pathology observed in TLE patients, especially those that are resistant to treatment (Blumcke et al., 2013). Neuronal loss in TLE (typically in hippocampal areas CA1, CA3, and the hilar of the DG along with other hippocampal-associated regions) is thought to occur from seizure-induced excitotoxicity, where neuronal hyperactivity during a seizure triggers a series of intracellular events leading to cell death (Niquet, 2012). Surgical resection of atrophied tissue can be effective for stopping seizures in those with treatment-resistant TLE, although long-term follow-ups demonstrate seizure relapse in some patients, which suggests other mechanisms of seizure generation (Blumcke et al., 2013).

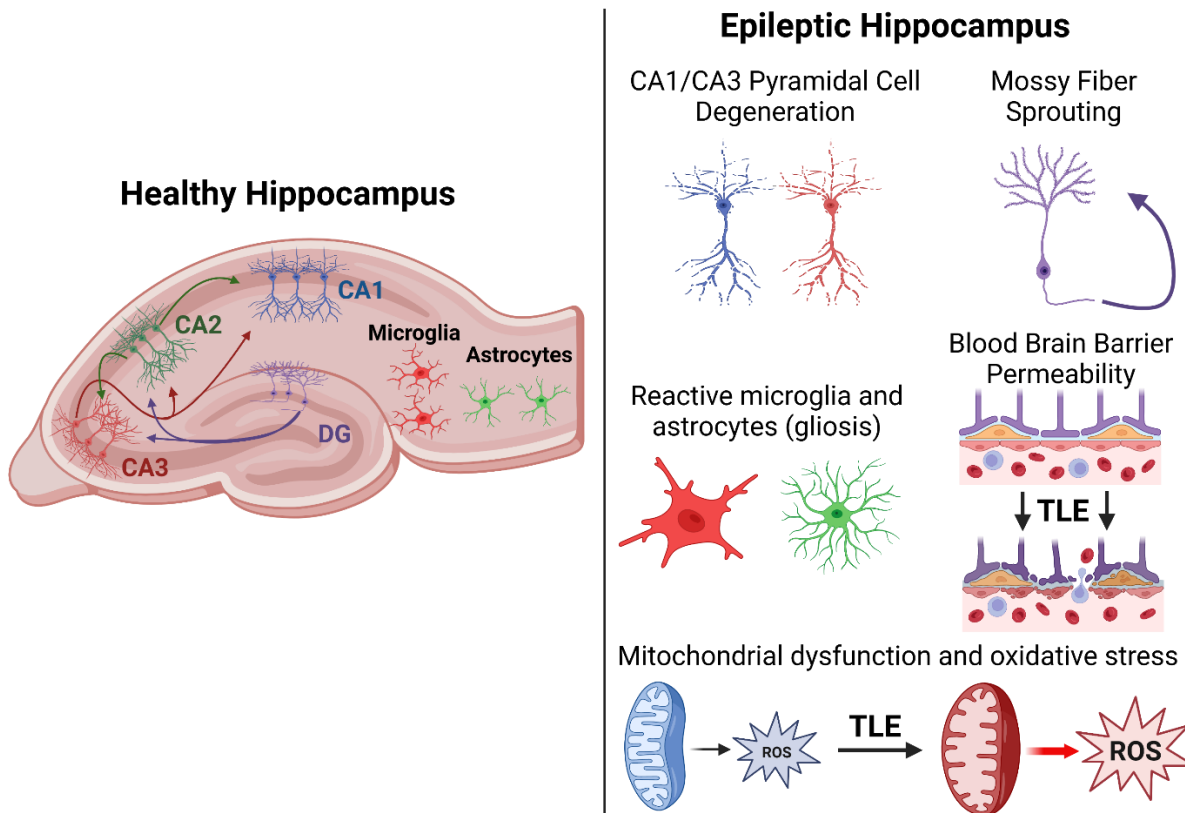


Figure 7. Common pathological hallmarks of TLE. In a healthy hippocampus, circuitry is unaltered, neurons are healthy and functioning normally, glial cells (microglia and astrocytes) are resting, the blood brain barrier is intact, and mitochondria produce physiological levels of reactive oxygen species (ROS) for energy production in neurons. In the epileptic hippocampus of TLE patients and rodents: 1) the pyramidal cells of area CA1 and CA3 are susceptible to degeneration, which can lead to hippocampal sclerosis and cognitive impairment; 2) axonal mossy fibers from granule cells can form recurrent, excitatory connections with themselves to sustain seizure activity; 3) microglia and astrocytes become reactive in response to hyperexcitability and neuronal damage, which can further exacerbate pathology; 4) the blood brain barrier becomes leaky and dysfunctional, which permits the entry of large molecules and cell into the brain and compromising barrier integrity; 5) the high energy demand needed to sustain seizure activity can lead mitochondrial dysfunction, which can cause excessive levels of ROS and subsequent oxidative stress. Created in BioRender.

Mossy fiber sprouting is another common pathological hallmark and is often associated with hippocampal sclerosis. Mossy fibers are the axonal projections from granule cells of the DG, which normally project to excitatory mossy cells in the hilar region of the DG, inhibitory interneurons of the DG, and excitatory pyramidal cells of CA3. During mossy fiber sprouting in TLE, granule cells of the DG undergo plasticity that promotes axon formation and synaptogenesis onto granule cells, which forms recurrent, excitatory connections, excitatory PCs, and to a lesser extent GABAergic interneurons. Mossy fiber sprouting is associated with hippocampal hyperexcitability, although it remains unclear if this is a driver of seizure activity or epileptogenesis (Buckmaster, 2012).

Seizures and TLE cause activation of astrocytes and microglia in what is known as reactive gliosis, particularly in the hippocampus. Reactive gliosis is common at sites of epileptiform activity and neurodegeneration (forming a glial scar) and is thought to play a causal role in epileptogenesis. Microglia are the first glial cell activated by seizure activity, where neuronal or astrocytic release of neurotransmitters or other molecules (e.g., ATP) mediates their reactivity. While surveying microglia have characteristic small soma and long processes, activated microglia undergo a pronounced morphological change displaying larger soma and shorter processes. Morphological change can be visualized using immunohistochemistry (IHC) against ionized calcium binding adaptor molecule 1 (IBA1). During and following seizure activity, activated microglia can engulf hyperactive dendrites and clear debris from damaged cells. In turn, microglia express and release a number of inflammatory mediators that can activate astrocytes and modulate neuronal excitability. In TLE, microglia can become persistently reactive, which have been shown to promote neurodegeneration and epileptogenesis in the hippocampus (Devinsky et al., 2018; Eyo et al., 2017).

Astrocytes play an important role in TLE as they are important for maintaining ion gradients, glutamate/GABA concentration, and adenosine/ATP at synapses through calcium-

dependent vesicular release and uptake/efflux via channels (Clastadonte, 2012). Astrocytes can be activated by a variety of inflammatory cytokines, neurotransmitters, and other molecules similar to microglia. Reactive astrocytes in TLE also undergo morphological change, where some become hypertrophic and their processes may abnormally overlap with other astrocytes depending on the extent of astrocytic reactivity. Glial fibrillary acidic protein (GFAP) is expressed by most reactive astrocytes and is visualized with IHC to determine the extent of astrocyte activation (Sofroniew and Vinters, 2010). Reactive astrocytes can facilitate neuronal hyperexcitability and epileptogenesis through changes in glutamine synthetase and glutamate transporter expression (altering glutamate and GABA concentration at synapses), adenosine kinase expression (altering inhibitory adenosine concentration at synapses, which is anticonvulsant), and potassium channel and chloride transporter expression that affects extracellular ionic gradients and therefore neuronal excitability. Reactive astrocytes also release inflammatory cytokines and gliotransmitters to facilitate microglia activation and synchronize hyperexcitable neurons to promote seizure development (Devinsky et al., 2018).

The blood brain barrier (BBB) is the principal protective barrier of the brain, consisting of endothelial cells that form tight junctions, perivascular pericytes, and the end feet of astrocytes. The BBB prevents all but the smallest and least polar molecules (e.g. gaseous O₂ and CO₂ and small, lipophilic drugs) to access the brain. The BBB regulates the flow of nutrients (e.g. glucose and lipids), ions (e.g. potassium and calcium), and other biological molecules into the brain and prevents infections and pathological agents from entering (Abbott et al., 2006). In TLE, the BBB often increases in permeability due to a brain insult or inflammation, allowing infiltration of vasculature proteins and cells that are not usually found in the brain including serum albumin and peripheral immune cells. BBB dysfunction is common in TLE patients, associated with seizure frequency, and associated with reactive astrocytes, which can further precipitate BBB dysfunction (Friedman, 2012).

Oxidative stress and mitochondrial dysfunction have also been investigated as contributing factors to epileptogenesis and other hallmark pathologies (e.g. neuronal cell death) caused by seizure (Shin et al., 2011). In neurons, mitochondria produce ATP via oxidative phosphorylation in the electron transport chain (ETC), maintain the electrical potential of the cell, metabolize amino acids for neurotransmitter synthesis, regulate intracellular calcium levels, and control cell death. During mitochondrial respiration, reactive oxygen species (ROS) including superoxide (O_2^-) and hydrogen peroxide (H_2O_2) are formed and released from the ETC, and ROS is important for many physiological processes as they regulate the function of mitochondrial enzymes, membrane transporters, and ion channels. Under physiological and pathological stimuli, large increases of intracellular calcium flux are buffered in part by mitochondria, and calcium buffering into the mitochondria is associated with enhanced ROS production and alterations in mitochondrial membrane potential (Kann and Kovacs, 2007). In TLE models, excessive ROS can contribute to excitotoxic neuronal cell death and damage proteins, lipids, and DNA through oxidation. Additionally, seizure activity enhances nitric oxide (NO) production, which can modify ion channels and enzymatic proteins to affect their function or react with O_2^- to produce the highly reactive peroxynitrite. Peroxynitrite reacts strongly with proteins, membrane lipids, and DNA and can impair neuronal metabolism and function when produced in excess. To protect against ROS-induced damage during seizure activity, antioxidant enzymes like superoxide dismutase (SOD), which detoxifies O_2^- to H_2O_2 , and catalase, which detoxifies H_2O_2 to water, are upregulated following seizure activity (Waldbaum and Patel, 2010). Indeed, mitochondrial dysfunction may contribute to seizure generation and epileptogenesis as evidenced by mice with partial or complete loss of the mitochondrial manganese SOD (MnSOD or SOD2), which have spontaneous seizures and are more sensitive to the behavioral and pathological effects of KA-induced seizure activity (Liang and Patel, 2004; Liang et al., 2012). However, NADPH oxidase (NOX) and xanthine oxidase have emerged as primary sources of ROS generation and ROS-induced cell death and lipid oxidation after NMDAR activation, suggesting alternative, non-

mitochondrial ROS sources as mechanisms of oxidative stress during seizure activity (Brennan et al., 2009; Kovac et al., 2014).

1.9. Area CA2 function, emerging role in TLE, and implications for RGS14

Area CA2 is positioned between CA1 and CA3 but has been largely understudied relative to its neighbors. Although original characterization of the PCs in CA2 noted distinct morphological and connectivity differences compared to PCs in CA3 and CA1, CA2 was thought to be a transition zone between the two regions. Recent work has provided renewed insight into CA2, which is now hypothesized to regulate information flow through the hippocampus by acting as a hub for alternative circuits to the classical trisynaptic pathway (EC>DG>CA3>CA1) (Lehr et al., 2021) (Figure 6). CA2 receives input from glutamatergic Schaffer collateral axons of CA3 PCs, layer II of the medial and lateral EC, mossy fibers of DG granule cells, neuropeptidergic neurons in paraventricular nucleus and supramammillary nucleus of the hypothalamus, cholinergic neurons of the medial septum and diagonal band of Broca, serotonergic neurons of the median Raphe nucleus, and dopaminergic neurons of the locus coeruleus and ventral tegmental area. CA2's major output is onto the basal dendrites of CA1 stratum oriens, where deep layer CA1 PCs receive input, in contrast to CA3 PCs that preferentially target the proximal dendrites of superficial CA1 PCs located in the stratum radiatum. Moreover, CA2 PCs form recurrent connections with itself, inhibitory interneurons in CA2, and recurrent loops with area CA3 PCs, layer II of the medial EC, the lateral septum, and the supramammillary nucleus. Intriguingly, CA2 is unique relative to CA3 and the DG as it projects bilaterally (connecting hippocampi across hemispheres) and across the transverse axis of the hippocampus, allowing for direct information flow from the memory-oriented dorsal hippocampus to the emotion-oriented ventral hippocampus (Middleton and McHugh, 2020). Overall, the vast and recursive nature of CA2 connections allow the small, mostly overlooked region to exert fine control of excitatory network activity within and outside the hippocampus.

Demonstrating their exceptional and unusual properties, CA2 PCs are wrapped in perineuronal nets (PNNs) similar to parvalbumin interneurons (Carstens et al., 2016), surrounded by a variety of inhibitory interneurons that provide dominant inhibition over the area (Botcher et al., 2014; Piskorowski and Chevaleyre, 2013), have high intrinsic calcium buffering capacity (Simons et al., 2009), contain an abundance of receptors that allow it to integrate a host of neuromodulatory inputs (Lehr et al., 2021), and display a unique molecular profile with a high expression of mRNAs encoding unique intracellular regulators (e.g. RGS14) and mitochondrial/metabolic enzymes (Dudek et al., 2016; Farris et al., 2019). All of these properties are important for regulating CA2 PC function and plasticity, as manipulating them has been shown to affect plasticity in CA2 (Lehr et al., 2021). Chemogenetic and optogenetic manipulation of CA2 activity has uncovered its importance in a number of hippocampal functions including encoding and remapping of place fields (Alexander et al., 2016; Kay et al., 2016), the generation of hippocampal sharp wave ripples (SPW-Rs) important for memory encoding and replay (Oliva et al., 2016), and modulation of hippocampal oscillations associated with information flow into and out of the hippocampus (Alexander et al., 2018). Moreso, CA2 has been shown to be necessary for a growing number of behaviors including social memory (Hitti and Siegelbaum, 2014), aggressive behavior (Leroy et al., 2018), and novelty detection of social stimuli (Donegan et al., 2020), and its role in social behavior has spurred investigation into its function in disorders that affect social function like autism spectrum disorders and schizophrenia (Donegan et al., 2020; Modi et al., 2019).

One of the most fascinating aspects of CA2 PCs is its resistance to excitotoxic degeneration after a number of excitotoxic insults, which is stark contrast to the PCs of CA3 and CA1 that are more susceptible and degenerate following hippocampal injury (Hatanpaa et al., 2014; Thom, 2014). This is a common phenomenon in TLE patients with hippocampal sclerosis (Blumcke et al., 2013) and has been repeatedly demonstrated in a number of animal models of

TLE (Curia et al., 2008; Levesque and Avoli, 2013). While this phenomenon has been observed for several decades, the mechanisms by which CA2 is impervious to excitotoxic injury is currently unknown but is thought to be related to the number of aforementioned mechanisms that also contribute to its resistance to plasticity. Superior calcium extrusion in CA2 PCs may prevent the triggering of cell death by excessive calcium influx, PNNs that enshroud the neurons may act as a protective barrier, and the dominant inhibition provided by interneurons may prevent excessive excitation that would trigger excitotoxicity (Dudek et al., 2016). There is also rationale for neuroprotective molecules that are highly expressed in CA2 like the adenosine 1 receptor (A1R), which is neuroprotective and antiseizure (Cunha, 2005), and striatal enriched protein tyrosine phosphatase, which has been demonstrated to protect neurons against excitotoxicity (Goebel-Goody et al., 2012). Although many of these mechanisms likely afford CA2's resistance to damage, no studies to date have evaluated which are important to the phenotype.

Instead, studies have investigated the ability of CA2 to regulate hippocampal excitability, seizure generation, and promote epileptiform activity and TLE pathology. Several reports have demonstrated CA2's capacity for generating epileptiform activity. In resected tissue from TLE patients, CA2 displayed interictal spikes associated with hypersynchronous firing of excitatory PCs (Wittner et al., 2009). In vivo recordings during SE and spontaneous seizures following SE in TLE models also show epileptiform activity in CA2, namely burst firing during SE and hypersynchronous spiking during spontaneous seizure activity (Haussler et al., 2016). Even prior to the development of spontaneous seizures, CA2 exerts control over hippocampal excitability by influencing the inhibitory drive in the recurrent CA3 circuit. When chronically (but not acutely) inhibited, CA2 loses inhibitory control over the circuit, resulting in hippocampal hyperexcitability, the appearance of epileptiform activity in CA3 and CA1, and sensitivity to KA-induced seizures (Boehringer et al., 2017). Likewise, acute inhibition had no effect on SE induction when PILO was used (Whitebirch et al., 2022). In animal models of TLE, CA2 PCs, like the granule cells of the

DG, disperse into CA3 and CA1 following SE (Hausssler et al., 2016; Tulke et al., 2019). Intriguingly, mossy fibers have been shown to sprout and synapse onto cell bodies of CA2 PCs in animal models of TLE and resected tissue from TLE patients (Freiman et al., 2021; Hausssler et al., 2016; Tulke et al., 2019), suggesting that CA2 may receive enhanced excitatory input from granule cells to propagate epileptiform activity. Promotion of mossy fiber plasticity in CA2 is associated with increases in BDNF expression and epileptiform activity in the area in a mouse model of TLE (Tulke et al., 2019). Given neighboring CA3 and CA1 often degenerate during TLE, DG>CA2 connections may present a pathological, excitatory network that persists to route information through the hippocampal network while also promoting seizure activity (Kilias et al., 2022). Lastly, it was recently shown that after the development of spontaneous seizures, CA2 exhibited increased intrinsic excitability and reduced synaptic inhibition, leading to increased excitatory output onto CA1 PCs and action potential firing in CA1. Moreso, inhibition of CA2 after the development of spontaneous seizures reduced convulsive and nonconvulsive seizure frequency without affecting seizure duration or severity (Whitebirch et al., 2022). Given the powerful and expansive excitatory connections into CA2 and away from the region, it is reasonable that CA2 may be central to seizure propagation as well as generation within the hippocampus. However, what cell intrinsic factors that are responsible for CA2's contribution to seizure generation and TLE pathogenesis remain unknown.

In CA2 physiology, RGS14 reduces intrinsic CA2 PC excitability and suppresses synaptic potentiation and structural plasticity at CA3-CA2 synapses (Evans et al., 2018b; Lee et al., 2010). This is in stark contrast to CA3-CA1 synapses that robustly express plasticity. RGS14 suppresses glutamate-induced calcium transients and modulates G protein, ERK, and calcium-dependent signaling in CA2 PCs to limit plasticity at CA3-CA2 synapses (Evans et al., 2018b; Lee et al., 2010). Increased excitatory input from CA3 and enhanced excitability in CA2 may therefore result in a hyperactive CA2 in RGS14 KO mice, similar to what is observed in epileptic CA2 (Whitebirch

et al., 2022). Interestingly, CA2 in both RGS14 KO mice and TLE mice exhibit significantly enhanced input resistance and current-evoked action potential firing (Lee et al., 2010; Whitebirch et al., 2022), which may contribute to a hyperexcitable CA2 and affect seizure generation. Therefore, RGS14 could be an intrinsic component of CA2 PCs that is important for its ability to modulate seizure activity in the hippocampus, where RGS14 KO may enhance the generation or propagation of seizure activity by affecting intrinsic signaling and physiological properties of CA2 PCs, although this hypothesis has yet to be tested.

Another recent and intriguing finding regarding RGS14 KO mice is the enhanced metabolic capacity of these mice due to novel effects by RGS14 on mitochondrial bioenergetics and function in brown adipocytes. Enhancement of metabolism in this tissue is associated with enhanced exercise capacity and longevity, suggesting RGS14 has a major effect on physiology via its effects on mitochondrial metabolism (Vatner et al., 2023; Vatner et al., 2018). Coincidentally, CA2 PCs also have an enhanced metabolic profile and are enriched with mitochondrial and metabolic mRNA transcripts relative to CA1 and CA3 (Farris et al., 2019), implicating a common role for RGS14 in mitochondrial metabolism in both cell types. Although RGS14 is highly expressed in area CA2, its effects on mitochondrial function and metabolism in CA2 under physiological or pathological conditions has not been explored despite the high energetic demand on mitochondria in both neurons and brown adipocytes (Attwell and Laughlin, 2001; Magistretti and Allaman, 2015; Shinde et al., 2021).

Lastly, in neurons of the CNS, RGS14 has been exclusively studied during physiological context (i.e., learning and memory), while its contribution to pathology remains unknown. In the periphery, however, RGS14 has been shown to be protective against injury, where its expression is modulated by cardiac injury in cardiomyocytes and ischemic-reperfusion injury in hepatocytes. When RGS14 is ablated in these cells, cell death and inflammation are worsened, while RGS14 overexpression attenuates this pathology, providing rationale for a protective role for RGS14 (Li

et al., 2016; Zhang et al., 2022). Despite these recent studies, the protective capacity of RGS14 and its levels of expression following brain insult have not been evaluated. In fact, RGS14 is highly and specifically expressed in CA2 PCs, which are highly resistant to injury and degeneration caused by injury (Hatanpaa et al., 2014). Therefore, there exists a strong possibility that RGS14 is an essential protective component of CA2 PCs and may influence other pathology (e.g., oxidative stress, glial activation) following insult (i.e., SE). While intriguing and ripe for study, this hypothesis remains unevaluated.

1.10. Research focus of the dissertation project

Because RGS14 is important for CA2 function in the brain and is protective against injury in the periphery, CA2 modulates seizure activity, and PCs of CA2 are resistant to injury, it stands to reason that RGS14 may be protective in CA2 and/or modulate the activity of CA2 upon hippocampal insult and thereby influencing seizure activity. Therefore, we proposed that RGS14 in CA2 PCs may be protective and/or modulate CA2 activity during seizure by influencing CA2 excitability and/or intracellular signaling, which may have effects on seizure sensitivity and typical TLE pathology caused by SE. To test this hypothesis, we used kainic acid induction of status epilepticus (KA-SE) to induce seizure activity, excitotoxic injury, and hippocampal pathology in WT and RGS14 KO mice to see if loss of RGS14 sensitized mice to the effects of KA-SE (Figure 8). Additionally, we sought to determine how RGS14 may be affording this protection. Here, we report that RGS14 protein is upregulated in hippocampus following KA-SE induction, and that loss of RGS14 accelerated the onset of behavioral seizures and mortality during seizure. Using proteomic approaches, we determined changes in the hippocampal proteome in RGS14 KO animals, and identified altered metabolic/mitochondrial protein expression in RGS14 KO mice after seizure activity.

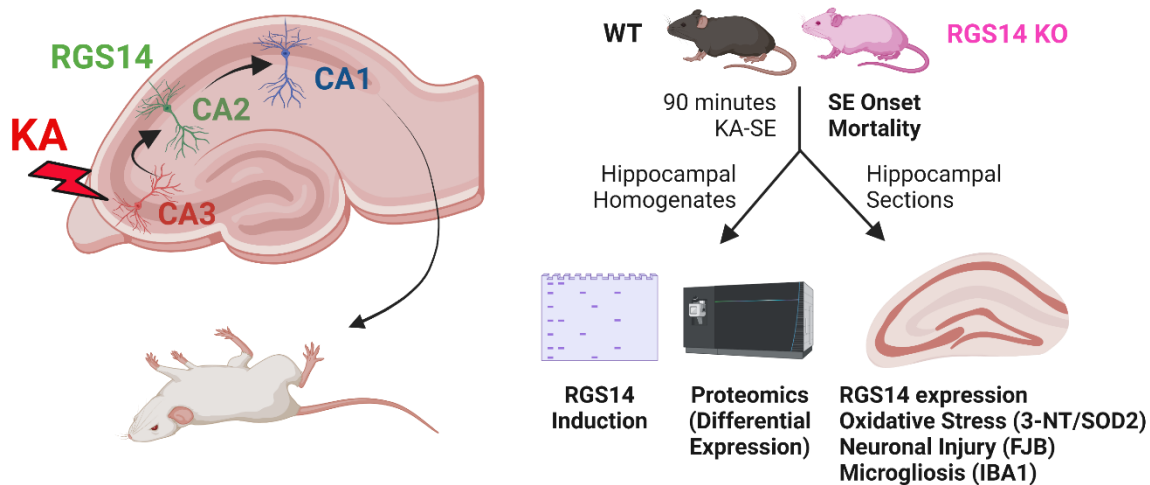


Figure 8. The kainic acid model of status epilepticus induction (KA-SE) used to evaluate the effects of RGS14 on hippocampal seizure activity and pathology. Kainic acid (KA) was administered (intraperitoneal) to WT and RGS14 KO mice to initiate seizure activity in the hippocampus. Mice were monitored for SE induction (>Stage 3 convulsive seizures) and mortality for 90 minutes following KA administration, and seizures were terminated following the 90 minute period. Of the surviving mice, hippocampi were dissected to evaluate RGS14 protein expression in WT mice (1, 3, or 7 days after KA-SE) and differences in the hippocampal proteome (proteomics) between WT and RGS14 KO mice, and fixed hippocampal sections were obtained to determine spatial RGS14 expression patterns within the hippocampus in WT mice and pathological hallmarks (oxidative stress, neuronal injury, and microgliosis) one day following KA-SE in WT and RGS14 KO mice. Created in BioRender.

Further investigation identified RGS14 localization to mitochondria in area CA2, and we provide evidence that RGS14 suppresses mitochondrial oxygen consumption *in vitro*. Consistent with this function, we show that mice lacking RGS14 exhibit enhanced hippocampal oxidative stress and altered seizure-induced glia response but without affecting CA2's resistance to injury *in vivo* (Harbin et al., 2023). Together, the findings of this dissertation suggest that RGS14 serves a previously unappreciated role in limiting behavioral seizure activity and hippocampal seizure pathology.

2. Materials and Methods

2.1. Animal Care

Male and female C57BL/6J wild-type (WT) and RGS14 KO mice ages 3-7 months were used in this study. Animals in all experiments were housed under a 12 h/12 h light/dark cycle with access to food and water ad libitum. All experimental procedures conformed to US NIH guidelines and were approved by the animal care and use committees (IACUC) of Emory University.

2.2. Kainic acid-induction of status epilepticus and monitoring of status epilepticus

Seizure-induction protocols using KA were followed as described (Rojas et al., 2014). WT and RGS14 KO mice were individually housed in clean mouse cages without access to food and water 30 minutes prior to KA injection. KA (3 mg/mL) was prepared on the day of experimentation by dissolving KA (Tocris, 0222) in a 0.9% bacteriostatic saline solution. Mice were injected intraperitoneally (i.p.) with a single, 30 mg/kg dose of KA or 0.3 mL of saline (control). Immediately after injection, mice were monitored and scored for seizure behavior using a modified Racine scale (Racine, 1972; Rojas et al., 2014) (Table 1). Each mouse was given a behavioral seizure score from a scale of 0-6 every 5 minutes for 90 minutes. Mice were scored based off the most severe seizure behavior that was observed during the 5-minute interval. When a mouse reached mortality, they were given a score of 7, which was not included in the mean behavioral seizure score and no further scores were given for those mice. Ninety minutes after injection, all mice were injected intraperitoneally with 10 mg/kg diazepam to terminate seizure activity. After seizure termination, mice remained singly housed, and food (dry and moistened) and water were returned to the cage, and monitored for well-being.

Table 1. Modified Racine scale to evaluate behavioral seizure progression in mice

Behavioral Score	Motor Behavior
0 Normal Behavior	walking, exploring, sniffing, grooming
1 Freeze Behavior	immobile, staring, rigid posture, hunched
2 Automatisms	head bobbing, face washing, whisker twitching, chewing, stargazing
3 Early Seizure Behavior	Myoclonic jerk, partial or whole body clonus
4 Moderate Seizure Behavior	rearing with bilateral forelimb clonus
5 Advanced Seizure Behavior	rearing and falling, loss of posture
6 Intense Seizure Behavior	tonic clonic seizure with running/bouncing
7 Death	

2.3. Hippocampal tissue collection

To collect hippocampal sections for histology, male and female mice were anesthetized with sodium pentobarbital (Fatal Plus, 380 mg/kg, i.p.) and euthanized by transcardial perfusion with 4% paraformaldehyde (PFA) in PBS one day after KA or saline injection or seven days after KA injection. After decapitation, mouse brains were dissected and post-fixed in 4% PFA at 4°C for 24 hours. After post-fix, brains were transferred to a 30% sucrose in PBS solution for 72 hours. Mouse brains were embedded in optimal cutting temperature (OCT) medium (Fisher Healthcare, 23730571), and coronal sections of hippocampus were collected at a thickness of 40 µm on a cryostat. Hippocampal sections were stored in 0.02% sodium azide in PBS at 4°C until they were evaluated for neuropathology. For proteomics and Western Immunoblot, mice were anesthetized with isoflurane followed by rapid decapitation and dissection of whole hippocampi. Whole hippocampi were snap frozen in liquid nitrogen and stored at -80°C until homogenization.

2.4. Western Immunoblotting

Frozen hippocampi were thawed on ice and homogenized in a modified RIPA buffer [150 mM NaCl, 50 mM Tris, 1 mM EDTA, 2 mM DTT, 5 mM MgCl₂, 1X protease inhibitor (Roche, A32955) 1X Halt phosphatase inhibitor (ThermoFisher, 78428)]. Cells were lysed in modified RIPA buffer for 1 hour at 4°C, end-over-end. Lysates were cleared, and proteins were denatured by boiling in Laemmli buffer for 5 minutes (stored at -20°C until immunoblotting). Samples were resolved on 4-20% Mini-PROTEAN® TGX™ precast protein gels (BioRad, 4561094), and gels were UV-activated for 45 seconds for total protein illumination (BioRad Stain-Free Technology) (Gilda and Gomes, 2015). Samples were then transferred to nitrocellulose membranes, and total protein was detected by activating membranes with ultraviolet light. Membranes were incubated in blocking buffer (5% non-fat milk in TBS containing 0.1% Tween-20 and 0.02% sodium azide) for 1 hour at room temperature. Membranes were incubated with anti-RGS14 (Neuromab, 75-170; 1:500) diluted in blocking buffer at 4°C overnight. Membranes were washed thrice with TBS

containing 0.1% Tween-20 followed by incubation with goat anti-mouse IgG HRP-conjugate (Jackson ImmunoResearch, 115-035-003; 1:5000). Membranes were washed thrice with TBS containing 0.1% Tween-20, and enhanced chemiluminescence was used to develop the blots. Blots were imaged using a ChemiDoc MP Imager (BioRad). ImageLab (BioRad) software was used for densitometry analysis of RGS14 bands, and quantified band density was normalized to total protein content. Normalized RGS14 band densities are expressed relative to the mean of the saline group.

2.5. Immunohistochemistry

To determine protein expression levels in tissue by immunohistochemistry (IHC), free floating hippocampal sections from KA- and saline-treated WT and RGS14 KO mice were subjected to antigen retrieval by boiling sections in 10 mM citrate buffer for 3 minutes and blocked in 5% normal goat serum in 0.1% Triton-PBS (blocking solution) for 1 hour at room temperature. Sections were incubated overnight at 4°C with primary antibody specific for RGS14 (Neuromab, 75-170, 1:500, WT sections only), IBA1 (Wako, 019-19741, 1:1000), GFAP (Synaptic Systems, 173-004, 1:1000), 3-nitrotyrosine (Abcam, ab61392, 1:500), or SOD2 (Proteintech, 24127-1-AP, 1:1000) diluted in blocking solution. Sections were washed thrice with PBS prior to incubation with the appropriate fluorescent secondary. Goat anti-mouse Alexa Fluor Plus 488 (ThermoFisher, A32723, 1:500), goat anti-rabbit Alexa Fluor 546 (ThermoFisher, A-11010, 1:500), or NeuroTrace™ 660 Nissl (ThermoFisher, N21483, 1:500) were diluted in blocking solution, and sections were blocked from light and incubated in secondary antibody solution for 2 hours at room temperature. Sections were washed thrice with PBS and mounted onto SuperFrost Plus microscope slides (Thermo Fisher Scientific). Once dried, sections were coverslipped with DAPI Fluoromount G (Southern Biotech, 0100-20) and stored away from light at 4°C prior to imaging.

2.6. Fluorescent Imaging and quantification of immunofluorescence

Fluorescent micrographs were collected from dorsal hippocampal sections using a Leica DM6000B epifluorescent upright microscope at 5X, 10X, and 20X magnifications using the appropriate wavelength filters. Images magnified at 20X were processed, analyzed, and quantified using ImageJ software. For RGS14 and SOD2, standardized regions of interests were drawn around each layer [stratum radiatum (SR), stratum pyramidale (SP), stratum oriens (SO)] of each CA field (CA1, CA2, CA3) and the dentate gyrus (DG). For 3-nitrotyrosine and GFAP, a standardized ROI was drawn around each CA field incorporating the three layers (SR, SP, SO). Quantification for 3-nitrotyrosine and GFAP was performed this way because staining was consistent throughout all layers for each stain, while immunofluorescence of RGS14 and SOD2 expression was noticeably different depending on the layer of analysis. For quantification of raw immunofluorescence, background correction and intensity thresholding (Otsu method) were performed consistently across all images for each ROI prior to quantifying raw immunofluorescence.

2.7. Quantification of microglia cell counts and size

For the microglia marker ionized calcium binding adaptor molecule 1 (IBA1), a standardized region of interest was drawn for each CA subfield incorporating the SR, SP, and SO and the DG incorporating the hilus, granule cell layer, and molecular layer. Background subtraction, intensity thresholding (Otsu method), and size and shape criteria for microglia (25-1000 μm^2 , circularity 0.05-1) were applied consistently across all images for each ROI using ImageJ software. Cell counts and area of IBA1 positive cells were quantified for each image. Microglia density is expressed as the number of cells divided by the area of ROI, and average size is expressed as the mean area of IBA1 positive cells.

2.8. Tissue homogenization and digestion of proteomics

Each tissue sample was added to 250 μ L of urea lysis buffer (8 M urea, 10 mM Tris, 100 mM NaH_2PO_4 , pH 8.5, including 2.5 μ L (100x stock) HALT(-EDTA) protease and phosphatase inhibitor cocktail (Pierce)) in a 1.5 mL Rino tube (Next Advance) harboring stainless steel beads (0.9-2 mm in diameter). Samples were homogenized twice for 5-minute intervals in the cold room (4 °C). Protein homogenates were transferred to 1.5 mL Eppendorf tubes on ice and were sonicated (Sonic Dismembrator, Fisher Scientific) thrice for 5 sec each with 5 sec intervals of rest at 30% amplitude to disrupt nucleic acids and were subsequently centrifuged at 4° C. Protein concentration was determined by the bicinchoninic acid (BCA) method, and samples were frozen in aliquots at -80 °C. Protein homogenates (100 μ g) were treated with 1 mM DTT at room temperature for 30 min, followed by 5 mM iodoacetimide at room temperature for 30 min in the dark. Protein samples were digested with 1:25 (w/w) lysyl endopeptidase (Wako) at room temperature overnight. Next day, samples were diluted with 50 mM NH_4HCO_3 to a final concentration of less than 2 M urea and were further digested overnight with 1:25 (w/w) trypsin (Promega) at room temperature. The resulting peptides were desalted with HLB column (Waters) and were dried under vacuum.

2.9. Liquid chromatography coupled to tandem spectrometry (LC-MS/MS)

The data acquisition by LC-MS/MS was adapted from a published procedure (Seyfried et al., 2017). Derived peptides were resuspended in the loading buffer (0.1% trifluoroacetic acid, TFA) and were separated on a Water's Charged Surface Hybrid (CSH) column (150 μ m internal diameter (ID) x 15 cm; particle size: 1.7 μ m). The samples were run on an EVOSEP liquid chromatography system using the 15 samples per day preset gradient (88 min) and were monitored on a Q-Exactive Plus Hybrid Quadrupole-Orbitrap Mass Spectrometer (ThermoFisher Scientific). The mass spectrometer cycle was programmed to collect one full MS scan followed by 20 data dependent MS/MS scans. The MS scans (400-1600 m/z range, 3 x 10⁶ AGC target,

100 ms maximum ion time) were collected at a resolution of 70,000 at m/z 200 in profile mode. The HCD MS/MS spectra (1.6 m/z isolation width, 28% collision energy, 1 x 10⁵ AGC target, 100 ms maximum ion time) were acquired at a resolution of 17,500 at m/z 200. Dynamic exclusion was set to exclude previously sequenced precursor ions for 30 seconds. Precursor ions with +1, and +7, +8 or higher charge states were excluded from sequencing.

2.10. Label-free quantification (LFQ) using MaxQuant

Label-free quantification analysis was adapted from a published procedure (Seyfried et al., 2017). Spectra were searched using the search engine Andromeda, integrated into MaxQuant, against mouse database (86,470 target sequences). Methionine oxidation (+15.9949 Da), asparagine and glutamine deamidation (+0.9840 Da), and protein N-terminal acetylation (+42.0106 Da) were variable modifications (up to 5 allowed per peptide); cysteine was assigned as a fixed carbamidomethyl modification (+57.0215 Da). Only fully tryptic peptides were considered with up to 2 missed cleavages in the database search. A precursor mass tolerance of ± 20 ppm was applied prior to mass accuracy calibration and ± 4.5 ppm after internal MaxQuant calibration. Other search settings included a maximum peptide mass of 6,000 Da, a minimum peptide length of 6 residues, 0.05 Da tolerance for orbitrap and 0.6 Da tolerance for ion trap MS/MS scans. The false discovery rate (FDR) for peptide spectral matches, proteins, and site decoy fraction were all set to 1 percent. Quantification settings were as follows: re-quantify with a second peak finding attempt after protein identification has completed; match MS1 peaks between runs; a 0.7 min retention time match window was used after an alignment function was found with a 20-minute RT search space. Quantitation of proteins was performed using summed peptide intensities given by MaxQuant. The quantitation method only considered razor plus unique peptides for protein level quantitation.

2.11. Differential expression analysis

LFQ normalized abundances summarized for protein level quantification based on parsimoniously assembled razor plus unique peptides in MaxQuant were considered for statistical comparisons between WT and RGS14 KO sample abundances after either SAL or KA. Prior to statistical comparison, network connectivity was used to identify and remove sample outliers, which were defined as samples of 3 or more standard deviations away from the mean. In addition, only proteins with quantitation in more than 50% of the samples were included and log₂ transformed. Significantly differentially proteins between groups were defined used one-way ANOVA with Tukey's comparison post hoc test. Differential expression displayed as volcano plots were generated using the ggplot2 package.

2.12. Weighted gene correlation network analysis (WGCNA)

The Weighted Gene Correlation Network Analysis (WGCNA; version 1.69) algorithm was used to generate co-expression modules from the mouse brain proteome as previously described (Johnson et al., 2020). The WGCNA::blockwiseModules function was run with soft threshold power at 9.5, deepsplit of 2, minimum module size of 30, merge cut height at 0.07, mean topological overlap matrix (TOM) denominator, using bicor correlation, signed network type, pamStage and pamRespectsDendro parameters both set to TRUE and a reassignment threshold of 0.05. This function calculates pair-wise biweight mid-correlations (bicor) between protein pairs. The resulting correlation matrix is then transformed into a signed adjacency matrix which is used to calculate a topological overlap matrix (TOM), representing expression similarity across samples for all proteins in the network. This approach uses hierarchical clustering analysis as 1 minus TOM and dynamic tree cutting lends to module identification. Following construction, module eigenprotein (ME) values were defined – representative abundance values for a module that also explain modular protein covariance. Pearson correlation between proteins and MEs was used as a module membership measure, defined as kME.

2.13. Gene ontology (GO) and cell type marker enrichment analyses

Gene ontology (GO), Wikipathway, Reactome and molecular signatures database (MSigDB) term enrichment in our gene sets of mouse network module members and significantly differentially changed protein subsets was determined by gene set enrichment analysis (GSEA) using an in-house developed R script (<https://github.com/edammer/GOparallel>). Briefly, this script performs one tailed Fisher's exact tests (FET) enabled by functions of the R piano package for ontology enrichment analysis on gene sets downloaded from <http://baderlab.org/GeneSets>, which is maintained and updated monthly to pull in current gene sets from more than 10 different database sources including those mentioned above (Reimand et al., 2019; Varemo et al., 2013). Redundant core GO terms were pruned in the GOparallel function using the minimal_set function of the ontologyIndex R package (Greene et al., 2017).

Cell type enrichment was also investigated as previously published (Johnson et al., 2022; McKenzie et al., 2017; Seyfried et al., 2017). An in-house marker list combined previously published cell type marker lists from Sharma et al. (Sharma et al., 2015) and Zhang et al. (Zhang et al., 2014) were used for the cell type marker enrichment analysis for each of the five cell types assessed (neuron, astrocyte, microglia, oligodendrocyte and endothelial). If, after the lists from Sharma et al. and Zhang et al. were merged, gene symbol was assigned to two cell types, we defaulted to the cell type defined by the Zhang et al. list such that each gene symbol was affiliated with only one cell type. Fisher's exact tests were performed using the cell type marker lists to determine cell type enrichment and were corrected by the Benjamini-Hochberg procedure.

2.14. Additional statistical analyses for proteomics

All proteomic statistical analyses were performed in R (version 4.0.3). Box plots represent the median and 25th and 75th percentile extremes; thus the hinges of a box represent the interquartile range of the two middle quartiles of data within a group. Error bars extents are defined

by the farthest data points up to 1.5 times the interquartile range away from the box hinges. Correlations were performed using biweight midcorrelation function from the WGCNA package. Module membership graphs were created using the iGraph R package (v1.2.6).

2.15. Immunogold electron microscopy

Mouse brain tissue sections from wild type animals containing the dorsal hippocampus were processed for a pre-embedding immunogold procedure to characterize subcellular RGS14 expression in area CA2 as previously performed (Squires et al., 2018a). The sections were pre-incubated in a 1% sodium borohydride/PBS solution for 20 min and washed in PBS. Sections were then put in a cryoprotectant solution for 20 minutes before being frozen at -20°C . Sections were then thawed and returned to a graded series of cryoprotectant and PBS. This was followed by an incubation in 5% milk diluted in PBS for 30 min and then overnight incubation at room temperature in primary RGS14 antibody solution consisting of RGS14 antibody (rabbit pAb – Protein Tech, 16258-1-AP; 1:4000 dilution) and 1% dry milk in TBS-gelatin buffer (0.02 M, 0.1% gelatin, pH 7.6). After this incubation, sections were rinsed in TBS-gelatin and incubated for 2 hours with secondary goat anti-rabbit Fab fragments conjugated to 1.4-nm gold particles (1:100; Nanoprobes, Yaphank, NY) and 1% dry milk in TBS-gelatin to limit cross-reactivity of the secondary antibody. To optimize RGS14 visualization, sections underwent incubation for approximately 10 min in the dark with a HQ Silver Kit (Nanoprobes) to increase gold particle sizes to 30–50 nm through silver intensification. The sections were then rinsed in phosphate buffer (0.1 M, pH 7.4) and treated with 0.5% osmium for 10 min and 1% uranyl acetate in 70% ethanol for 10 min, followed by dehydration with increasing ethanol concentrations. They were then placed in propylene oxide, embedded in epoxy resin (Durcupan ACM, Fluka, Buchs, Switzerland) for at least 12 hours, and baked in a 60°C oven for 48 hours. As controls, sections were incubated in a solution devoid of the RGS14 antibody but containing the secondary antibody and the rest of the immunostaining protocol remained the same as above.

2.16. Measurement of Mitochondrial Respiration using Seahorse XF Cell Mitochondrial Stress Test in HEK293T cells

The measurement of mitochondrial respiration was performed as previously described with modifications (Morris et al., 2021). Briefly, HEK293T cells were cultured in Dulbecco's essential medium (DMEM; Gibco, 11-995-040) supplemented with 10% fetal bovine serum and 1% penicillin/streptomycin and incubated at 37°C, 5% CO₂ until the time of seeding or passaging. Cells were maintained by passaging every 2-3 days when cells reached 70-80% confluency. Mitochondrial respiration was evaluated using a XFe96 Extracellular Flux Analyzer (Agilent Seahorse Bioscience Inc., Billerica, MA) and Seahorse CF Cell Mito Stress Test Kit (Agilent, 103015-100) according to manufacturer's instructions. Briefly, cells were seeded into a Seahorse XFe96 microplate (Agilent, 103794-100) at 15,000 cells/well and incubated for 24 hr at 37°C, 5% CO₂. FLAG-RGS14 or pcDNA3.1 (negative control) plasmids (Shu et al., 2007) were transiently transfected using transfection medium DMEM supplemented with 5% FBS and 1% penicillin/streptomycin and polyethyleneimine (PEI) as the transfection reagent. Cells were then incubated for 24 hr at 37°C, 5% CO₂ to ensure adequate expression of both constructs. After transfection, cells were switched to Seahorse XF Base Medium supplemented with 1mM L-glutamine, 5.5 mM D-glucose, and 2 mM sodium pyruvate (pH of 7.4) and equilibrated in this medium for 30 minutes. Oxygen consumption rate (OCR) was measured prior to and after sequential treatment with 1 μM oligomycin (mitochondrial complex V inhibitor), 0.5 μM carbonilcyanide p-trifluoromethoxyphenylhydrazone (FCCP) (ATP synthase inhibitor and proton uncoupler), and 0.5 μM rotenone/antimycin A (Complex I/III inhibitor). Basal respiration, mitochondrial ATP-linked respiration, maximal respiration, proton leak, spare respiratory capacity, and non-mitochondrial linked respiration were determined using the XF Wave 2.1 software. Cell lysates were collected in lysis buffer, and Pierce BCA assay was used to determine protein concentration. OCR values were normalized to HEK293T protein concentration in the same

sample and were expressed as mean \pm SEM. Western immunoblotting to confirm protein expression was performed as stated above using anti-FLAG HRP-conjugated antibody (Sigma Aldrich, A8592; 1:15,000) to verify transfection and expression of FLAG-RGS14.

2.17. FluoroJade B (FJB) tissue staining

To assess for neurodegeneration one day after KA-SE, FluoroJade B (FJB) (Histochem, #1FJB, Jefferson, AR) was used to label and quantify degenerating neurons (Schmued et al., 1997) according to manufacturer's instructions with modifications (Rojas et al., 2014). Briefly, hippocampal sections were mounted and dried on SuperFrost Plus microscope slides. Once dried, sections were sequentially immersed with 80% EtOH, 70% EtOH, and ddH₂O for 2 minutes each. Sections were incubated with 0.06% KMnO₄ (dissolved in ddH₂O) for 10 minutes and rinsed twice with ddH₂O for 2 minutes each to remove all traces of KMnO₄. Sections were incubated in a 0.0004% solution of Fluoro-Jade B for 30 minutes covered from light. Sections were then rinsed thrice with ddH₂O for 1 minute each and air dried for 24 hours while covered from light. Sections were cleared with xylenes for 5 minutes and coverslipped with DPX (Electron Microscopy Sciences, Hatfield, PA) mounting medium. FJB labeled neurons were visualized and imaged using a Leica DM6000B epifluorescent upright microscope with filters for fluorescein or FITC at 10X and 20X magnifications. For each animal, 20X representative images were collected from dorsal hippocampal CA fields, and 10X representative images were collected from the entorhinal/perirhinal cortex, lateral amygdala, and dorsomedial thalamus. For quantification of CA3 neuronal injury, 20X CA3 images were collected unilaterally from 3 sections (per animal) that were observed to have the highest number of FJB+ cells in CA3. FJB+ cells in the stratum pyramidale (SP) layer were counted by a blinded observer throughout the entire CA3 region for those 3 sections using DotDotGoose (Ersts, American Museum of Natural History, Center of Biodiversity and Conservation, version 1.5.3). For CA3 quantification, cell counts are represented as the mean number of FJB+ cells across the 3 sections for each animal.

2.18. Statistical analysis

All statistical analysis other than that done for proteomics was performed in GraphPad Prism (version 9.3.1). Data were subjected to Grubb's outlier analysis prior to statistical comparisons. For behavioral seizure experiments, Gehan-Breslow-Wilcoxon test was used to determine differences between survival curves, and Fisher's exact test was used to determine contingency of genotype on binned mortality and overall mortality. Multiple t-tests were used to compare mean behavioral seizure score at each time point during the 90 minute behavioral seizure period, and unpaired Student's t-test was used to compare mean latency to Stage 3 seizure activity between genotypes. Two-way ANOVA with Sidak post-hoc comparison was used to assess effects of genotype and sex on latency to mortality and Stage 3 seizure activity. One-way ANOVA with Dunnett's post-hoc comparisons was used to compare mean RGS14 expression (band density from immunoblot) in hippocampal lysates, and unpaired Student's t-tests were used to compare mean RGS14 immunofluorescence between SAL and 1d KA treatments. Unpaired Student's t-tests were used to compare OCR means between control and RGS14 overexpression groups, SOD2 mean immunofluorescence in CA1, GFAP- and IBA1-related parameters at 7 day KA timepoints, and mean number of FJB+ neurons in CA3 between WT and RGS14 KO mice after KA-SE. For comparison 3-NT and SOD2 mean immunofluorescence and IBA1+ microglia cell density and mean area at 1 day KA timepoints, two-way ANOVA with Tukey's or Sidak's post-hoc analysis was used.

3. Results

3.1. Loss of RGS14 increases susceptibility to KA-induced seizures by expediting entry into SE and mortality (Harbin et al., 2023)

To test seizure susceptibility in RGS14 KO mice, we administered a single dose of 30 mg/kg KA by intraperitoneal (i.p.) injection into WT (n = 39 total; 26 males, 13 females) and RGS14 KO mice (n = 41 total; 25 males, 16 females) to induce status epilepticus (KA-SE) as previously described (Rojas et al., 2014). We monitored survival during seizure activity, progression of behavioral seizure severity, and latency to seizure staging for 90 minutes following KA administration. Behavioral seizure score (0-6) was measured every 5 minutes for 90 minutes using a modified Racine scale (see Materials and Methods and Table 1) until termination of seizure with diazepam (10 mg/kg, i.p.). Status epilepticus was defined as 30 minutes or more of continuous Stage 3 or higher seizure activity.

After KA administration, we observed that all mice regardless of genotype either entered SE (30 min or longer of > Stage 3 behavioral seizure activity) or died at higher stage seizures (data not shown). Comparison of survival curves between WT and RGS14 KO mice demonstrated that RGS14 KO mice died significantly quicker than WT mice (Fig. 9A), and the mean latency to mortality was significantly reduced (12.6 minutes faster) in the RGS14 KO mice (Fig. 9B). At the 30-minute time interval, nearly half of RGS14 KO mice (49%, 19 of 41) reached mortality, while less than one-quarter of WT mice (23%, 6 of 39) reached mortality at the same interval (Fig. 9A). Of the mice that reached mortality, significantly more RGS14 KO mice (76%, 19 of 24) died in the first 30 minutes after KA administration compared to WT mice (33%, 6 of 18) (Fig. 9C). Surprisingly, there was no significant difference between the overall mortality rate between WT mice (46%, 18 of 39) and RGS14 KO mice (59%, 24 of 41) after the 90-minute seizure period (Fig. 9D).

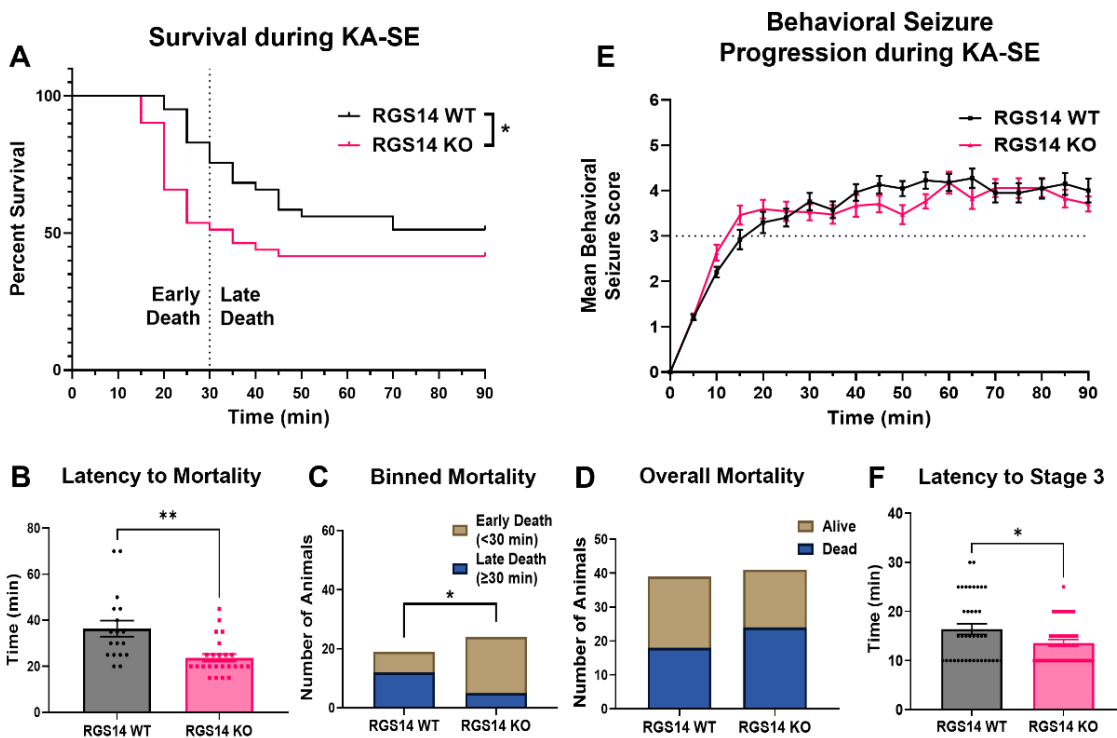


Figure 9. Loss of RGS14 increases susceptibility to KA-induced seizure by expediting mortality and entry into SE. (Harbin et al., 2023) (A) Survival curve comparing the percentage of alive animals between WT ($n = 39$) and RGS14 KO ($n = 41$) mice after 30 mg/kg KA injection shows RGS14 KO mice die quicker than WT mice following KA (KO/WT Hazard Ratio = 1.770, Mantel-Haenszel) (B) Mean latency to mortality in WT and RGS14 KO mice following KA injection (WT, 36.39 ± 3.52 min; RGS14 KO, 23.75 ± 1.63 min). (C) The number of animals that died in the first 30 minutes (Early Death; WT, $n = 6$; RGS14 KO, $n = 19$) or last 60 minutes (Late Death; WT, $n = 12$; RGS14 KO, $n = 5$) of the 90-minute seizure period. (D) The number of animals that were alive (WT, $n = 21$; RGS14 KO, $n = 17$) or dead (WT, $n = 18$; RGS14 KO, $n = 24$ dead) at the end of the 90-minute seizure period. (E) The mean behavioral seizure score plotted over time in WT ($n = 39$) and RGS14 KO ($n = 41$) mice. Seizure stage was scored every 5 minutes until seizure termination 90 minutes after KA injection. (F) The mean latency of animals to reach Stage 3 behavioral seizure activity after KA injection (WT, 16.41 ± 1.07 min; RGS14 KO, 13.54 ± 0.68

min). *Statistical analysis:* (A) Gehan-Breslow-Wilcoxon test to compare survival curves (* $p < 0.05$). (B, F) Unpaired t-test to compare latency to mortality (B; WT vs RGS14 KO, ** $p < 0.01$) and Stage 3 seizure (F; WT vs RGS14 KO, * $p < 0.05$) (C, D) Fisher's exact test to assess for contingency of genotype on binned morality (C, * $p < 0.05$) or overall mortality (D, $p > 0.05$). (E) Multiple t-tests were used to compare between genotypes at each time point ($p > 0.05$ for all time points). Error bars represent standard error of the mean (SEM). WT, wild-type; KA, kainic acid; SE, status epilepticus. (1.5 column)

Initial analysis of behavioral seizure scores demonstrated that WT and RGS14 KO mice progress similarly through behavioral seizure staging following KA (Fig. 9E). When latency to Stage 3 (i.e. SE) was compared between genotypes, we found RGS14 KO mice reached Stage 3 slightly but significantly quicker than WT mice (2.9 minutes faster) (Fig. 9F). Because seizure susceptibility can differ between males and females, we assessed the contribution of sex to the seizure phenotype (Fig. 10). We found only a main effect of genotype on the latency to mortality (Fig. 10A) and SE (Fig. 10B), where RGS14 KO had reduced latency to mortality in both males (12.1 minutes faster) and females (13.5 minutes faster). These data suggest that RGS14 limits the behavioral seizure response to KA, where loss of RGS14 expedites entry into SE and mortality following KA without affecting overall mortality.

3.2. RGS14 protein expression is upregulated following status epilepticus (Harbin et al., 2023)

Several studies have demonstrated that RGS14 expression is significantly altered in animal and cellular models of cardiac hypertrophy and hepatic ischemic-reperfusion injury (Li et al., 2016; Zhang et al., 2022), and that the expression of other RGS proteins is regulated by seizure activity (Gold et al., 1997). Therefore, we sought to determine whether RGS14 expression is altered following KA-SE (Fig. 11). One, three, or seven days after KA-SE, whole hippocampi were collected from WT mice for protein analysis, and Western blot was used to detect RGS14 expression in whole hippocampal lysate (Fig. 11A). Relative to saline-treated hippocampal tissue, there was a striking and significant upregulation of RGS14 protein following KA-SE. (Fig. 11B). Peaking one day after KA-SE, RGS14 expression is significantly induced more than 5-fold compared to saline (Fig. 11B). RGS14 expression remained high relative to saline three days after KA-SE (3.65 fold induction), but returned to near baseline levels 7 days after KA-SE (Fig. 11B). These findings suggest that RGS14 induction in the hippocampus is regulated by seizure activity and may play an important role in injury response following KA-SE.

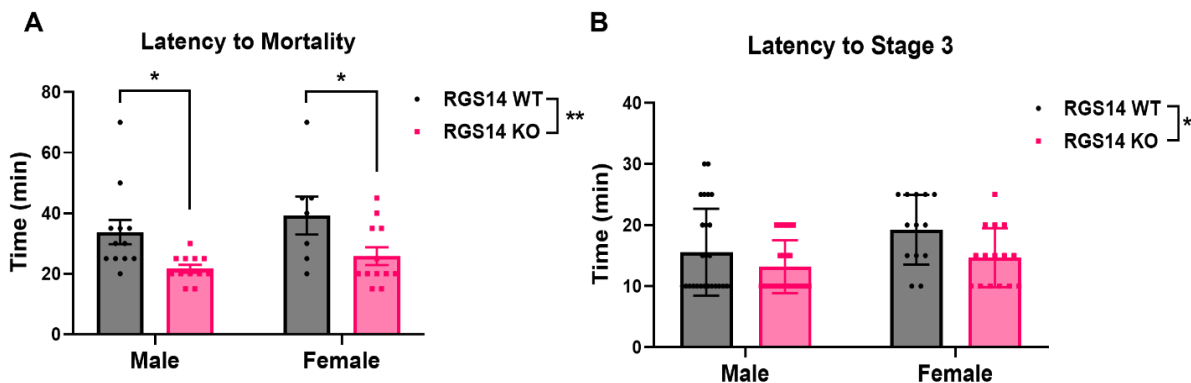


Figure 10. Behavioral sensitivity to KA-SE in RGS14 KO mice is not affected by sex. (Harbin et al., 2023) (A) Mean latency to mortality in male and female WT and RGS14 KO mice (males: WT, 33.75 ± 4.00 min; RGS14 KO, 21.67 ± 1.28 min) (females: WT, 39.29 ± 6.31 min; RGS14 KO, 25.83 ± 2.94 min). (B) Mean latency to Stage 3 behavioral seizure activity in male and female WT and RGS14 KO mice. *Statistical analysis:* (A, B) Two-ANOVA with Sidak post-hoc comparisons was used to compare mean latency to mortality (A; two-way ANOVA, $F = 12.60$ for genotype, $**p < 0.01$; Sidak, WT vs RGS14 KO, $*p < 0.05$) and Stage 3 seizure activity (two-way ANOVA, $F = 6.71$ for genotype, $*p < 0.05$). Error bars represent the SEM.

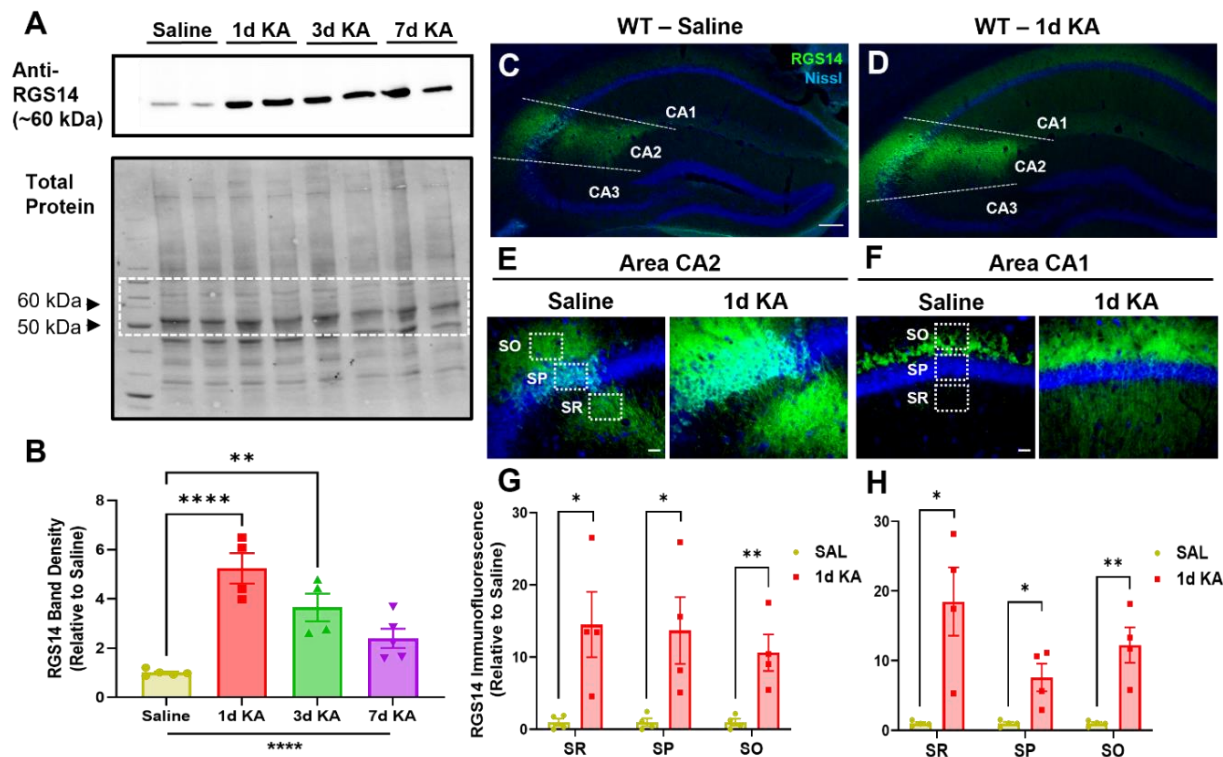


Figure 11. Hippocampal RGS14 protein expression is upregulated following KA-SE.

(Harbin et al., 2023) (A) Representative Western blot showing RGS14 protein expression (top) relative to total protein (bottom) in WT hippocampal lysate 1 day after saline ($n = 5$) or 1 ($n = 4$), 3 ($n = 4$) or 7 ($n = 5$) days after KA-SE. Dashed box in total protein blot represents strip used for RGS14 immunoblot. (B) Quantification of mean RGS14 protein band density normalized to total protein density (saline, 1.00 ± 0.06 ; 1d KA, 5.24 ± 0.62 ; 3d KA, 3.65 ± 0.56 ; 7d KA, 2.40 ± 0.39) (C, D) Representative IHC images of RGS14 expression in the dorsal hippocampus of WT mice 1 day after saline (C) or KA-SE (D). Dashed lines divide the CA1, CA2, and CA3 subregions of the hippocampus. Scale bar, 100 μm . (E) Representative IHC image of area CA2 1 day after saline or KA-SE. (F) Representative IHC image of area CA1 1 day after saline or KA-SE. Dashed boxes illustrate regions of quantification for pyramidal cell layers (SR, SP, SO) in area CA2 (E) and CA1 (F). Scale bar, 20 μm . (G) Mean RGS14 immunofluorescence ($n=4$ per treatment) in saline- and KA-treated CA2 SR (saline, 1.00 ± 0.49 ; 1d KA, 14.52 ± 4.52), SP (saline, 1.00 ± 0.54 ; 1d KA, 13.69 ± 4.63), and SO (saline, 1.00 ± 0.47 ; 1d KA, 10.62 ± 2.53). (H) Mean RGS14

immunofluorescence (n=4 per treatment) in saline- and KA-treated CA1 SR (saline, 1.00 ± 0.19 ; 1d KA, 18.51 ± 4.91), SP (saline, 1.00 ± 0.22 ; 1d KA, 7.61 ± 1.99), and SO (saline, 1.00 ± 0.19 ; 1d KA, 12.26 ± 2.54). *Statistical Analysis:* (B) One-way ANOVA with Dunnett post-hoc comparisons to compare mean RGS14 band density (one-way ANOVA, $F = 17.65$ for treatment, **** $p < 0.0001$; Dunnett's, 1d KA vs SAL, $p < 0.0001$; 3d KA vs SAL, $p < 0.01$; 7d KA vs SAL, $p > 0.05$). (G, H) Unpaired t-tests to compare mean RGS14 immunofluorescence in CA2 (SAL vs 1d KA: SR, SP, * $p < 0.05$; SO, ** $p < 0.01$) and CA1 (SAL vs 1d KA: SR, SP, * $p < 0.05$; SO, ** $p < 0.01$). $p > 0.05$ is considered not significant (ns). Error bars represent the SEM. IHC, immunohistochemistry; SR, stratum radiatum; SP, stratum pyramidale; SO, stratum oriens.

To determine where in the hippocampus RGS14 expression is being induced, IHC was performed on dorsal hippocampal sections collected from WT mice one day after KA-SE or saline (SAL) (Fig. 11C-H). In saline-treated WT mice (Fig. 11C), RGS14 expression was mostly restricted to the cell bodies (*stratum pyramidale*, SP) and dendrites (*stratum radiatum*, SR, and *stratum oriens*, SO) of area CA2 PCs (Fig. 11E). Additionally in saline-treated animals, we observed modest RGS14 expression in the SO of CA1, where CA2 axons project to CA1 pyramidal cell (Fig. 11F). One day following KA-SE (Fig. 11D), we detected a robust and significant upregulation of RGS14 in PCs throughout each layer of CA2 (fold induction relative to saline: 14.5 in SR; 13.7 in SP; 10.6 in SO) (Fig. 11E, G). Similarly, we observed significant upregulation of RGS14 expression in area CA1 one day after KA-SE, strikingly in the SR where proximal dendrites of CA1 receive projections mostly from CA3 (fold induction relative to saline: 18.5 in SR, 7.6 in SP, 12.3 in SO) (Fig. 11F, H). However, it should be noted that the upregulated RGS14 expression in CA1 was still considerably lower relative to CA2, and its expression in CA1 was still more prominent in the SO, where CA2 axons terminate, relative to cell bodies in the SP or proximal dendrites in the SR.

Together, this demonstrates that RGS14 expression is robustly induced by KA-SE within hippocampal areas CA2 and CA1 (Fig. 11E, F), which likely reflects RGS14 upregulation in CA2 PC dendrites (CA2 SR, SO), cell bodies (CA2 SP), and axons (CA1 SO) (Fig. 11G) as well as CA1 PC dendrites (CA1 SR, SO) and cell bodies (CA1 SP) (Fig. 11H). Importantly, this is the first evidence demonstrating that RGS14 expression is activity-dependent in the hippocampus, suggesting that RGS14 may serve a protective role in this brain region following seizure.

3.3. Metabolic and mitochondrial proteins are differentially expressed between WT and RGS14 KO mice 1 day after KA-SE (Harbin et al., 2023)

To better understand how RGS14 may be influencing seizure activity in the hippocampus and the effects of losing RGS14 induction following seizure activity, we performed a proteomics analysis on hippocampal tissue taken from WT and RGS14 KO mice 1 day after saline or KA-SE treatment (n=5 per genotype and treatment). Whole hippocampi were homogenized, digested, and subjected to LC-MS/MS, and label-free quantitation (LFQ) was used to obtain relative protein abundance in each sample. Protein abundance was compared within treatment (SAL or KA), between genotype (WT vs RGS14 KO) to identify differentially expressed proteins (DEPs) in RGS14 KO hippocampi (Fig. 12A, B). From these analyses, 45 proteins in the SAL treatment and 49 proteins in the KA treatment were found to be significantly up or downregulated between WT and RGS14 KO groups (adjusted $p < 0.05$), where 9 proteins were differentially expressed after both saline and KA treatments (Fig. 12C). These proteins are visualized in a volcano plot as either downregulated (left side) or upregulated (right side) in RGS14 KO hippocampi relative to WT hippocampi (Fig. 12A) (comprehensive table of DEPs listed in Table 2).

Gene ontology (GO) analysis was performed on up- and downregulated DEPs in SAL-treated mice identify common cellular pathways and processes associated with the DEPs that may influence sensitivity to KA (Fig. 12D). GO terms related to G-protein processes like “G-protein beta subunit binding”, “G-protein Alpha Subunit Binding”, “Gtpase Activating Protein Binding”, and “Morphogenesis” were associated with proteins downregulated in RGS14 KO (Fig. 12D, left), which is unsurprising as we and others have shown the capacity of RGS14 to tightly regulate GPCR and G-protein activation (Harbin et al., 2021) and dendritic spine morphology (Evans et al., 2018b).

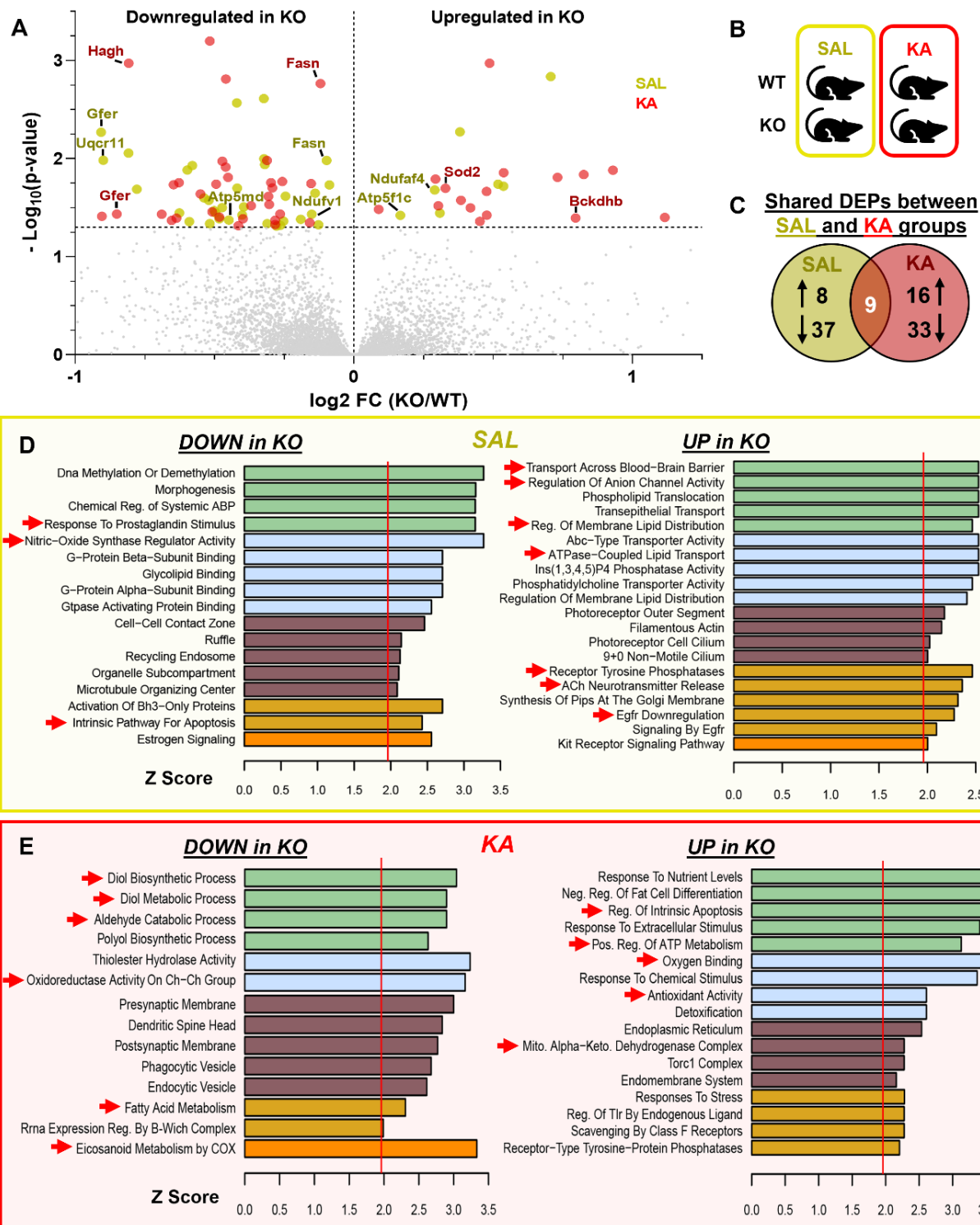


Figure 12. Differential expression analysis of the hippocampal proteome reveals altered mitochondrial and metabolic protein expression in RGS14 KO versus WT mice. (Harbin et al., 2023) (A) Volcano plot showing differentially expressed proteins (DEPs) one day after SAL

(yellow) or KA-SE (red) treatment in RGS14 KO hippocampus relative to WT plotted by their $-\log_{10}(\text{p-value})$ and \log_2 fold change (KO/WT). Proteins were considered significantly downregulated if the adjusted p-value < 0.05 , \log_2 fold change (KO/WT) < 0 and significantly upregulated if the adjusted p-value < 0.05 , \log_2 fold change (KO/WT) > 0 (n = 5 per genotype/condition). Labeled dots represent DEPs involved with cellular metabolism and localize to the mitochondria. (B) Diagram illustrating between-genotype, within-treatment comparisons used to determine DEPs. (C) Venn diagram showing the number of upregulated or downregulated proteins in RGS14 KO relative to WT after SAL or KA-SE and DEPs common to both treatment groups. (D-E) Gene ontology analysis demonstrates similar biological function and processes of DEPs that are either downregulated (DOWN) or upregulated (UP) in RGS14 KO hippocampi one day after SAL (D) or KA-SE (E). *Red arrows* indicate ontologies of interest that may influence seizure susceptibility (D) or mitochondrial metabolism and oxidative stress (E).

A			SAL			B			KA		
Upregulated in KO			Downregulated in KO			Upregulated in KO			Downregulated in KO		
Protein	Adj. p-value	Log2 FC (KO/WT)	Protein	Adj. p-value	Log2 FC (KO/WT)	Protein	Adj. p-value	Log2 FC (KO/WT)	Protein	Adj. p-value	Log2 FC (KO/WT)
Ehbp1	0.00342	1.848	Rgs14	0.00003	-4.239	Apob	0.03976	1.116	Rgs14	0.00005	-4.070
Ppfia4	0.00146	0.707	Tpm1	0.04297	-1.405	Ehbp1	0.01315	0.930	Sf3b1	0.03869	-0.904
Them6	0.01911	0.537	Spag7	0.00010	-1.054	Txndc12	0.01455	0.825	Gfer	0.03674	-0.851
Ocr1	0.01824	0.518	Gfer	0.00540	-0.907	Bckdhb	0.04040	0.796	Fto	0.00107	-0.808
Abcb1a	0.00534	0.381	Uqcr11	0.01041	-0.899	Mlst8	0.01556	0.731	Hnrnp3	0.03684	-0.690
Ndufaf4	0.03588	0.309	Rap2c	0.00878	-0.808	Ppfia4	0.01394	0.538	Srgap2	0.04268	-0.654
Sh3kbp1	0.02090	0.290	Nfix	0.02050	-0.779	Arsb	0.00106	0.488	Prrc2c	0.01850	-0.647
Atp5f1c	0.03784	0.167	Pigu	0.03585	-0.626	Cygb	0.03770	0.477	Gabbr1	0.04053	-0.637
			Fto	0.01307	-0.597	Tmed7	0.02162	0.477	Elmo1	0.01756	-0.627
			Syt11	0.04393	-0.591	Trappc8	0.04369	0.452	Stx8	0.02297	-0.551
			Naa15	0.01176	-0.579	Dlgap2	0.03178	0.419	Hagh	0.00063	-0.517
			Trappc8	0.02520	-0.537	Acat2	0.02662	0.385	C2cd4c	0.03492	-0.508
			Naaa	0.02662	-0.521	Sod2	0.02007	0.329	Trappc13	0.01821	-0.494
			Ggact	0.04601	-0.517	Sort1	0.03027	0.303	Anxa3	0.03948	-0.483
			Psap	0.03392	-0.501	Ssr1	0.01621	0.293	Cacna1e	0.01062	-0.472
			Srrm2	0.03583	-0.496	Eno1	0.03296	0.090	Ptgr2	0.01220	-0.460
			Ndr4	0.04098	-0.483				Rgs7bp	0.00155	-0.459
			Rab9a	0.03169	-0.472				Ubr4	0.01557	-0.451
			Atp5md	0.04234	-0.448				Bola2	0.04830	-0.414
			Tipr1	0.00271	-0.420				Dgke	0.04097	-0.398
			Ddost	0.01995	-0.418				Esd	0.03030	-0.368
			Scg5	0.03750	-0.401				Mpp3	0.01045	-0.311
			Edc4	0.03111	-0.395				Acaa1a	0.02432	-0.306
			Erlin2	0.00245	-0.323				Asah1	0.02940	-0.303
			Akt1	0.01005	-0.322				Npc1	0.01759	-0.297
			Agfg2	0.01151	-0.319				Psmc6	0.01991	-0.292
			Scn1b	0.04604	-0.310				Tipr1	0.04249	-0.282
			Dynl1	0.04879	-0.277				Ncam1	0.04696	-0.282
			Alcam	0.04788	-0.263				Sh3kbp1	0.03674	-0.265
			Ggt7	0.04351	-0.252				Hdhd2	0.01715	-0.257
			G6pdx	0.02414	-0.245				Spr	0.04502	-0.158
			Slc4a4	0.04152	-0.190				Actr1b	0.01800	-0.153
			Ndufv1	0.03694	-0.151				Fasn	0.00172	-0.119
			Gnas	0.02256	-0.139						
			Cct5	0.04734	-0.127						
			Actn1	0.01044	-0.097						
			Fasn	0.01851	-0.087						

Table 2. Comprehensive list of differentially expressed proteins (DEPs) between WT and RGS14 KO after SAL or KA treatment. (Harbin et al., 2023) (A) List of upregulated (left) or downregulated (right) DEPs in RGS14 KO hippocampi one day after saline treatment, their adjusted p-values, and the fold change of abundance (\log_2 FC (KO/WT)). (B) List of upregulated (left) or downregulated (right) DEPs in RGS14 KO hippocampi one day after saline treatment, their adjusted p-values, and the fold change of abundance (\log_2 FC (KO/WT)). FC, fold change.

However, we were surprised to find GO terms like “Response to Prostaglandin Stimulus”, “Nitric-Oxide Synthase Regulator Activity”, and “Intrinsic Pathway for Apoptosis” to be associated with downregulated proteins in RGS14 KO hippocampi (Fig 12D, left), suggesting RGS14 may influence nitric oxide levels and regulate prostaglandin and cellular stress signals. Proteins that were upregulated in RGS14 KO hippocampi after SAL were associated with lipid membrane dynamics and membrane transport (e.g. “Regulation of Membrane Lipid Distribution”, “ATPase-Coupled Lipid Transport”, “Transport Across Blood-Brain Barrier”), receptor tyrosine signaling (e.g. “Receptor Tyrosine Phosphatases”, “EGFR Downregulation”), and acetylcholine neurotransmission (“ACh neurotransmitter Release”) (Fig. 12D, right). We and others have demonstrated RGS14 interacts with small monomeric G proteins like H-Ras to modulate MAPK/ERK signaling (Shu et al., 2010; Willard et al., 2009), making it plausible that RGS14 KO would alter tyrosine receptor signaling dynamics within CA2 pyramidal cells. Although RGS14 has never been demonstrated to modulate lipid dynamics or distribution, blood brain barrier transport, or acetylcholine release, this data demonstrates loss of RGS14 may act upstream to dysregulate a number of cellular pathways that contribute to KA seizure susceptibility in RGS14 KO mice. However, it should be noted that only 8 upregulated proteins were used in this GO analysis, so it may be unlikely that RGS14 majorly affects all of these cellular processes.

To determine alterations in cellular processes caused by loss of RGS14 induction following seizure activity, we performed GO analysis 1 day after KA-SE. After KA treatment, significantly downregulated proteins in RGS14 KO hippocampi were associated with GO terms “Diol Biosynthetic Process”, “Diol Metabolic Process”, “Aldehyde Catabolic Processes”, “Oxidoreductase Activity on Ch-Ch Group”, and “Fatty Acid Metabolism” (Fig. 12E, left), suggesting possible dysregulation of cellular metabolism in RGS14 KO mice following seizure activity. Strikingly, the most enriched GO term associated with proteins downregulated in KO mice was “Eicosanoid Metabolism by COX.” Cyclooxygenase 2 (COX-2) is induced after seizure

activity and its conversion of arachidonic acid to prostaglandins that contribute to epileptic pathological responses (Rojas et al., 2019). Proteins that are upregulated in RGS14 KO hippocampi were associated with GO terms “Regulation of Intrinsic Apoptosis”, “Positive Regulation of ATP Metabolism”, “Oxygen Binding”, “Antioxidant Activity”, and “Mitochondrial Alpha-Ketoglutarate Dehydrogenase Complex” (Fig. 12E, right). Proteins that localize to the mitochondria or are involved in cellular metabolic regulation are highlighted in the volcano plot (Fig. 12A). Of interest, DEPs in RGS14 KO at baseline include complex I (Ndufaf4), III (Uqcr11), and V (Atp5md, Atp5f1c) components of the ETC, and DEPs in RGS14 KO following KA-SE included a subunit of the alpha-ketoglutarate dehydrogenase complex Bckdhb and the mitochondrial superoxide dismutase SOD2. All of these proteins are critical for proper mitochondrial function, and their altered expression in the RGS14 KO hippocampus may exacerbate oxidative stress and seizure pathology (Folbergrova and Kunz, 2012; Shin et al., 2011).

Complimentary to this analysis, we also determined DEPs altered after KA-SE (between treatment) in either WT or RGS14 KO hippocampi (within genotype) (Fig. 13A, B). We found 69 DEPs (34 upregulated, 35 downregulated) in WT mice and 50 DEPs (27 upregulated, 23 downregulated) in RGS14 KO mice, where only 8 proteins were common between the genotypes (Fig. 13) (complete list of DEPs found in Table 3). Again, we used GO analysis on each set of DEPs (Fig. 13D, E), and we compared and contrasted the two GO analyses to provide further insight into KA-induced changes in the RGS14 KO hippocampus relative to WT. Proteins associated with gene expression, protein translation, and protein folding were commonly upregulated in both WT and RGS14 KO (Fig 13D, E), which is expected as neuronal activity promotes transcription and translation (Fernandez-Moya et al., 2014; Yap and Greenberg, 2018).

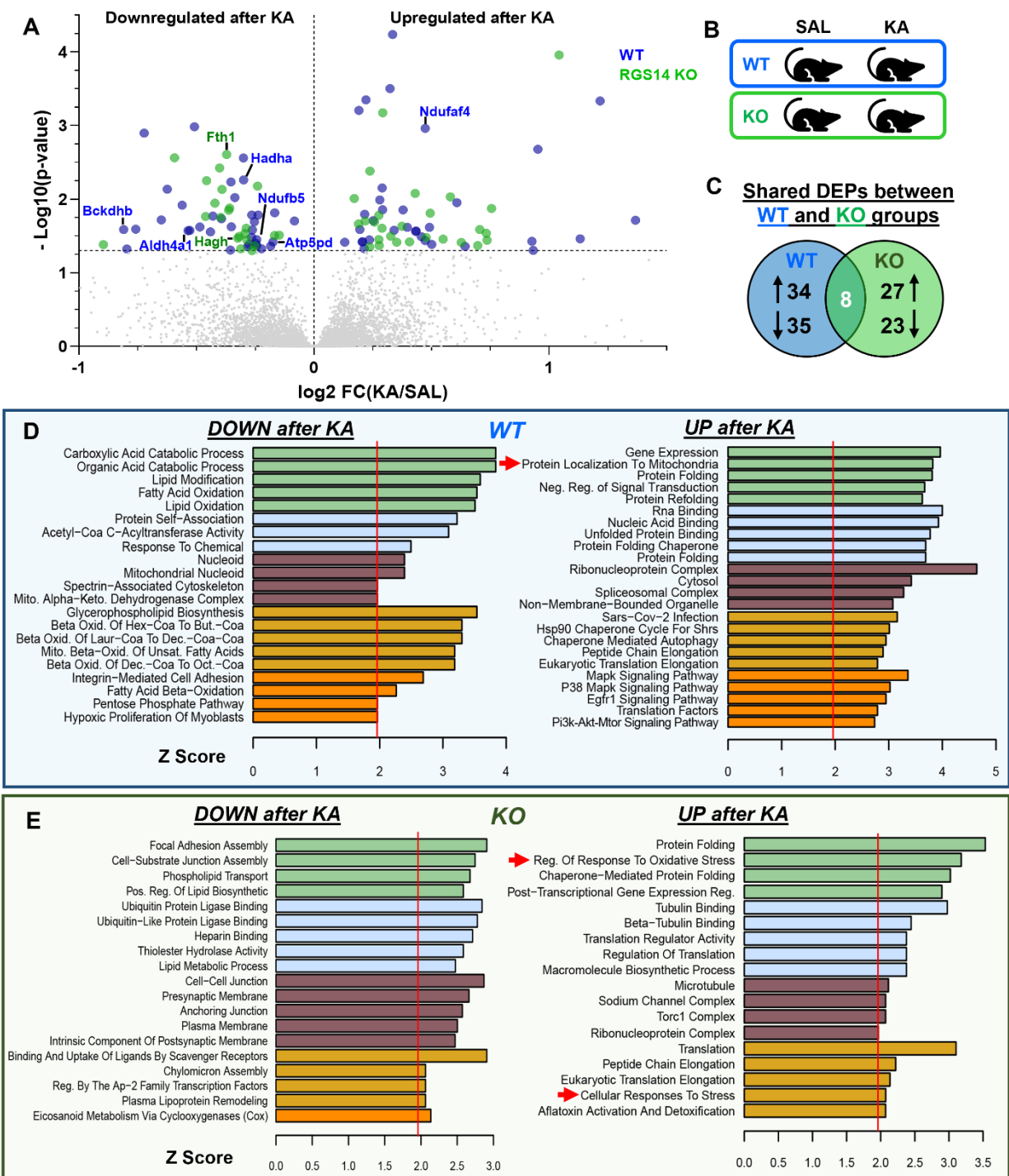


Figure 13. Comparison of WT and RGS14 KO hippocampal proteome after KA-SE suggests oxidative stress as a potential consequence of RGS14 KO. (Harbin et al., 2023) (A) Volcano plot showing differentially expressed proteins (DEPs) in WT or RGS14 KO one day after KA-SE plotted by their $-\log_{10}(\text{p-value})$ and \log_2 fold change (KA/SAL). Proteins were considered

significantly downregulated if the adjusted p-value < 0.05 , \log_2 fold change (KA/SAL) < 0 and significantly upregulated if the adjusted p-value < 0.05 , \log_2 fold change (KA/SAL) > 0 ($n = 5$ per genotype/condition). Labeled dots represent DEPs involved with cellular metabolism and localize to the mitochondria. (B) Diagram illustrating within-genotype, between-treatment comparisons used to determine DEPs. (C) Venn diagram showing the number of upregulated or downregulated proteins following KA-SE in WT or RGS14 KO hippocampi and DEPs common to both genotypes. (D-E) Gene ontology analysis demonstrates similar biological function and processes of DEPs that are either downregulated (DOWN) or upregulated (UP) following KA-SE in WT (D) or RGS14 KO A (E). Red arrows indicate ontologies of interest related to metabolic and mitochondrial function.

A			WT			B			RGS14 KO		
Upregulated			Downregulated			Upregulated			Downregulated		
after KA			after KA			after KA			after KA		
Protein	Adj. p-value	Log2 FC (KA/Sal)	Protein	Adj. p-value	Log2 FC (KA/Sal)	Protein	Adj. p-value	Log2 FC (KA/Sal)	Protein	Adj. p-value	Log2 FC (KA/Sal)
Lrrfip1	0.04855	2.039	Bckdhb	0.02584	-0.810	Spag7	0.00011	1.043	Ehbp1	0.02550	-1.389
Hspb1	0.01937	1.367	Tinagl1	0.04738	-0.796	Srrm2	0.01341	0.755	Rnf141	0.04137	-0.896
Dnajb5	0.00046	1.217	Kcnj10	0.02556	-0.758	Eif5b	0.03604	0.736	Cacna1e	0.00274	-0.593
Ybx1	0.03460	1.132	Naa15	0.00127	-0.722	Cmp1	0.02918	0.733	Ptgr2	0.01712	-0.461
Vgf	0.00210	0.952	Ank1	0.01913	-0.649	Mlst8	0.02592	0.705	Srprb	0.00560	-0.457
Castor2	0.04962	0.932	Abcd3	0.00731	-0.624	Dnajb5	0.04264	0.697	Mark3	0.01132	-0.422
Lsm3	0.03750	0.927	Snrpa1	0.01207	-0.561	Syt11	0.03861	0.626	Pmm1	0.00377	-0.402
Ptpn5	0.04391	0.643	Ggact	0.02672	-0.535	Sez6l	0.00928	0.580	Pip5k1a	0.01768	-0.397
Rps27	0.01114	0.608	Aldh4a1	0.02659	-0.529	Trappc8	0.03487	0.549	Rgs7bp	0.00735	-0.391
Psmb5	0.04123	0.500	Hectd4	0.00104	-0.508	Dlgap2	0.01553	0.495	Fth1	0.00248	-0.371
Fmn1	0.02409	0.491	Cygb	0.02392	-0.486	Cnn3	0.03324	0.477	Mtmr1	0.01415	-0.363
Prmt1	0.03650	0.473	Trappc8	0.02779	-0.440	Scn1b	0.00837	0.430	Apoe	0.01321	-0.359
Ndufaf4	0.00109	0.473	Scg5	0.01695	-0.430	Msi2	0.03794	0.407	Hagh	0.03390	-0.324
Ddi2	0.03225	0.456	Dhd1	0.01846	-0.393	Kif3a	0.02329	0.374	Ncam1	0.03203	-0.318
Btf3	0.02712	0.434	Pnmal2	0.04917	-0.356	Tbca	0.03857	0.352	Sorbs1	0.04719	-0.312
Spon1	0.02731	0.433	Akt1	0.00585	-0.353	Celf2	0.03192	0.326	Mblac2	0.02923	-0.294
Rab8a	0.02410	0.397	C20orf27	0.02376	-0.352	Sgta	0.00067	0.292	Mpp3	0.02482	-0.288
Eif1	0.01400	0.379	Tipr1	0.00950	-0.337	Ssr1	0.02485	0.289	Abcb1a	0.03589	-0.285
G3bp2	0.02647	0.341	Erlin2	0.00276	-0.300	Asb8	0.04264	0.277	Sh3kbp1	0.04989	-0.264
Tpt1	0.00006	0.334	Hadha	0.00548	-0.300	Ggt7	0.03534	0.276	Scfd1	0.04290	-0.253
Hsph1	0.00032	0.324	Sorbs1	0.04445	-0.282	Slc27a4	0.01662	0.276	Xpnpep1	0.00664	-0.240
Sh3kbp1	0.01395	0.291	Hadhb	0.04115	-0.277	Farsb	0.02048	0.257	Sh3bgrl	0.03115	-0.168
Rps16	0.00703	0.290	Alcam	0.03304	-0.265	Tpt1	0.00416	0.237	Actr1b	0.03090	-0.148
Dnaja1	0.01025	0.280	Scfd1	0.01639	-0.265	Rps9	0.04456	0.237			
Grb2	0.01957	0.252	Pgls	0.02616	-0.262	Hsph1	0.01982	0.218			
Eef1a1	0.03566	0.235	Hnrnpr	0.02022	-0.253	P4hb	0.02167	0.189			
Eef2	0.00045	0.221	Dgkg	0.03988	-0.247	Eef2	0.00978	0.171			
Tra2a	0.01602	0.215	Agfg2	0.04260	-0.244						
Rheb	0.04696	0.214	Ndufb5	0.03526	-0.244						
Kiaa0513	0.03774	0.206	Prxl2a	0.01638	-0.237						
Rpl13	0.03803	0.205	Pitpnm1	0.04720	-0.223						
Hsp90ab1	0.02585	0.195	Ahcy	0.04338	-0.184						
Hpcal4	0.00062	0.191	Atp5pd	0.03795	-0.174						
Hspa8	0.03850	0.131	L1cam	0.01534	-0.167						
			Actn1	0.01974	-0.083						

Table 3. Comprehensive list of differentially expressed proteins (DEPs) one day after KA-SE in WT or RGS14 KO hippocampi. (Harbin et al., 2023) (A) List of upregulated (left) or downregulated (right) DEPs one day following KA-SE in WT hippocampi, their adjusted p-values, and the fold change of abundance (log2 FC (KA/SAL)). (B) List of upregulated (left) or downregulated (right) DEPs one day following KA-SE in RGS14 KO hippocampi, their adjusted p-values, and the fold change of abundance (log2 FC (KA/SAL)). FC, fold change.

In contrast, while upregulated proteins in WT were associated with the GO term “Protein Localization To Mitochondria” (Fig. 13D), upregulated proteins in RGS14 KO lacked this ontology and instead were associated with GO terms “Regulation of Response to Oxidative Stress” and “Cellular Response to Stress”, further implicating that RGS14 may be important in regulating mitochondrial response to seizure activity and loss of RGS14 could promote oxidative stress.

3.4. WGCNA Analysis reveals significant alterations of protein modules related to cellular/lipid metabolism and astrocytes in RGS14 KO hippocampi (unpublished data)

To further expand on our proteomics analysis, we used weighted gene correlation network analysis (WGCNA) to cluster proteins into modules with similar expression patterns across groups as we have previously performed (Gerber et al., 2019) (Fig. 14). Proteins were clustered into 35 distinct modules that were determined to co-express with each other (Fig. 14A). By comparing these modules with DEPs identified in our differential expression analysis, four modules of interest (M5 green, M19 light yellow, M27 white, M15 midnight blue) were found to be significantly associated with the DEPs from the differential expression (Fig. 14B). M5 and M19 were chosen for further analysis based on their significant association with proteins in WT but not RGS14 KO hippocampi that were downregulated by KA. M27 was of interest because this module was significantly associated with proteins that differed between WT and RGS14 KO after KA, while M15 was selected due to its association with DEPs between WT and RGS14 KO after saline (baseline). Each module contains a hub protein (eigengene) identified as the first principal component that drives the expression changes and is representative of the expression of the other module proteins (Langfelder and Horvath, 2007). Eigengene values from each of the four modules significantly varied across group (Fig. 14C). Similar to what was seen in the module-trait relationships (Fig. 14B), eigengenes from M5 and M19 modules were considerably lower after KA treatment in WT mice but decreased only slightly after KA treatment in RGS14 KO (Fig. 14C).

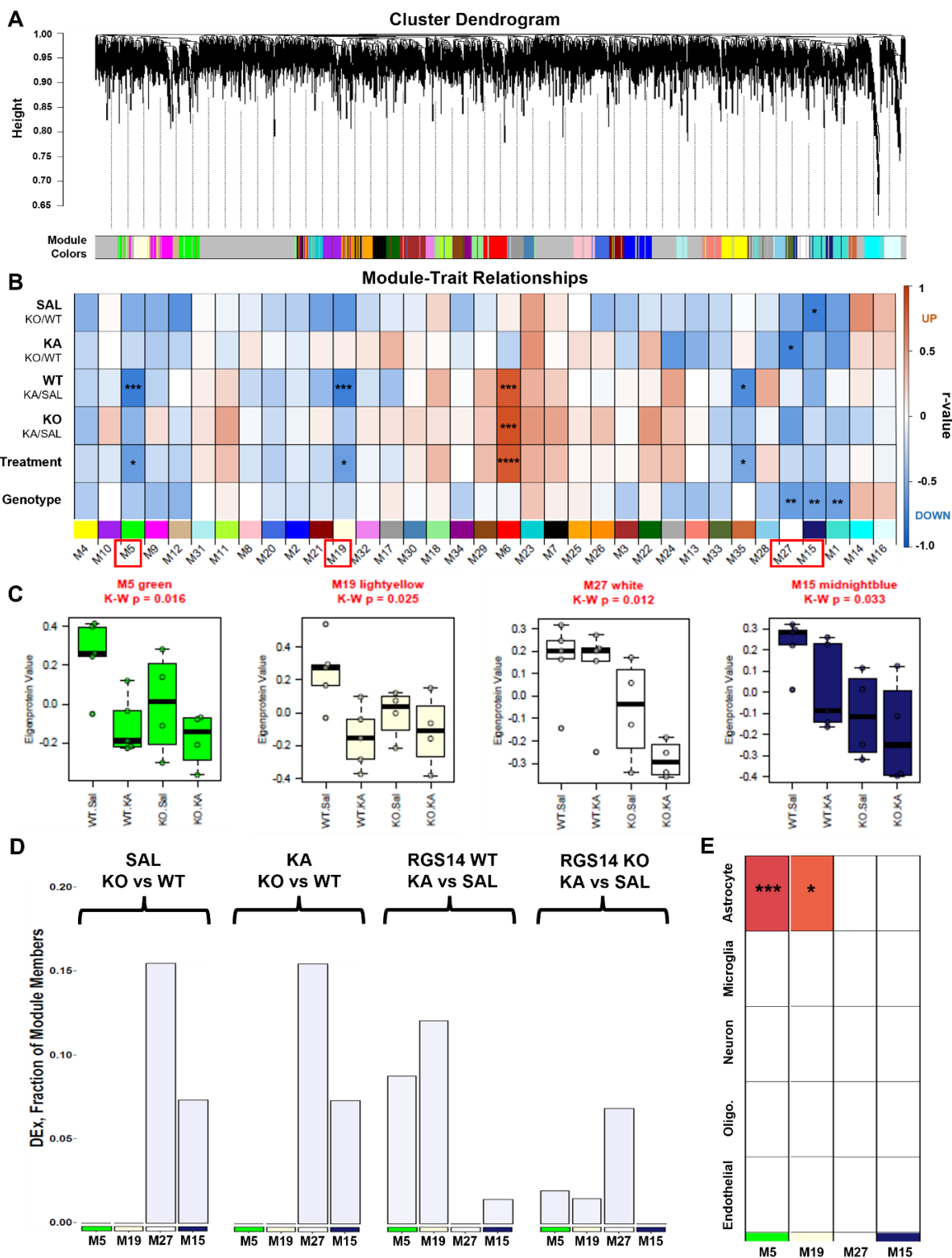


Figure 14. WGCNA uncovers modules of hippocampal proteins that exhibit different expression patterns between WT and RGS14 KO. (unpublished data) (A) Cluster dendrogram

demonstrating the clustering of proteins based on similarity of expression. Peaks represent proteins and the height of peaks represent the degree of relation to the expression module (colored bars below). (B) Heat map showing the degree of correlation of modules with the DEPs identified from differential expression analysis for each comparison and if the expression changes are driven by treatment or genotype. Red represents modules of proteins that were similarly upregulated (positive correlation), while blue represents modules of proteins that were similarly downregulated (negative correlation). (C) Box plots representing the expression pattern of eigengenes that significantly varied between groups. (D) Fraction of DEPs for each differential expression comparison that are represented by the selected modules. (E) Cell-type enrichment analysis demonstrating modules that are enriched with proteins specific to primary brain cell types for each of the selected modules. * $p < 0.05$, ** $p < 0.01$, *** $p < 0.001$, **** $p < 0.0001$.

Comparing between WT and RGS14 KO, the eigengene for M27 differed more within the KA-treated groups whereas the eigengene for M15 differed more within the saline-treated groups (Fig. 14C). Accordingly, M27 and M15 modules contained an appreciable proportion of DEPs that were significantly different between genotypes (Fig. 14D). Likewise, M5 and M19 modules were represented more by DEPs that significantly differed after KA treatment in WT mice compared to RGS14 KO mice (Fig. 14D). When cell-type enrichment was performed on each of the modules, M5 and M19 modules were significantly enriched with proteins associated with astrocytes, while M27 and M15 modules were not associated with any particular cell-type (Fig. 14E). Overall, this corroborates our findings from differential expression analysis, highlighting modules of proteins that are also significantly altered in RGS14 KO mice at baseline or after KA-SE, while unveiling a possible alteration in astrocytic proteins caused by KA-SE in WT mice but not RGS14 KO mice.

Because co-expression modules may reflect shared biological function of protein members, we performed GO analysis on the four modules of interest to determine what biological and cellular processes were associated with each module (Fig. 15). Similar to WT proteins that were downregulated after KA-SE (Fig. 13D), the M5 module contained proteins associated with fatty acid oxidation and metabolism particularly in the mitochondria (e.g. "Mitochondrial Fatty Acid Beta-Oxidation") (Fig. 15A), which makes sense as this module also showed downregulation following KA-SE in WT (Fig. 14). This further emphasizes a role for RGS14 in regulating cellular metabolism during seizure activity, where energy metabolism and mitochondrial function during periods of seizure activity may differ between WT and RGS14 KO hippocampi and contribute to seizure-induced oxidative stress. While ontologies related to fatty acid metabolism were by far the most enriched, the ontology "Regulation of Potassium Ion Transport" was also enriched in this module (Fig. 15A). This is of particular interest as maintenance of potassium gradients is a key component of excitability and seizure occurrence and regulated primarily by astrocytes (Sofroniew and Vinters, 2010).

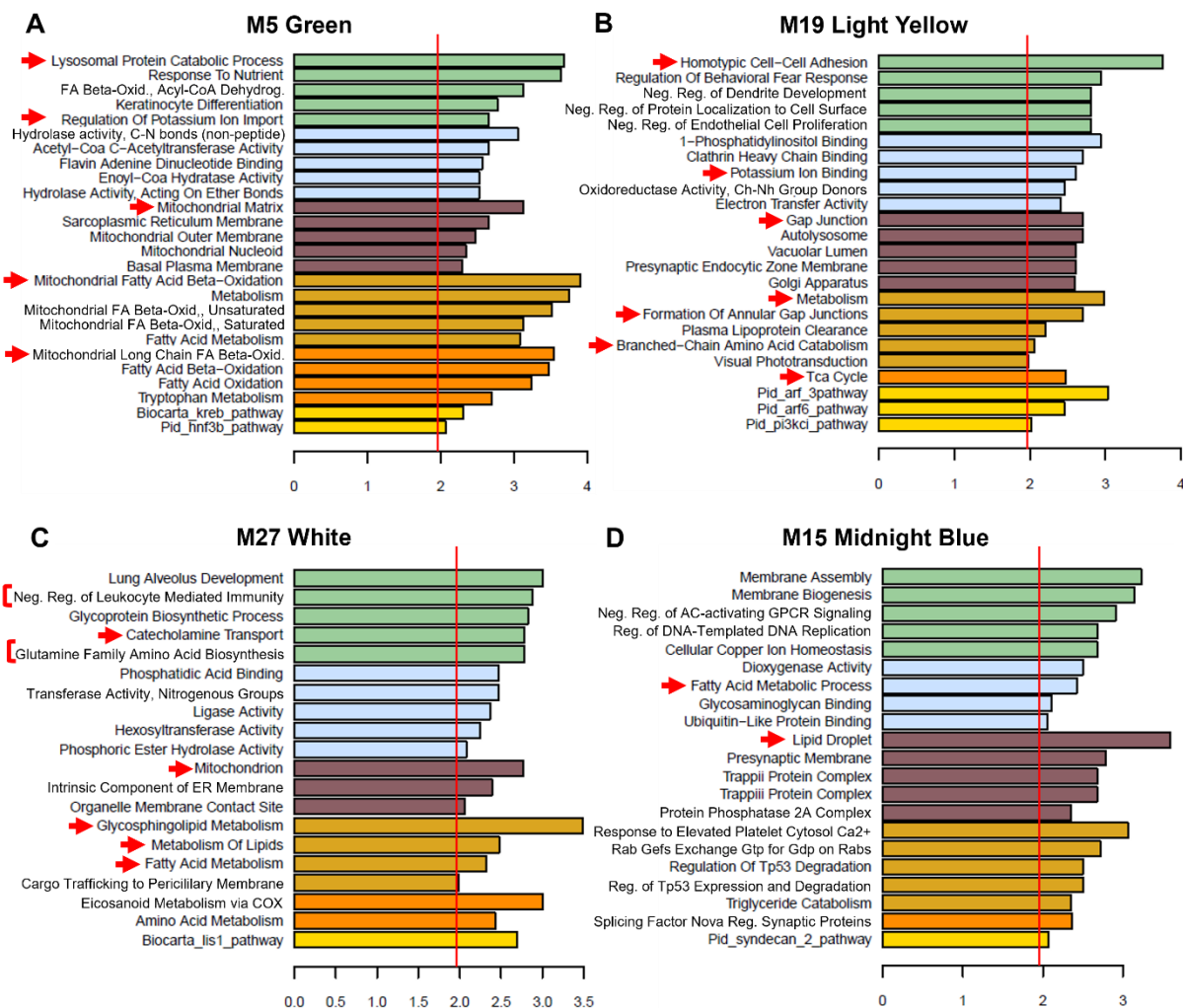


Figure 15. Gene ontology of WGCNA further demonstrates altered metabolic processes altered in RGS14 KO mice. (unpublished data) (A) Plots of significant ontologies associated with proteins in the M5 green module. (B) Plots of significant ontologies associated with proteins in the M19 light yellow module. (C) Plots of significant ontologies associated with proteins in the M27 white module. (D) Plots of significant ontologies associated with proteins in the M15 midnight blue module. Red arrows and brackets indicate ontologies of interest, particularly those related to metabolism and mitochondrial function.

Because this module was also associated with astrocytic proteins (Fig. 14E), this data also suggests a potential dysfunction in astrocytic handling of potassium or astrocytic energy metabolism.

In the M19 module, some of the most enriched ontologies were related to cell-cell adhesion and gap junctions (e.g. “Homotypic Cell-Cell Adhesion”, “Gap Junction”) with some ontologies also related cellular metabolism (e.g. “Metabolism”) (Fig. 15B), which support the proteomics findings thus far. Changes in cell adhesion and gap junctions may reflect RGS14’s ability to suppress synaptic plasticity, as cell adhesion molecules are important mediators of structural enlargement at synapses (Missler et al., 2012). Because this module was also associated with the ontology “Potassium Ion Binding” and astrocytes (Fig. 14E), which form cell-cell junctions with themselves and other cell types (Bennett et al., 2003), this may further indicate dysregulation of astrocytic function in RGS14 KO mice. M27 and M15 modules also contained modules related to metabolism and mitochondrial function (e.g. “Glycosphingolipid Metabolism” and “Mitochondrion” in M27; “Fatty Acid Metabolic Process” in M15) (Fig. 15C, D), and the most enriched ontology in M15 was “Lipid Droplet” (Fig. 15C), which further implicates dysregulation of cellular and lipid metabolism as a potential effect of RGS14 deletion. Additionally, ontologies like “Catecholamine Transport” and “Glutamine Family Amino Acid Biosynthesis” in the M27 module may indicate perturbations in neurotransmitter synthesis and transmission in RGS14 KO mice, where ontologies like “Neg. Reg. of Leukocyte Mediated Immunity” and “Eicosanoid Metabolism” may suggest impairment of inflammatory processes following KA-SE (Fig. 15C). Overall, our findings here corroborate our findings from differential expression where loss of RGS14 impacts a spectrum of predicted and novel cellular pathways, the most prominent being alterations in cellular metabolism and mitochondrial function that may have effects on seizure-induced oxidative stress.

3.5. RGS14 localizes to mitochondria in CA2 PCs and reduces mitochondrial respiration in vitro (Harbin et al., 2023)

Among the protein pathways most affected by loss of RGS14, those associated with mitochondrial function and oxidative stress were most surprising and of interest. To explore a possible role for RGS14 in mitochondrial function, we first tested whether RGS14 localizes to the mitochondria in area CA2 PCs. We used immunogold-labeled electron microscopy (EM) to visualize RGS14 in subcellular structures within area CA2 PCs of untreated WT mice (Fig. 16A). RGS14 immunogold labeling is indicated by spherical black particles in proximal dendrites (Fig. 16A, top left and bottom left panels) or cell bodies (Fig. 16A, top center and far right panels). RGS14 immunogold labeling was associated with the external and crista membranes of mitochondria in both dendrites and cell bodies of CA2 pyramidal cells (Fig. 16A). Control sections from CA2 tissue processed for the immunogold reaction without the RGS14 antibody were almost completely devoid of gold particles over mitochondria (Fig. 16B), indicating the specific localization of RGS14 in mitochondria of CA2 pyramidal neurons.

To determine if RGS14 has an impact on mitochondrial function, we measured oxygen consumption rate (OCR) under basal conditions and following pharmacological inhibition of the ETC in HEK293T cells. We found that cells expressing RGS14 (Fig. 16E) had an overall lower OCR profile compared to cells not expressing RGS14 (Fig. 16C), indicating that RGS14 reduces mitochondrial respiration and is consistent with a previous report that RGS14 had effects on mitochondrial respiration in brown adipose tissue (Vatner et al., 2018). We analyzed the area under the curve to quantify different mitochondrial respiration parameters (Gu et al., 2021) and found that RGS14 reduced basal respiration (28.7% reduction relative to control) and maximal respiration (23.3% reduction relative to control) without affecting proton leak, ATP-linked respiration, spare capacity, and non-mitochondrial respiration (Fig. 16D).

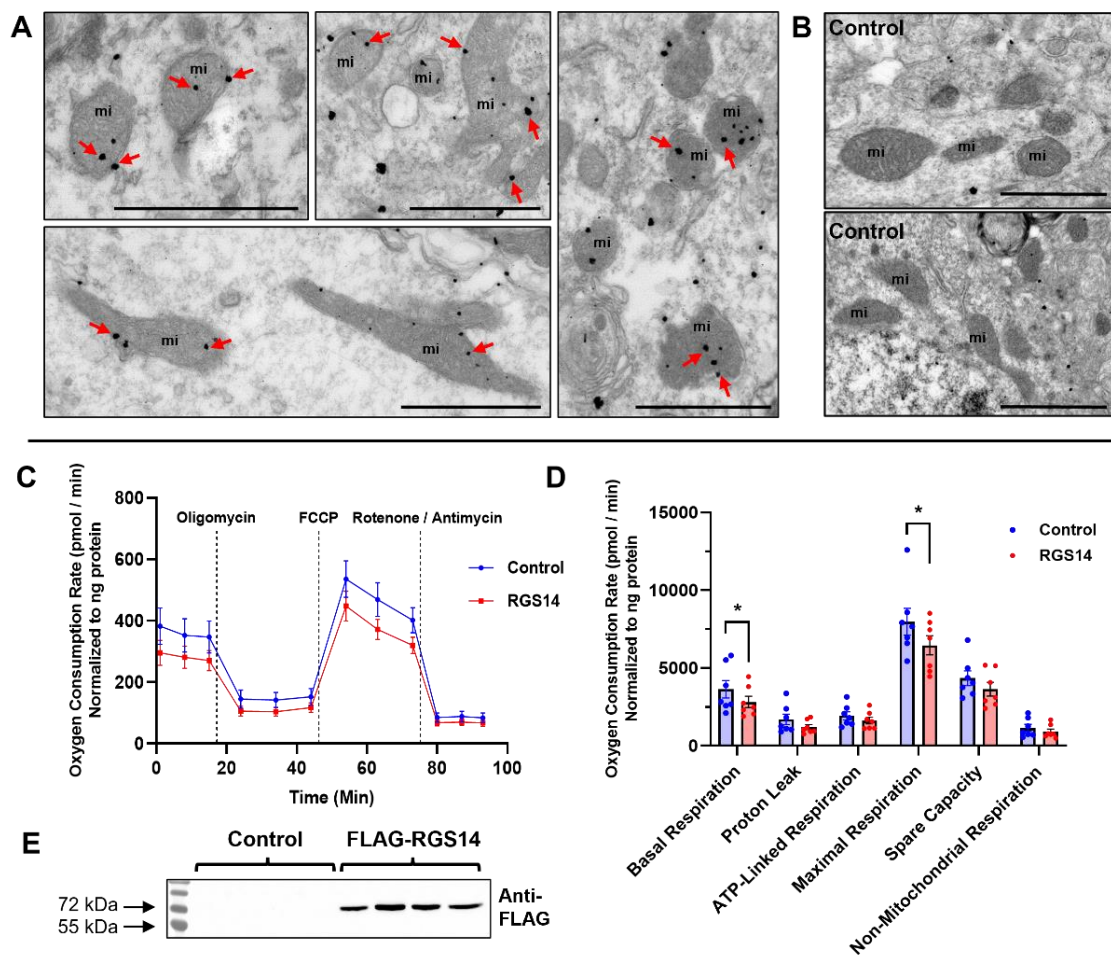


Figure 16. RGS14 localizes to mitochondria in CA2 PCs and reduces mitochondrial respiration *in vitro*. (Harbin et al., 2023) (A) Electron micrographs of CA2 hippocampal region showing RGS14 immunogold labeling in mitochondria. *Top left* and *bottom left* panels depict labeling in dendritic processes, while *center* and *right* panels show neuronal cell body labeling. Gold labeling can be found both on the external and crista membranes of the mitochondria (red arrows). (B) Negative control micrographs showing non-specific immunogold background labeling from sections incubated without the RGS14 antibody. Note the lack of labeling over mitochondria. Scale bars: 1 μm . (C) Normalized oxygen consumption rate plotted over time in HEK293T cells expressing pcDNA3.1 (control) or FLAG-RGS14 (RGS14) during a mitochondrial stress test. Measurements start at baseline and are followed by sequential treatments of cells with mitochondrial inhibitors oligomycin, FCCP, and rotenone/antimycin A. (D) Quantification of

parameters derived from panel (C) that are representative mitochondrial function during the assay (n = 7 per transfection condition). (E) Representative Western blot verifying overexpression of RGS14 in HEK293T cells transfected with FLAG-RGS14 compared to pcDNA3.1 (control).

Statistical Analysis: (D) Unpaired t-tests to compare mean OCR between control vs RGS14 groups (basal respiration, 3627.11 ± 297.19 vs 2819.16 ± 196.95 , *p < 0.05; maximal respiration, 7965.98 ± 430.71 vs 6458.40 ± 324.92 , *p < 0.05). Error bars represent the SEM. FCCP, carbonilcyanide p-trifluoromethoxyphenylhydrazone.

Together, this data supports a role for RGS14 in the regulation of mitochondrial function, possibly in area CA2 where metabolic function and mitochondrial gene expression is enriched (Farris et al., 2019).

3.6. RGS14 is necessary for SOD2 induction in area CA2 and prevents 3-nitrotyrosine accumulation (Harbin et al., 2023)

Superoxide and other reactive metabolites are generated by seizure activity, and this seizure-induced oxidative stress plays an important role in mediating seizure pathology (Puttachary et al., 2015). SOD2 is the primary enzyme that detoxifies mitochondrial superoxide, and its altered expression or activity can be deleterious (Holley et al., 2011). Loss of SOD2 exacerbates KA-induced oxidative stress, hippocampal hyperexcitability, and cell death, whereas SOD2 overexpression ameliorates these effects (Liang et al., 2000; Liang and Patel, 2004). We noted that SOD2 was significantly upregulated in RGS14 KO hippocampi after KA as identified by our proteomics (Fig. 12A and Table 2).

Because RGS14 localized to mitochondria in area CA2 (Fig. 16) and loss of RGS14 altered mitochondrial superoxide metabolic pathways (Figs. 12-15), we examined the impact of RGS14 loss and seizure on SOD2 protein expression and oxidative stress in hippocampal area CA2 (Fig. 17A-C). We used IHC to quantify SOD2 expression across the hippocampus one day after saline or KA-SE (Fig. 17A). In area CA2, SOD2 expression in both cell bodies (SP) and proximal dendrites (SR) was noticeably similar between WT (Fig. 17A, top left) and RGS14 KO (Fig. 17A, bottom left) after saline treatment. Contrary to our proteomic results, we observed a remarkable increase of SOD2 expression in WT CA2 (Fig. 17A, top right) that was not evident in RGS14 KO CA2 (Fig. 17A, bottom right). In CA2 cell bodies (SP), SOD2 expression was significantly altered by genotype, treatment, and an interaction between the two (Fig. 17B), where post-hoc analysis revealed higher levels of SOD2 in KA-treated WT mice compared to SAL-treated WT CA2 (71.55 fold higher) or KA-treated KO CA2 (7.71 fold higher).

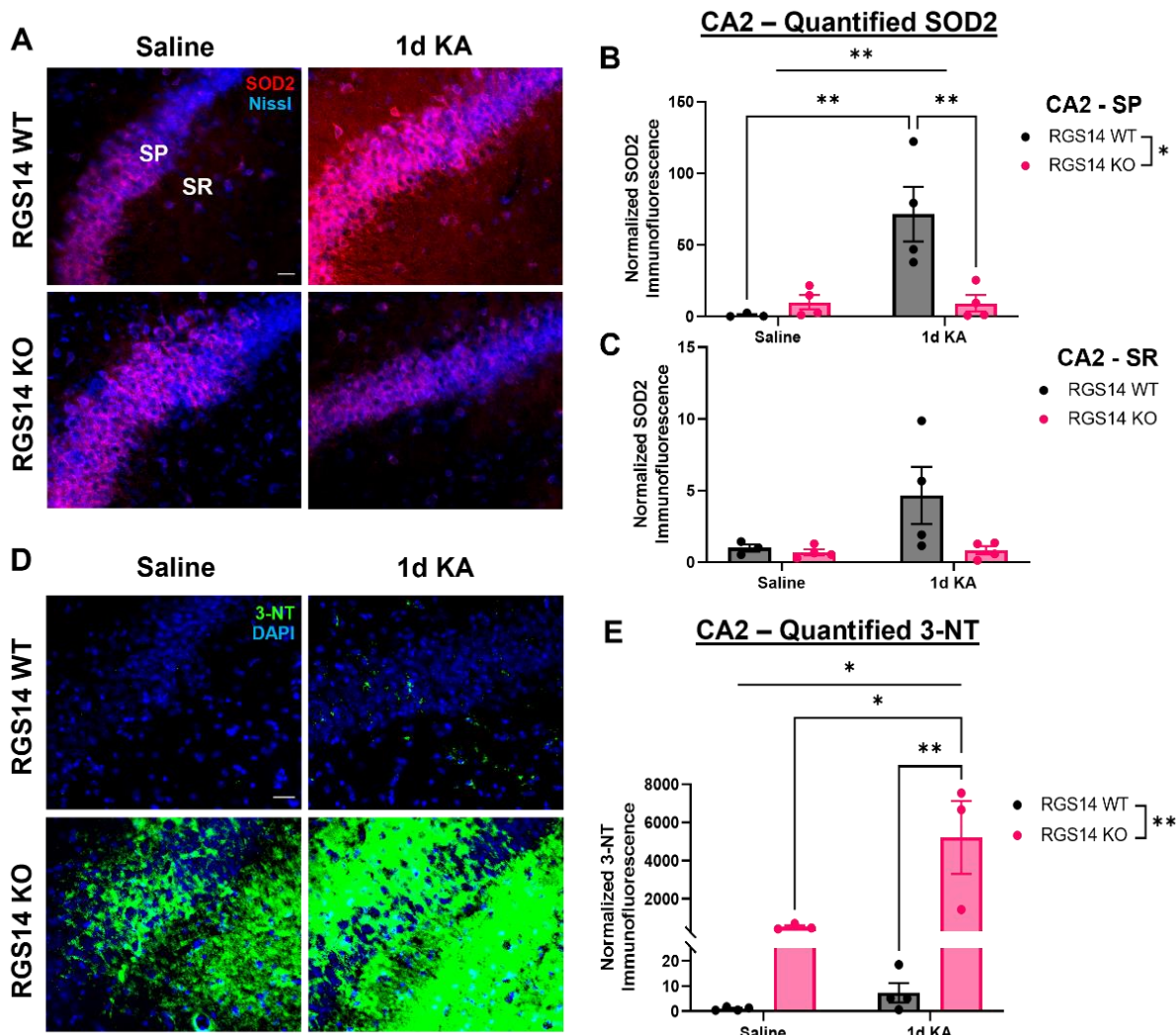


Figure 17. RGS14 is necessary for SOD2 induction in area CA2 and prevents 3-nitrotyrosine accumulation. (Harbin et al., 2023) (A) Representative IHC images of superoxide dismutase 2 (SOD2) expression in WT and RGS14 KO CA2 one day after saline or KA-SE. Note the induction of SOD2 expression after KA-SE in WT but not RGS14 KO CA2. SP and SR represent regions of analysis for cell body (SP) and dendritic (SR) layers of CA2. Scale bar, 20 μ m. (B) Mean SOD2 immunofluorescence in the cell bodies (SP) of CA2 expressed relative to saline-treated WT mean (SAL: WT, n=3, 1.00 ± 0.76 ; RGS14 KO, n=4, 10.09 ± 4.93 ; 1d KA: WT, n=4, 71.55 ± 19.06 ; RGS14 KO, n=4, 9.28 ± 5.76). (C) Mean SOD2 immunofluorescence in the proximal dendrites (SR) of CA2 expressed relative to saline-treated WT mean (SAL: WT, $1.00 \pm$

0.26; RGS14 KO, 0.70 ± 0.21 ; 1d KA: WT, 4.65 ± 2.00 ; RGS14 KO, 0.84 ± 0.29). (D) Representative IHC images of 3-nitrotyrosine (3-NT) staining in WT and RGS14 KO CA2 one day after saline or KA-SE. 3-NT is detected in striking abundance in RGS14 KO mice compared to WT mice, an effect that is exacerbated following KA-SE. Scale bar, 20 μm . (E) Mean immunofluorescence of 3-NT staining in area CA2 expressed relative to saline-treated WT mean (SAL: WT, $n=4$, 1.00 ± 0.32 ; RGS14 KO, $n=3$, 532.56 ± 83.88 ; 1d KA: WT, $n=4$, 7.33 ± 3.86 ; RGS14 KO, $n=3$, 5213.93 ± 1908.17). *Statistical analysis*: (B, C, E) Two-way ANOVA with Tukey post-hoc comparisons used to compare group means (B, two-way ANOVA, $F = 5.68$ for genotype, $*p < 0.05$; $F = 9.77$ for treatment, $*p < 0.05$; $F = 10.23$ for interaction, $**p < 0.01$; Tukey's, WT SAL vs WT KA, $**p < 0.01$; WT KA vs KO KA, $**p < 0.01$) (E, two-way ANOVA, $F = 12.89$ for genotype, $**p < 0.01$; $F = 8.61$ for treatment, $*p < 0.05$; $F = 8.56$ for interaction, $*p < 0.05$; Tukey's, KO SAL vs WT KA, $*p < 0.05$; WT KA vs KO KA, $**p < 0.01$). Error bars represent the SEM. SP, stratum pyramidale; SR, stratum radiatum. 3-NT, 3-nitrotyrosine.

Although there was an apparent increase in SOD2 in CA2 dendrites (SR) in KA-treated WT mice relative to the other groups, these results were not statistically significant (Fig. 17C). In area CA1, we found SOD2 expression to be opposite of area CA2, where SOD2 expression is increased in KA-treated RGS14 KO compared to KA-treated WT (5.85 fold higher in SP; 8.48 fold higher in SR) (Fig. 18). This data suggests RGS14 could influence superoxide levels in the hippocampus by modulating SOD2 expression and also helps explain the paradoxical results between our proteomics and IHC, as whole hippocampi were used for proteomics and the volume of CA2 is considerably smaller than CA1 (Iglesias et al., 2015).

To determine if loss of RGS14 increases superoxide production and exacerbates oxidative stress, we evaluated the expression of hippocampal 3-nitrotyrosine (3-NT) using IHC one day after saline or KA-SE (Fig. 17D, E). Tyrosine oxidizes to 3-NT when exposed to peroxynitrite, a highly reactive species that forms from O_2^- and NO. 3-NT is commonly used as a marker for oxidative stress and can greatly impact protein function and signaling (Bandookwala and Sengupta, 2020; Campolo et al., 2020). Quite remarkably, we observed a dramatic increase of 3-NT staining in CA2 of RGS14 KO mice relative to WT after saline or KA-SE. (Fig. 17D). Quantification and comparison of 3-NT staining in area CA2 revealed a significant effect of genotype, treatment, and an interaction between treatment and genotype, suggesting loss of RGS14 and KA-SE influence the abundance of 3-NT in CA2 (Fig. 17E). Although post-hoc analysis showed no difference of CA2 3-NT staining between WT and RGS14 KO after saline treatment, we did find 3-NT abundance in KO CA2 was increased after KA compared to SAL-treated KO CA2 (9.79 fold higher) and KA-treated WT CA2 (72.87 fold higher) (Fig. 17E). Although RGS14 modulates SOD2 expression in CA1, we observed no genotype or treatment differences in 3-NT staining in this area (data not shown).

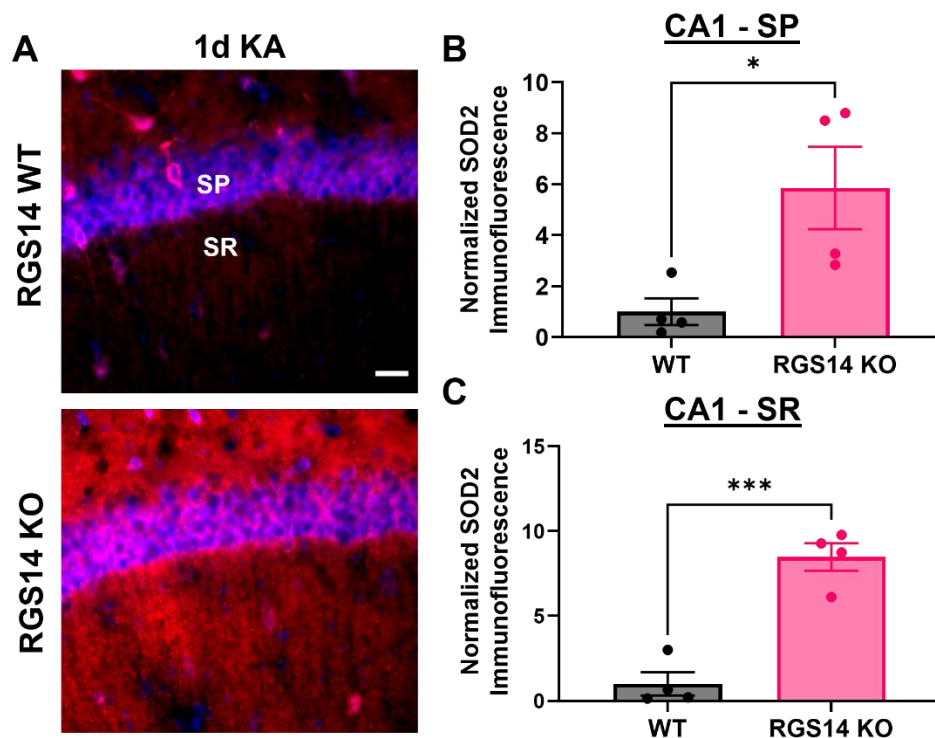


Figure 18. SOD2 is upregulated in area CA1 of RGS14 KO mice one day after KA-SE. (Harbin et al., 2023) (A) Representative IHC images of superoxide dismutase 2 (SOD2) expression in WT and RGS14 KO CA2 one day after KA-SE. SP and SR represent regions of analysis for cell body (SP) and dendritic (SR) layers of CA2. (B) Mean SOD2 immunofluorescence in the SP layer of CA1 expressed relative to WT mean (WT, 1.00 ± 0.52 ; RGS14 KO, 5.85 ± 1.62). (C) Mean SOD2 immunofluorescence in the SR layer of CA1 expressed relative to WT mean (WT, 1.00 ± 0.68 ; RGS14 KO, 8.48 ± 0.81). *Statistical analysis:* (B, C) Group means compared using unpaired t-tests (B, WT vs RGS14 KO, $*p < 0.05$) (C, WT, vs RGS14 KO, $***p < 0.001$). Error bars represent the SEM. SP, stratum pyramidale; SR, stratum radiatum.

Overall, these results provide compelling evidence that RGS14 limits excessive amounts of superoxide and prevents accumulation of 3-NT in area CA2 likely by regulating some aspects of mitochondrial function and promoting SOD2 expression after KA.

3.7. Loss of RGS14 does not alter early hippocampal neuronal injury in areas CA2 or CA1 after KA-SE (Harbin et al., 2023)

Because loss of RGS14 sensitized mice to behavioral seizures by KA (Fig. 9), we hypothesized that RGS14 KO mice would have more severe neurodegeneration in the hippocampus, possibly in CA2 PCs that are typically resistant to such injury (Hatanpaa et al., 2014; Steve et al., 2014) or CA1 PCs that also induce RGS14 expression after KA-SE. As such, we assessed hippocampal neuronal injury in the dorsal hippocampus as well as the subiculum, entorhinal/perirhinal cortices, lateral amygdala, and dorsomedial thalamus one day following KA-SE in WT and RGS14 KO mice using Fluoro-Jade B (FJB), a sensitive dye that labels degenerating neurons after SE (Schmued et al., 1997). Somewhat unexpectedly, we observed no FJB labeling in hippocampal areas CA1 (Fig. 19D) or CA2 (Fig. 19E) of either WT (Fig. 19A) or RGS14 KO mice (Fig. 19B). However, FJB labeling in area CA3 was observed in both WT and RGS14 KO mice (Fig. 11F), where neuronal injury was expected and is typically observed after KA-SE (Ben-Ari and Cossart, 2000). RGS14 KO mice appeared to have increased FJB labeling in CA3 relative to WT mice (Fig. 19F), though quantification and comparison of FJB+ cell counts in CA3 revealed no significant differences between WT and RGS14 KO mice (Fig. 19C), likely due to the high variability of FJB labeling between RGS14 KO mice. Moreover, we observed no labeling in the subiculum (Fig. 19G), the perirhinal/entorhinal cortex (Fig. 19H), the lateral amygdala (Fig. 19I), or dorsomedial thalamus (Fig. 19J), where neuronal injury from KA-SE has also been reported (Rusina et al., 2021). Contrary to our hypothesis, these results suggest RGS14 is not necessary for protection against early excitotoxic injury caused by KA-SE in CA2 or CA1 PCs, where RGS14 was found to be upregulated at the same time point (Fig. 11).

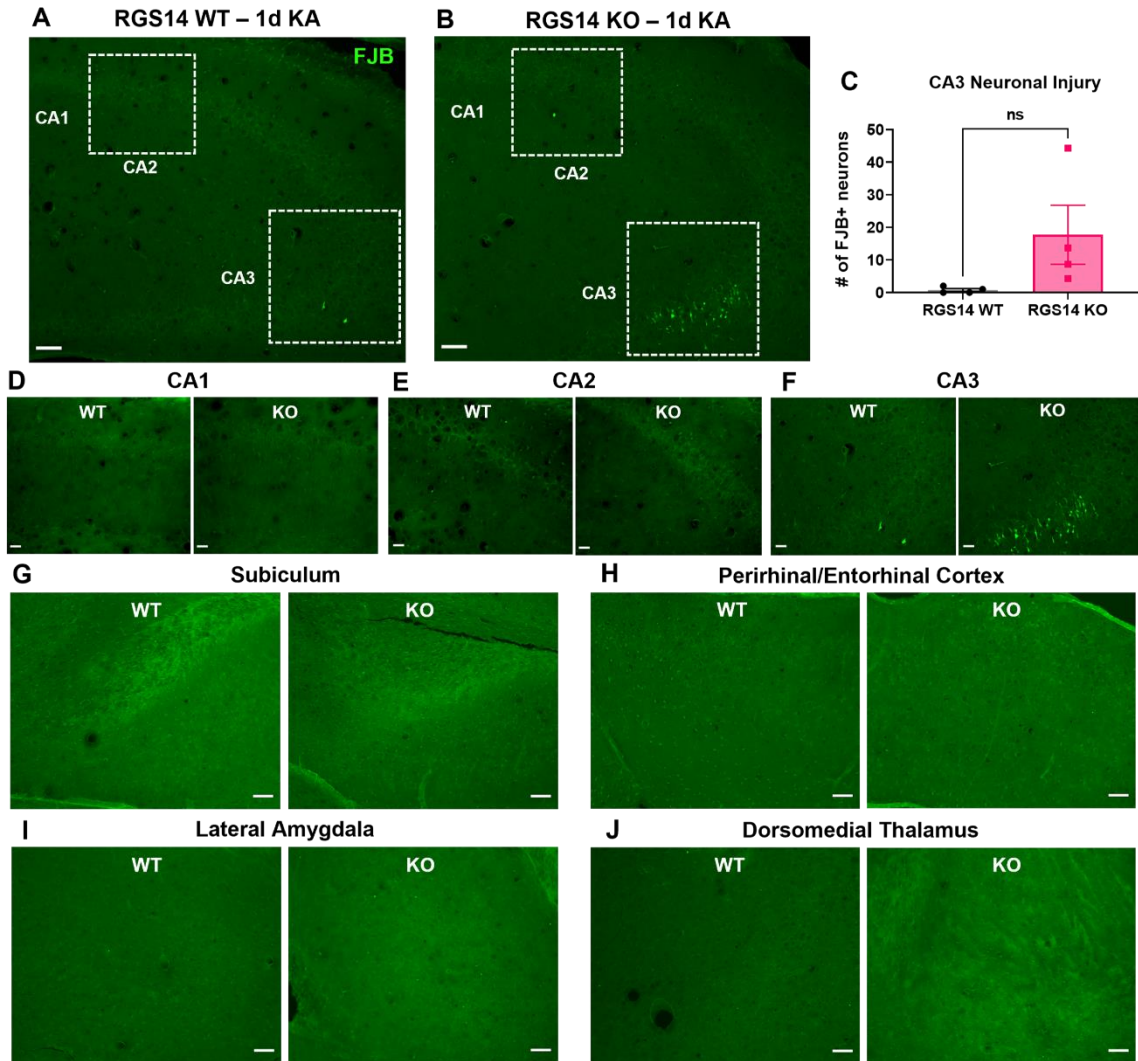


Figure 19. Loss of RGS14 does not alter early hippocampal neuronal injury in areas CA2 or CA1 after KA-SE. (Harbin et al., 2023) (A-B) Representative FluroJade B (FJB) staining in WT (A) and RGS14 KO (B) dorsal hippocampi 1 day following KA-SE (A). Dashed box represents the injured region of area CA3. Scale bar, 50 μ m. (C) Mean number of FJB+ neurons in area CA3 of the dorsal hippocampus after KA-SE (n = 4 per genotype) (WT, 0.75 ± 0.48 ; RGS14 KO, 17.75 ± 9.06) (D-F) Representative images of area CA1 (D), CA2 (E), and CA3 (F) in WT and RGS14 KO mice. Scale bar, 20 μ m. (G-J) Representative images of the subiculum, perirhinal/entorhinal cortex, lateral amygdala, and dorsomedial thalamus in WT and RGS14 KO mice. Scale bar, 50

μm . *Statistical Analysis:* (C) Unpaired t-test was used to compare mean number of FJB+ neurons (WT vs RGS14 KO, $p > 0.05$). Error bars represent the SEM.

3.8. *RGS14* is required for glial response to KA-SE (Harbin et al., 2023 and unpublished data)

Hippocampal microgliosis shortly follows SE, such that microglia are recruited to sites of hyperexcitability and are activated by a variety of factors that induce morphological changes (Hiragi et al., 2018). As a final examination of seizure pathology, we sought to determine if loss of *RGS14* altered microglial recruitment and activation to the hippocampus following KA-SE. To test this hypothesis, we performed IHC using IBA1 as a marker to specifically label microglia and quantify microglial number and size in the hippocampus of WT and *RGS14* KO mice one day after saline or KA-SE (Fig. 20A). Overall, we observed no visible differences in microglial number or morphology between saline-treated WT and *RGS14* KO (Fig. 12A, top panels). However, while there was a noticeable increase in IBA1 immunoreactivity in WT hippocampus after KA-SE, such was not the case in *RGS14* KO mice (Fig. 20A, bottom panels), suggesting that *RGS14* could mediate microglial activation.

To determine microglia reactivity (increase in number and size of microglia) and potential subregional differences in microglial activation between WT and *RGS14* KO hippocampi, we quantified the density of IBA1+ microglia (number of microglia/area of analysis) and area of IBA1+ microglia for each hippocampal subregion. In CA1 (Fig. 20B), we found a significant effect of genotype on microglia density with significantly more microglia in WT CA1 compared to *RGS14* KO CA1 after KA-SE (85% increase) (Fig. 20C). Additionally, there was a significant effect of genotype and interaction between treatment and genotype on microglia size in CA1, where microglia were significantly larger in KA-treated WT mice compared to SAL-treated WT (104% larger) or KA-treated *RGS14* KO (141% larger) (Fig. 20D). In CA2 (Fig. 20E), we observed a significant effect of treatment and genotype on microglia density, where there were significantly more microglia in KA-treated WT CA2 compared to SAL-treated WT (92% increase) or KA-treated *RGS14* KO CA2 (156% increase) (Fig. 20F). Subsequently, there was an effect of treatment on microglia size in CA2, where only WT microglia increased in size following KA-SE (99% larger)

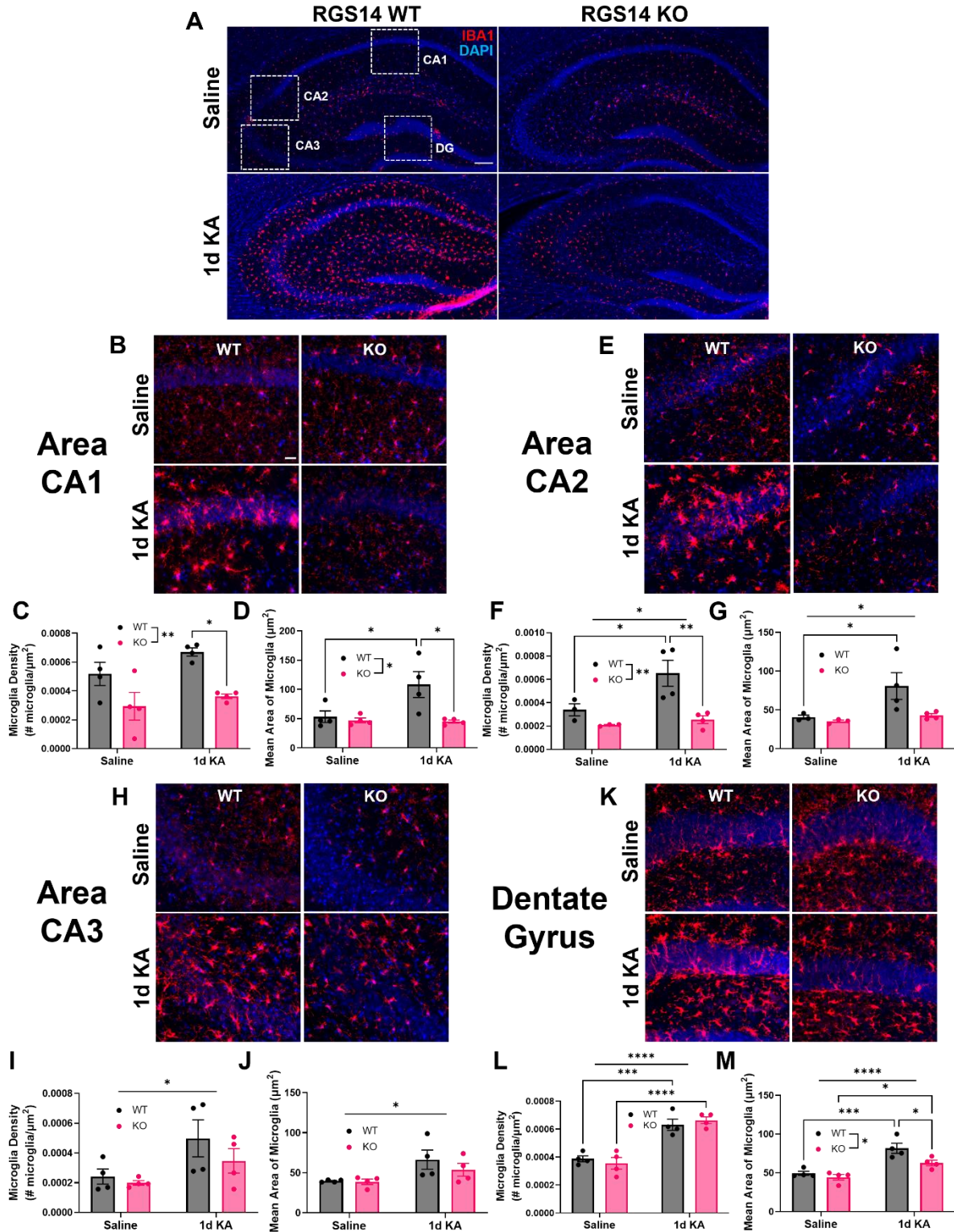


Figure 20. RGS14 is required for microglial recruitment and activation in hippocampal areas CA1 and CA2. (Harbin et al., 2023) (A) Representative IHC images of ionized calcium

binding adaptor molecule 1 (IBA1) as a marker of microglia and DAPI (nuclei marker) in the dorsal hippocampus of WT and RGS14 KO mice one day after saline or KA-SE. Scale bar, 100 μm . (B, E, H, K) Representative IHC images of IBA1 expression in area CA1 (B), CA2 (E), CA3 (H), and DG (K) in WT and RGS14 KO mice one day after saline or KA-SE. Scale bar, 20 μm . (C) Mean microglial density for CA1 (# microglia/ $\mu\text{m}^2 \text{e-04}$) (SAL: WT, 5.19 ± 0.80 ; KO, 2.94 ± 0.96 ; 1d KA: WT, 6.71 ± 0.28 ; KO, 3.63 ± 0.16). (D) Mean area (size) of IBA1+ microglia in CA1 (μm^2) (SAL: WT, 53.19 ± 9.85 ; KO, 47.09 ± 4.22 ; 1d KA: WT, 108.31 ± 22.13 ; KO, 45.02 ± 2.60). (F) Mean microglial density for CA2 (# microglia/ $\mu\text{m}^2 \text{e-04}$) (SAL: WT, n=3, 3.39 ± 0.52 ; KO, n=3, 2.08 ± 0.05 ; 1d KA: WT, 6.52 ± 1.11 ; KO, 2.54 ± 0.33). (G) Mean area (size) of IBA1+ microglia in CA2 (μm^2) (SAL: WT, n=3, 40.61 ± 2.68 ; KO, n=3, 35.34 ± 1.61 ; 1d KA: WT, 80.84 ± 17.26 ; KO, 42.91 ± 2.37). (I) Mean microglial density for CA3 (# microglia/ $\mu\text{m}^2 \text{e-04}$) (SAL: WT, 2.42 ± 0.51 ; KO, 1.99 ± 0.15 ; 1d KA: WT, 4.99 ± 1.24 ; KO, 3.47 ± 0.82). (J) Mean area (size) of IBA1+ microglia in CA3 (μm^2) (SAL: WT, 53.19 ± 9.85 ; KO, 47.09 ± 4.22 ; 1d KA: WT, 108.31 ± 22.13 ; KO, 45.02 ± 2.60). (L) Mean microglial density for DG (# microglia/ $\mu\text{m}^2 \text{e-04}$) (SAL: WT, 3.87 ± 0.21 ; KO, 3.55 ± 0.42 ; 1d KA: WT, 6.31 ± 0.40 ; KO, 6.63 ± 0.25). (M) Mean area (size) of IBA1+ microglia in CA1 (μm^2) (SAL: WT, 49.37 ± 2.61 ; KO, 44.44 ± 3.68 ; 1d KA: WT, 81.71 ± 6.50 ; KO, 62.72 ± 3.60). n=4 per genotype and condition unless noted otherwise. *Statistical analysis*: Two-way ANOVA with Tukey's or Sidak's post-hoc comparisons was used to compare mean microglial density (C, F, I, L) and area (D, G, J, M) between treatment and genotype (C, two-way ANOVA, $F = 16.95$ for genotype, $**p < 0.01$; Sidak's, WT KA vs KO KA, $*p < 0.05$) (D, two-way ANOVA, $F = 7.87$ for genotype, $*p < 0.05$; $F = 5.35$ for interaction, $*p < 0.05$; Tukey's, WT SAL vs WT KA, $*p < 0.05$; WT KA vs KO KA, $*p < 0.05$) (F, two-way ANOVA, $F = 13.41$ for genotype, $**p < 0.01$; $F = 6.22$ for treatment, $*p < 0.05$; Tukey's, WT SAL vs WT KA, $*p < 0.05$; WT KA vs KO KA, $**p < 0.01$) (G, two-way ANOVA, $F = 5.29$ for treatment, $*p < 0.05$; Sidak's, WT SAL vs WT KA, $*p < 0.05$) (I, two-way ANOVA, $F = 6.58$ for treatment, $*p < 0.05$) (L, two-way ANOVA, $F = 7.81$ for treatment, $*p < 0.05$) (B, two-way ANOVA, $F = 68.49$ for treatment, $****p < 0.0001$; Sidak's, WT SAL vs WT

KA, *** $p < 0.001$; KO SAL vs KO KA, **** $p < 0.0001$) (M, two-way ANOVA, $F = 7.58$, * $p < 0.05$; $F = 33.93$ for treatment, **** $p < 0.0001$; Tukey's, WT SAL vs WT KA, *** $p < 0.001$; KO SAL vs KO KA, * $p < 0.05$; WT KA vs KO KA, * $p < 0.05$). Error bars represent the SEM.

(Fig. 20G). This was a surprising result as pronounced microglial activation typically follows intense seizure activity (Eyo et al., 2017) and RGS14 KO mice had a more severe seizure response to KA (Fig. 9). Interestingly, RGS14 expression in glia has not been demonstrated, which could indicate a neuronal mechanism of promoting microgliosis. However, this suggests that RGS14 is necessary for microglia activation after KA-SE in hippocampal area CA1 and CA2, where RGS14 expression was coincidentally found to be upregulated (Fig. 11).

In contrast to area CA1 and CA2, we found that IBA1+ microglia were similarly activated between WT and RGS14 KO in area CA3 (Fig. 20H). In CA3, there was only a significant effect of treatment on IBA1+ microglia density (Fig. 20I) and average IBA1+ microglia area (Fig. 20J) with no significant differences between groups in post-hoc analysis. In the DG (Fig. 20K), KA-SE increased microglia density regardless of genotype (63% increase in WT; 86% increase in KO) (Fig. 20L). We also found a significant effect of both treatment and genotype on average IBA1+ microglia area in the DG (Fig. 20M). Although microglia from both WT DG and RGS14 KO DG were significantly larger after KA-SE compared to saline counterparts (65% larger in WT; 41% larger in KO), KO microglia from DG were slightly but significantly smaller than WT DG microglia after KA-SE (30% smaller) (Fig. 20M). To see if this effect persisted at a later time point, we performed the same analysis in WT and RGS14 KO hippocampi seven days after KA-SE (Fig. 21). Similarly, we found that WT mice had significantly more microglia relative to RGS14 KO mice in both CA1 (161% increase) (Fig. 21A, B) and CA2 (141% increase) (Fig. 21D, E). However, average microglial size did not differ between genotypes in CA1 (Fig. 21C) or CA2 (Fig. 21F). At this time point, microglia density was similar to that observed at 1 day after KA-SE, while microglial size was more similar to that observed in saline controls (Fig. 20), indicating that only WT microglia are recruited and activated to sites of injury or hyperexcitability and remain there at later time points following KA-SE (albeit in a different morphological or activation state), whereas RGS14 KO microglia fail to become recruited or activated at any of the observed time points.

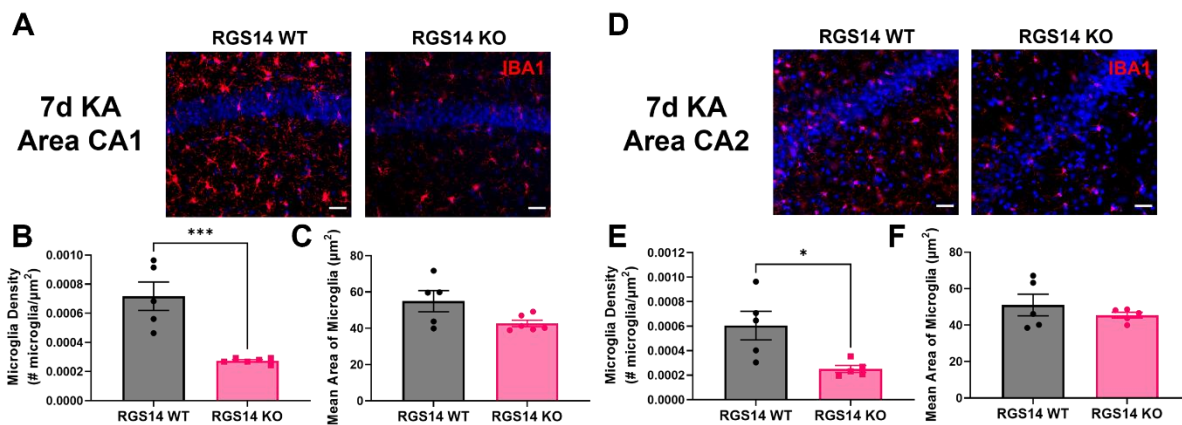


Figure 21. Reduction in microglial density persists 7 days after KA-SE in RGS14 KO mice.

(unpublished data) (A) Representative IHC images of IBA1 in the dorsal hippocampal area CA1 of WT and RGS14 KO mice seven days after KA-SE. Scale bar, 20 μm . (B) Mean microglial density for CA1 (# microglia/ μm^2 e-04) (WT, n=5, 7.17 ± 0.97 ; RGS14 KO, n=6, 2.74 ± 0.08). (C) Mean area (size) of IBA1+ microglia in CA1 (μm^2) (WT, n=5, 54.96 ± 5.83 ; KO, n=6, 42.67 ± 1.77). (D) Representative IHC images of IBA1 in the dorsal hippocampal area CA2 of WT and RGS14 KO mice seven days after KA-SE. Scale bar, 20 μm . (E) Mean microglial density for CA2 (# microglia/ μm^2 e-04) (WT, n=5, 6.05 ± 1.16 ; RGS14 KO, n=5, 2.51 ± 0.29). (F) Mean area (size) of IBA1+ microglia in CA2 (μm^2) (WT, n=5, 51.02 ± 5.95 ; KO, n=5, 45.42 ± 1.60). *Statistical analysis:* Group means were compared using unpaired t-test. (B, WT vs RGS14 KO, ***p < 0.001) (C, WT vs RGS14 KO, p > 0.05) (E, WT vs RGS14 KO, *p < 0.05) (F, WT vs RGS14 KO, p > 0.05). Error bars represent the SEM.

Taken together, this data suggests RGS14 is required for microgliosis in area CA1 and CA2, but not CA3 or DG following KA-SE, a novel finding for a protein whose expression is restricted to neurons in the brain, and establishes a clear role for RGS14 in determining early seizure pathology.

Like microglia, astrocytes also become reactive from activating factors released from neurons and microglia following SE, which causes a marked increase in the number GFAP-expressing astrocytes (i.e. astrogliosis) although delayed and subsequent to microgliosis (Sano et al., 2021). Because microglial response was suppressed in RGS14 KO mice (Fig. 20, 21) and our findings from WGCNA revealed reductions in astrocytic proteins that may alter their function, we sought to determine if astrocyte reactivity was also altered in RGS14 KO mice compared to WT mice using IHC to visualize GFAP+ astrocytes in the dorsal hippocampus and quantify GFAP immunoreactivity (Fig. 22). One day following KA-SE or saline, we observed an apparent decrease in GFAP immunoreactivity in CA1 of RGS14 KO mice relative to WT (Fig. 22A), particularly following KA-SE. However, there was no statistically significant effect of genotype or treatment on GFAP immunoreactivity (Fig. 22C). Because astrocyte response is typically delayed compared to microglial response following SE (Sano et al., 2021), which may explain the lack of treatment effect one day following KA-SE, we quantified GFAP immunoreactivity seven days after KA-SE in CA1 (Fig. 22B). At this later time point, we found GFAP immunoreactivity was significantly decreased in CA1 of RGS14 KO mice compared to WT (95% decrease) (Fig. 22D), demonstrating that loss of RGS14 impacts astrocyte reactivity to KA-SE similar to what was seen for microglia. In area CA2, we again saw a remarkable decrease in GFAP expression in RGS14 KO mice (Fig. 22E), an effect that became more pronounced one day after KA-SE. Indeed, there was a main effect of genotype on GFAP immunoreactivity in CA2 (Fig. 22G), suggesting that astrocytes from RGS14 KO animals may have impaired function regardless of treatment in CA2.

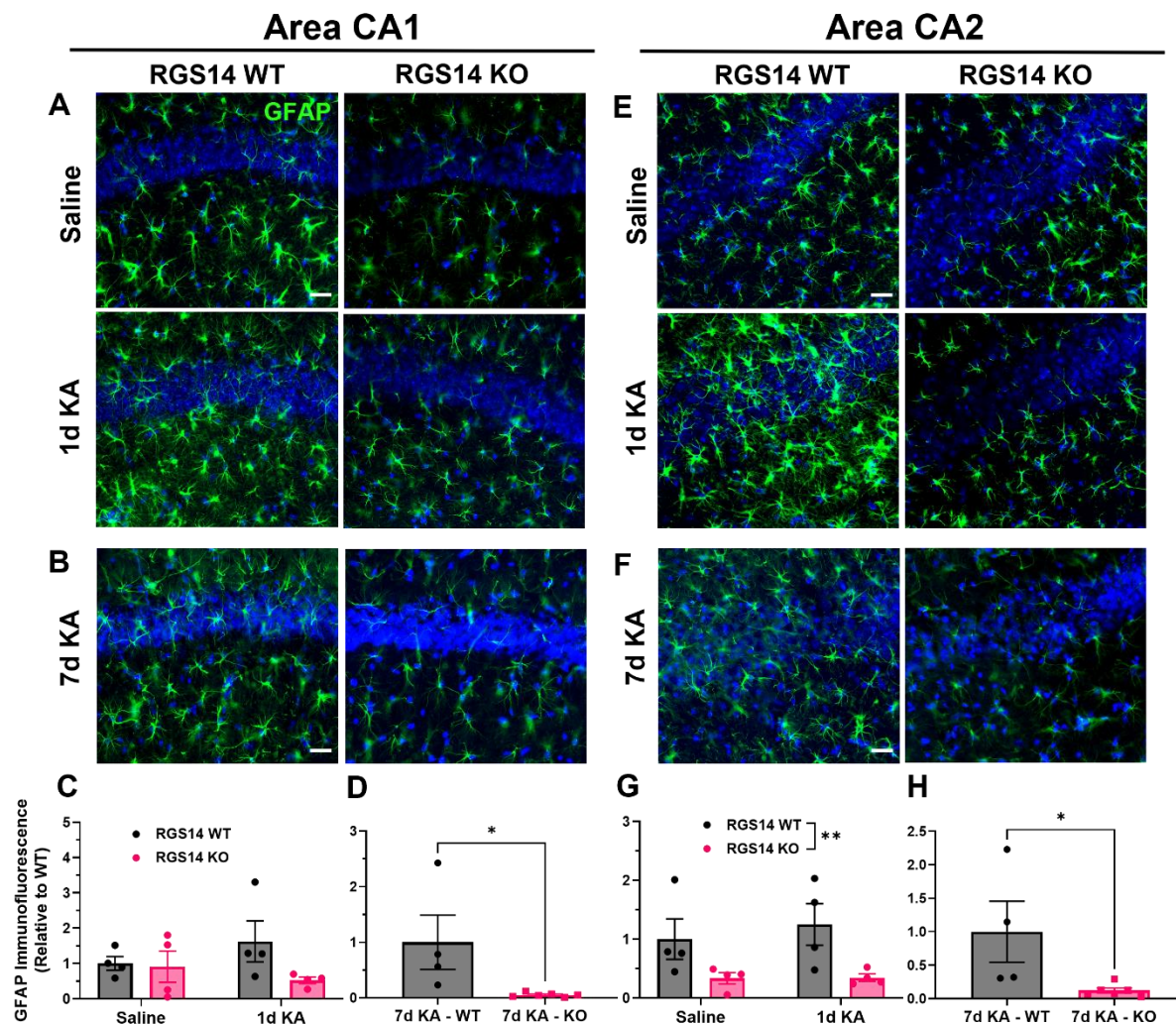


Figure 22. Loss of RGS14 causes deficits in astrocyte reactivity following KA-SE.

(unpublished data) (A, B) Representative IHC images of GFAP in the dorsal hippocampal area CA1 of WT and RGS14 KO mice one day after KA-SE or saline (A) or seven days after KA-SE (B). Scale bar, 20 μ m. (C) Mean GFAP immunofluorescence one day after saline or KA-SE in CA1 relative to saline-treated WT mean (SAL: WT, n=4, 1.00 ± 0.19 ; RGS14 KO, n=4, 0.91 ± 0.44 ; 1d KA: WT, n=4, 1.62 ± 0.58 ; RGS14 KO, n=4, 0.52 ± 0.09). (D) Mean GFAP immunofluorescence seven days after KA-SE in CA1 relative to WT mean (WT, n=4, 1.00 ± 0.49 ; KO, n=6, 0.05 ± 0.02). (E, F) Representative IHC images of GFAP in the dorsal hippocampal area CA2 of WT and RGS14 KO mice one day after KA-SE or saline (E) or seven days after KA-SE

(F). Scale bar, 20 μm . (G) Mean GFAP immunofluorescence one day after saline or KA-SE in CA2 relative to saline-treated WT mean (SAL: WT, n=4, 1.00 ± 0.35 ; RGS14 KO, n=4, 0.33 ± 0.10 ; 1d KA: WT, n=4, 1.25 ± 0.35 ; RGS14 KO, n=4, 0.34 ± 0.06). (H) Mean GFAP immunofluorescence seven days after KA-SE in CA2 relative to WT mean (WT, n=5, 1.00 ± 0.45 ; KO, n=6, 0.12 ± 0.04) *Statistical analysis*: (C, G) For saline and one day KA groups, means were compared using two-way ANOVA with Sidak's post hoc comparison (G, two-way ANOVA, $F = 9.58$ for genotype, $**p < 0.01$). (D, H) For seven day KA groups, means were compared using unpaired t-tests (D, WT vs RGS14 KO, $*p < 0.05$) (H, WT vs RGS14 KO, $*p < 0.05$). Error bars represent the SEM.

Similarly, we observed a significant reduction in RGS14 KO GFAP expression seven days after KA-SE in CA2 (88% decrease) (Fig. 22F, H), further supporting an essential role for RGS14 in regulating aspects of astrocyte function and response to seizure activity in CA1 and CA2. Like microglia, RGS14 KO effects in astrocytes were specific to CA1 and CA2 as GFAP expression did not differ in CA3 or the DG (data not shown). Overall, the data here supports a necessary role for RGS14 in glial response to seizure activity, which occurs in a subregion dependent manner coincident with its upregulation following seizure.

4. Discussion

4.1. Summary of Findings

Here, we have shown that loss of RGS14 sensitizes mice to the behavioral effects of KA-SE demonstrated by expedited entry into SE and mortality. In response to seizure activity, RGS14 expression in WT mice was upregulated in the hippocampus, particularly in area CA2 and CA1 PCs, although RGS14 was still more abundantly expressed in CA2 relative to CA1. Using proteomics to assess molecular consequences of loss of RGS14, we observed an expected difference in expression of proteins related to G-protein signaling while unexpectedly finding proteins involved with NO synthase (NOS) activity, prostaglandin stimulation, lipid membrane dynamics, and neurotransmission that differed prior to seizure, which likely affect the sensitivity to KA behavioral seizures observed in RGS14 KO mice. Of processes that likely influence pathology following KA-SE, we saw an array of proteins involved with mitochondrial metabolism that were differentially expressed between WT and RGS14 KO hippocampi and modules of proteins associated with metabolism, fatty acid oxidation, and astrocytes that also differed in expression between WT and RGS14 KO after seizure activity. Accordingly, we observed for the first time that RGS14 localizes to mitochondria of PCs in area CA2 and that add-back of RGS14 to cells reduced mitochondrial respiration *in vitro*. Loss of RGS14 promoted the marked accumulation of 3-NT (a marker of oxidative stress) and prevented seizure induction of SOD2 (a mitochondrial enzyme that detoxifies the reactive metabolite superoxide) in CA2 PCs, suggesting exacerbated oxidative stress in the region. Although we found that RGS14 is not necessary for CA2's resistance to early seizure-induced neuronal injury, mice lacking RGS14 had a striking impairment in microgliosis and astrogliosis in areas CA1 and CA2 following KA-SE, suggesting RGS14 is required for neuroinflammatory response caused by seizure activity. Together, these results provide compelling evidence that RGS14 limits behavioral and pathological seizure

response to KA in the hippocampus, possibly by influencing the cellular excitability and metabolic profile of CA2 PCs (Harbin et al., 2023).

4.2. Neuronal mechanisms by which loss of RGS14 primes the hippocampus and the brain to seizure sensitivity caused by KA

While systemic KA administration can cause activation of KARs in a variety of brain regions that may contribute to seizure generation including the amygdala and entorhinal cortex, the hippocampus appears to be the most sensitive to generating epileptiform activity and degenerating due to neuronal hyperactivity (Levesque and Avoli, 2013). Because KARs are expressed pre- and postsynaptically on excitatory pyramidal cells, granule cells, and inhibitory interneurons within the hippocampus, there have been several proposed cellular mechanisms of how hippocampal seizure activity originates via KA activation (Lerma and Marques, 2013). There is a general consensus, however, that KA alters the E/I balance via enhancement of mossy fiber excitation from DG granule cells, suppression of GABAergic inhibition in CA3, or by other mechanisms to generate epileptiform (ictal) activity in the CA3 region (Lerma and Marques, 2013), which forms a recurrent collateral network similar to CA2 (Dudek et al., 2016). KA causes hypersynchronized neuronal activity of pyramidal cells in CA3 through the coordination of excitatory and inhibitory neuronal firing, which is thought to generate hippocampal oscillations that are associated with seizure activity. Hypersynchrony allows for propagation of epileptiform activity to spread from CA3 to CA1 and out of the hippocampus to connected structures causing epileptiform oscillations where the activity spreads (Ben-Ari and Cossart, 2000). Faster onset of SE (continuous limbic motor seizures) and mortality in RGS14 KO (Fig. 9, 10) (Harbin et al., 2023) suggests enhanced hippocampal excitability that causes faster generation of seizure activity within this CA3 network, quicker propagation of seizure activity from the hippocampus to associated structures, or both. CA2 PCs from RGS14 KO mice are intrinsically more excitable than those from WT mice, where KO CA2 PCs exhibit higher input resistance and have increased

firing upon current injections. While excitatory transmission at CA3>CA2 synapses in WT mice is typically weak, these synapses are strengthened in RGS14 KO mice and may result in additional excitatory input to CA2 during seizure activity (Lee et al., 2010). Additionally, RGS14 buffers dendritic calcium upon glutamate uncaging at CA2 synapses, which suggests loss of RGS14 could further enhance depolarizing responses from glutamate (Evans et al., 2018b). All of this indicates that RGS14 KO mice likely have hyperactive CA2 activity, which could influence seizure activity, and several recent reports support a role for CA2 in regulating hippocampal excitability that may initiate seizures and hippocampal oscillatory activity that may contribute to seizure propagation (Lehr et al., 2021).

One study demonstrated that CA2 controls the excitability of the hippocampal network, influences the nature of hippocampal oscillations, and regulates sensitivity to kainic acid (Boehringer et al., 2017). Here, they found CA2 activity recruits feed forward inhibition onto the recurrent CA3 network, and acute silencing of CA2 increased CA3 recurrent network excitability in vitro. Accordingly, chronic silencing of CA2 in vivo resulted in hyperexcitability of CA1 and CA3 and epileptiform-like spiking in the region, where HFOs associated with epileptiform activity were observed in CA1. Finally, chronic silencing of CA2 increased behavioral sensitivity to KA seizures in the same experimental paradigm that was used in this body of work. The findings in this report stand contrary to our hypothesis that behavioral seizure sensitivity to KA in RGS14 KO is a result of a hyperactive CA2. However, it should be noted that the connectivity and strength of the inhibitory network in RGS14 KO CA2 and CA3 has not been evaluated, so it is unknown whether feedforward inhibition onto CA3 by CA2 would similarly exist in RGS14 KO mice. Related, the epileptic CA2 has reduced inhibitory input (Whitebirch et al., 2022) and reduced expression of interneurons (Kilias et al., 2022), and if CA2 in RGS14 KO mice is similar to epileptic CA2, then we may also observe deficits in inhibition in RGS14 KO CA2. Additionally, chronic silencing of CA2 may have unforeseen consequences that alter hippocampal excitability not attributable to

CA2 PCs alone, including dysregulated activity of output structures regulated by CA2 or changes in local hippocampal circuitry or glial contributions. Along these lines, acute silencing of CA2 PCs did not trigger CA1 or CA3 hyperexcitability that was observed in chronic silencing conditions. Furthermore, this report did not evaluate hippocampal hyperexcitability events or epileptiform activity after enhancing CA2 activation, which may differ from acute or chronic silencing. However, it is possible that loss of RGS14 does not alter seizure initiation in the hippocampus, where the potentially hyperactive CA2 has no effect on seizure generation in the CA2/CA3 network or RGS14 expression outside of CA2 is more important for KA sensitivity (contributions of extrahippocampal RGS14 discussed further below).

KA-induced epileptiform activity in the hippocampus is associated with nonconvulsive seizures, while convulsive seizures stemming from limbic activation suggest propagation to extrahippocampal structures like the neocortex and motor cortex (Levesque and Avoli, 2013; Tse et al., 2014). Agreeing with this, we found that RGS14 KO mice progressed similarly through early, nonconvulsive seizure staging (Stages 1 and 2; data not shown), and genotype differences only emerged during convulsive, Stage 3 seizure activity. Additionally, loss of RGS14 dramatically hastened the mortality of mice, suggesting that epileptiform activity may propagate quicker to hindbrain structures controlling autonomic functions like heart rate and breathing (Li and Buchanan, 2019). Therefore, it may be more likely that RGS14 in CA2 gates output of seizure activity to CA1 and/or other outputs that would allow seizure activity to propagate more quickly out of the hippocampus. Because CA2 has a wide, bilateral output along and out of the hippocampus (Cui et al., 2013; Mercer et al., 2007), increased excitation onto and out of CA2 in RGS14 KO mice may propagate seizure activity to these regions more rapidly. Future studies can utilize CA2-specific deletion of RGS14 paired with EEG recording or voltage-dye measurements in the different hippocampal subregions of acute hippocampal slices *in vitro* or different CA2

output regions in vivo to better understand how the loss of RGS14 in CA2 specifically gates epileptiform activity within the hippocampus and propagates out of it.

In support of RGS14 regulating seizure propagation, CA2 has been repeatedly shown to regulate and possibly initiate certain forms of hippocampal oscillations, which are associated with the transition of synchronized neuronal activity from CA3 to CA1 and to extrahippocampal regions (Oliva et al., 2023). Gamma oscillations involve neuronal synchronization with firing rates between 30-100 Hz (low gamma 30-50 Hz; high gamma 50-100 Hz) (Colgin et al., 2009). Physiologically, hippocampal gamma oscillations are thought to underlie memory encoding (high gamma) and retrieval (low gamma) (Colgin et al., 2009), and recent evidence has demonstrated CA2 modifies hippocampal and extrahippocampal low gamma oscillations (Oliva et al., 2023). Enhancement of CA2 activity increases low gamma power in the hippocampus, and this activity coincides with increases in low gamma power in the medial prefrontal cortex, suggesting gamma oscillations in the hippocampus and then propagation to cortical structures is modified by CA2 activity (Alexander et al., 2018). During seizure activity caused by KA, low gamma oscillations occur early after KA administration in the hippocampus and have been proposed as a mechanism of seizure propagation from the limbic system to cortical regions associated with convulsive seizures (Levesque et al., 2009; Medvedev et al., 2000). Furthermore, increases in gamma power in the cortex are associated with convulsive seizures in KA-treated mice (Tse et al., 2014). If CA2 activity also modulates gamma oscillations during KA-induced seizure, then it may be that the increased excitability of CA2 in RGS14 KO mice enhances or quickens the formation of KA-induced low gamma oscillations in the hippocampus and expedites propagation of seizure activity to cortical structures and elsewhere.

Additionally, several reports now have shown that CA2 also regulates another important form of oscillatory activity: SPW-Rs, which are thought to facilitate memory transfer from the hippocampus to the neocortex and originally attributed to CA3 activity (Buzsaki, 2015; Oliva et

al., 2023). SPW-Rs originate from hypersynchronized bursts of CA3 PC firing onto CA1 dendrites that massively depolarizes CA1 PCs (sharp wave) followed by a 100-250 Hz oscillation in CA1 (ripple). This type of activity resembles interictal spikes and HFOs that precede seizure events in TLE and are generated by similar mechanisms, where sharp waves and spikes both originate from hypersynchronous firing of excitatory pyramidal cells and ripples and HFOs both rely on coordinated synchronicity of excitatory and inhibitory neuron populations (Buzsaki, 2015). CA2 can initiate SPW-Rs that can propagate to CA1 similar to CA3, and CA2 activity modulates the power of SPW-Rs in the hippocampus and cortex (Alexander et al., 2018; Oliva et al., 2016). Pathologically, SPW-Rs in the hippocampus are detected during KA-SE and in spontaneous seizures that develop following KA-SE (Buzsaki, 2015). RGS14, by enhancing the excitability of CA2, may therefore regulate SPW-R generation or the intensity of such events during seizure activity and represents another possible mechanism by which epileptiform activity can propagate out of the hippocampus more rapidly in RGS14 KO mice. Furthermore, gap junctions also seem to play an important role in generating SPW-Rs (Mylvaganam et al., 2014), and potential gap junction dysfunction in RGS14 KO hippocampi may offer another mechanism by which RGS14 could regulate this type of oscillation. To test this idea, follow-up studies could use in vivo EEG recordings in the hippocampus and associated structures (ideally paired and correlated with video of behavioral seizures) to determine if low gamma oscillations and/or sharp wave ripples are altered in RGS14 KO mice at rest or during seizure activity and if such changes correlate with progression of behavioral seizures.

Outside of the hippocampus, RGS14 expression and regulation in temporal lobe structures like the amygdala, entorhinal, and piriform cortex may also be important for behavioral seizure sensitivity to KA in RGS14 KO mice (Evans et al., 2014; Squires et al., 2021). The amygdala is of particular importance as it is highly susceptible to the seizurogenic and pathological effects of KA and electrical kindling (Ben-Ari et al., 1980; McIntyre and Gilby, 2008))

and exhibits synchronized epileptiform activity with the hippocampus (Levesque et al., 2009). RGS14 was recently shown to be expressed in the central amygdala (Squires et al., 2021), and although its function in this region remains untested, RGS14 here may be important for cued fear response and likely governs some aspect of neuronal function (Alexander et al., 2019). Epileptiform activity from the electrically stimulated central amygdala causes kindling of seizure activity to the perirhinal and piriform cortexes much quicker than stimulation of other amygdala nuclei, and central amygdala kindling with the perirhinal cortex was associated with forelimb clonus (Stage 3 seizure activity from the paradigm in our work) (Mohapel et al., 1996). Because global loss of RGS14 also decreased the latency to Stage 3 seizure activity (Fig. 9, 10) (Harbin et al., 2023), it is reasonable to hypothesize that RGS14 may regulate the propagation of seizure activity from the central amygdala to cortical structures. Interestingly, the amygdala (and specifically the central amygdala) is also connected to autonomic structures that regulate respiration, and stimulation of the central amygdala has been consistently shown to alter respiration patterns (Krohn et al., 2023). Several reports have demonstrated that the spread of seizure activity to the amygdala in humans are associated with apnea (temporary cessation of breathing) and oxygen desaturation (Dlouhy et al., 2015; Nobis et al., 2019; Rhone et al., 2020), and stimulation of the amygdala induces apnea in epileptic patients (Dlouhy et al., 2015; Rhone et al., 2020). If RGS14 regulates the excitability of the central amygdala (as it does in CA2), then loss of RGS14 could cause faster seizure propagation out of the central amygdala, which may contribute to the observed expedited mortality in RGS14 KO mice.

The parahippocampal cortexes (including the entorhinal and piriform cortices) are tightly connected to the hippocampus and amygdala of the limbic system and therefore are also implicated in temporal lobe seizure generation (Vismer et al., 2015). RGS14 is expressed in layers II/III of the entorhinal cortex and layer II of the piriform cortex, where its expression is more intense in the piriform cortex relative to the entorhinal cortex (Evans et al., 2014). Both the entorhinal

cortex and piriform cortex regulate sensory information transmitted to the limbic system (notably the hippocampus and amygdala), and, being highly interconnected themselves and with other cortical regions, these regions are highly seizurogenic and can help further synchronize neuronal activity to increase seizure intensity and propagation (Vismer et al., 2015). Of note, excitatory neurons of layers II and III of the entorhinal cortex send powerful excitatory drive to CA2, form LTP at synapses, and drive CA2 firing, which is opposite to what is measured at input from CA3 (Chevalleyre and Siegelbaum, 2010). Although the role of RGS14 in either of these regions is currently unknown, it stands to reason that RGS14 may help limit excitability, neuronal synchronization, seizure initiation, and seizure propagation within these regions as hypothesized in the limbic system. To assess RGS14's role in regulating seizure activity in extrahippocampal regions, future studies may utilize a combination of region-specific knockdown of RGS14, in vivo EEG recordings in the amygdala, entorhinal cortex, and piriform cortex, and paired measurements of behavioral seizure activity and autonomic function (e.g., respiration). Correlation between enhanced seizure activity in regions where RGS14 has been deleted and behavioral or physiological output would help unravel the role of RGS14 in controlling activity of these regions and if they are important for seizure phenomena similar to what has been described in this report. Additionally, using neuronal activity markers (e.g., c-Fos) shortly after seizure activity would also be important for identification of regions exhibiting increased neuronal activity in RGS14 KO mice (McIntyre and Gilby, 2008).

Lastly, there may be peripheral mechanisms that govern RGS14 KO sensitivity to KA. Our proteomics results suggested a potential alteration of BBB permeability as some proteins upregulated in RGS14 KO were associated with "Transport Across Blood Brain Barrier" at baseline (Fig. 12D), (Harbin et al., 2023) which may affect the uptake of KA into the brain. Out of the 8 upregulated proteins in RGS14 KO, Abcb1a (P-glycoprotein) was the only one that could influence BBB permeability (Table 2) (Harbin et al., 2023). However, we think this is unlikely as

P-glycoprotein effluxes drugs out of the brain and its upregulation would suggest less BBB penetrability (Schinkel, 1999). Additionally, KA crosses the BBB via passive diffusion, while P-glycoprotein utilizes active transport for membrane shuttling (Gynther et al., 2015; Schinkel, 1999), further arguing against BBB permeability as a mechanism of KA sensitivity in RGS14 KO mice. As another possibility, a recent study demonstrated increased blood flow to hindlimb skeletal muscle in RGS14 KO mice (Vatner et al., 2023), indicating enhanced perfusion may accelerate effects of KA. However, this effect was mediated by RGS14 actions in brown adipose tissue and likely does not suggest enhanced hippocampal perfusion that may contribute to the expedited behavioral effects of KA. As a final consideration, it is possible that RGS14 expression in cardiomyocytes or elsewhere in the periphery may contribute to expedited mortality in RGS14 KO mice, although RGS14-KO mice have normal cardiac function at baseline (Li et al., 2016). Even so, to mitigate influence of systemic effects, future experiments will measure epileptiform activity in acute slices from RGS14 KO mice in vitro or use intracerebral administration of KA to induce seizure activity in vivo.

4.3. Factors that may influence susceptibility to seizures and pathology based on hippocampal proteomics

Because RGS14 influences a number of intracellular signaling pathways and suppresses glutamatergic signaling in CA2 PCs (Harbin et al., 2021), we hypothesized that the ablation of RGS14 would cause pronounced changes in hippocampal protein dynamics at baseline that may help explain enhanced susceptibility to KA-SE. Because RGS14 is most abundantly expressed in CA2 PCs (relative to other subregions) in the hippocampus at baseline (Fig. 11) (Harbin et al., 2023), it is likely that any hippocampal proteome changes in RGS14 KO mice reflect the absence of RGS14 in CA2 and altered function of the region. However, it is possible that altered function of extrahippocampal regions that also express RGS14 and provide input to the hippocampus (e.g., central amygdala and parahippocampal cortices) also contribute to effects on protein

expression in the hippocampus. To assess these changes, we performed proteomics on WT and RGS14 KO hippocampal lysates after saline injection to identify proteins that were differentially expressed (DEPs) between genotypes and using GO to identify biological and cellular processes associated with DEPs (Fig. 12, Table 2). (Harbin et al., 2023) Although we have used this approach to identify novel RGS14 interacting partners in the brain (Evans et al., 2018a), this is the first time to our knowledge that molecular consequences from RGS14 KO have been evaluated anywhere in the brain.

Expectedly, our analysis showed that downregulated proteins were associated with G protein dependent signaling in RGS14 KO including G_{α_s} (G_{α_s}). This may reflect aberrant G protein signaling within the hippocampus and compensatory response from RGS14 KO as RGS14 modulates AC activity and subsequent cAMP accumulation via its GAP activity on activated $G_{\alpha_{i/o}}$ subunits. CA2 receives numerous neuromodulatory inputs, and there are a number of GPCRs abundant in CA2 that modulate its function, particularly synaptic plasticity (Lehr et al., 2021). One such GPCR is the $G_{\alpha_{i/o}}$ -coupled GPCR A1R, which is of particular interest in epilepsy as adenosine is generally considered anticonvulsive by decreasing neuronal excitability or neurotransmission (Spanoghe et al., 2020). Accordingly, A1R knockout in mice enhances susceptibility to KA-SE, where these mice exhibited enhanced seizure propagation and pathology (Beamer et al., 2021). A1R antagonism enhances excitatory transmission and restores synaptic plasticity at CA3>CA2 synapses (Lehr et al., 2021), and it is possible RGS14 inhibits G-protein signaling downstream of A1R by deactivating $G_{\alpha_{i/o}}$. If so, we would expect enhanced A1R and $G_{\alpha_{i/o}}$ signaling and lower levels of cAMP in CA2 of RGS14 KO mice. However, downregulation of G_{α_s} suggests enhanced G_{α_s} or depressed $G_{\alpha_{i/o}}$ signaling, and loss of RGS14 increases sensitivity to KA-SE, which reflects RGS14's anticonvulsant effects are likely not mediated through GAP effects on A1R. Related, evidence suggests that the RGS domain by which GAP activity is exerted may be less important in CA2 relative to its other domains (Squires et al., 2021). Supporting this,

inhibition of PKA, which is activated by cAMP, restores plasticity in RGS14 KO CA2 and indicates that RGS14 inhibits PKA activity at least during glutamatergic stimulation, which is opposite of what would be expected if RGS14 was primarily a GAP (Evans et al., 2018b).

RGS14 also binds Rap2 in rodent brain (Mittal and Linder, 2006; Traver et al., 2000), and decreased expression of Rap2c could also be due to a similar negative feedback response. If RGS14 binds Rap2 to inhibit its signaling in the hippocampus, then loss of RGS14 may enhance Rap2 mediated signaling and would require compensatory expression changes seen here. Rap2 mediates activation of JNK signaling and shifts signaling away from ERK activation (Ye and Carew, 2010), and decreased Rap2 expression may represent a compensatory response from enhanced JNK signaling or result in enhanced ERK signaling. A recent study demonstrated RGS14 in hepatocytes inhibits JNK and p38 MAPK signaling (but not ERK), demonstrating RGS14's broad control over small, monomeric G-protein and associated MAPK signaling (Zhang et al., 2022). Additionally, RGS14 binds activated H-Ras and Raf kinases upstream of ERK activation to limit ERK signaling (Shu et al., 2010; Vellano et al., 2013), and it is feasible that RGS14 KO enhances ERK signaling. Supporting this, RGS14 limits plasticity through a MEK/ERK-dependent mechanism in CA2 (Lee et al., 2010), and our proteomics data showed upregulated proteins were associated with receptor tyrosine protein phosphatases that may indicate enhanced kinase signaling (Fig. 12) (Harbin et al., 2023). MAPK signaling arms (MEK/ERK, JNK, and p38) can be activated by either GPCR or RTK signaling and affects properties of neuronal excitability through various mechanisms (Ye and Carew, 2010). KA administration causes activation of hippocampal MAPK signaling (Jeon et al., 2000), and modulation of the various MAPK signaling arms can differentially alter seizure susceptibility depending on the model of seizure induction (Hu et al., 2020; Nguyen et al., 2022; Tai et al., 2017). Therefore, dysregulation of MAPK signaling in CA2 (or elsewhere in the hippocampus) in RGS14 KO mice may also contribute to the susceptibility to KA-SE.

We also found that proteins associated with morphogenesis were downregulated in RGS14 KO hippocampi, which was expected as we have shown RGS14 inhibits glutamate-dependent increases in CA2 dendritic spine volume. Along these lines, RGS14 likely plays a major role in limiting glutamate signaling through NMDAR-dependent processes as RGS14 limits NMDAR-dependent calcium influx and plasticity (Evans et al., 2018b). By suppressing calcium transients from glutamate stimulation, RGS14 likely limits CA2 PC depolarization and calcium-dependent enhancement of synaptic potentiation and neuronal firing during seizure activity, which may contribute to sensitivity to KA-SE. RGS14 binds to $\text{Ca}^{2+}/\text{CaM}$ and $\text{CaMKII}\alpha$ and likely regulates their function in some capacity (Evans et al., 2018a), although if and how this occurs remains untested. CaM and CaMKII modulate the activity of hundreds of proteins and trigger downstream signaling that have profound consequences on neuronal excitability (Ben-Johny and Yue, 2014; Liu and Murray, 2012). As it relates to seizures, inhibition of CaMKII enhances seizure susceptibility and epileptiform activity originating from the limbic system in vivo (Butler et al., 1995) and in hippocampal slices in vitro (Butler et al., 1995). Therefore, calcium signaling dysregulation may also be important for the sensitivity of RGS14 KO mice to KA-SE.

Interestingly and unexpectedly, the GO pathway “Response to Prostaglandin Stimulus” was enriched in downregulated proteins caused by RGS14 KO (Fig. 12) (Harbin et al., 2023). Prostaglandins exert their effects through a number of GPCRs, including those coupled to Gi/o (Hata and Breyer, 2004), where RGS14 could limit their activity by acting through its GAP/RGS function. Prostaglandins like prostaglandin E2 (PGE2) are known to regulate membrane excitability, seizure response, and inflammation in the hippocampus (Chen and Bazan, 2005; Jiang et al., 2013; Rojas et al., 2014), which is coincident with the phenotype of RGS14 KO. Prostaglandins are synthesized from arachidonic acid via cyclooxygenases COX1 or the inducible COX2 (which is heavily implicated in seizure pathology) and exert their seizure-modifying effects through a variety of intracellular signaling pathways (Rojas et al., 2019), several of which RGS14

interacts with and regulates (Harbin et al., 2021). Also unexpected were GO terms associated with apoptosis, which suggests RGS14 influences components of apoptotic signaling in the hippocampus as it does in hepatocytes (Zhang et al., 2022), lipid membrane dynamics, distribution, and signaling, which may indicate RGS14 regulates the balance of lipid species through some unknown mechanism, and acetylcholine neurotransmission, which is well characterized as influencing seizure susceptibility in the hippocampus as demonstrated by the widespread use of seizure induction using muscarinic agonist PILO (Curia et al., 2008) and may reflect alterations in cholinergic input from areas like the lateral and medial septum that have are regulated by CA2 activity (Leroy et al., 2018; Pimpinella et al., 2021). Finally, one of the most enriched and unexpected of enriched GO terms were related to DNA methylation and NOS activity. NOS is regulated by a number of extracellular and intracellular mediators, and NO is able to modulate neuronal excitability through post-translational mechanisms on ion channels that may contribute to enhanced excitability in CA2 (Spiers and Steinert, 2021). Supporting this, we found that 3-NT (a product of NO and O₂⁻) is massively induced in RGS14 KO CA2 at baseline (Fig. 17) (Harbin et al., 2023), suggesting the enhanced production of NO in CA2 that may affect cellular function of PCs and the surrounding environment as NO is able to diffuse through the membrane (Spiers and Steinert, 2021). Overall, this data suggests RGS14 alters the expression of signaling and other cellular components, likely in CA2 PCs where it is highly expressed at baseline, to limit susceptibility to KA-SE in mice prior to seizure induction.

Because we observed RGS14 protein was robustly induced in expression in the PCs of area CA1 and CA2 and this effect was largest one day following KA-SE (Fig. 11) (Harbin et al., 2023), we presumed that proteomic analysis at this time point would provide valuable insight into hippocampal processes that RGS14 could be affecting upon its induction. Comparing proteomes between genotypes one day after KA-SE, we observed proteins downregulated in RGS14 KO were associated with oxidation-reduction processes, organic molecule catabolism and synthesis,

and fatty acid metabolism, whereas those upregulated in RGS14 KO were associated with apoptotic response, ATP metabolism, and oxidant/antioxidant activity (Fig. 12E) (Harbin et al., 2023), indicating that loss of RGS14 induction may promote metabolic dysfunction and oxidative stress. Indeed, many of the DEPs in RGS14 KO hippocampi localize to the mitochondria and make up components of the ETC, citric acid (TCA) cycle, or fatty acid metabolic pathways even at baseline (Fig. 12A, Table 2). When identifying proteins that were significantly altered by KA within each genotype (Fig. 13, Table 3), we found that most proteins downregulated in WT hippocampi were highly associated with fatty acid oxidation processes, which were not seen in RGS14 KO (Fig. 13D, E) (Harbin et al., 2023). The data here suggests that seizure activity modulates metabolic response in WT hippocampi, and this response may be dysregulated in RGS14 KO, particularly as it relates to fatty acid oxidation. Further supporting this idea, WGCNA analysis identified four co-expression modules of proteins that significantly differed between WT and RGS14 KO (Fig. 14) (unpublished data), and proteins in these modules were associated with mitochondrial metabolism and fatty acid oxidation, especially the M5 module that followed an expression trend similar to what in our differential expression analysis (proteins related to fatty acid oxidation are downregulated in WT but not in RGS14 KO hippocampi) (Fig. 15) (unpublished data). The consequence of metabolic dysregulation in RGS14 KO hippocampi could be enhanced oxidative stress caused by seizure activity. Indeed, some proteins upregulated in RGS14 KO were associated with regulation of oxidative stress, which was not seen in WT mice (Fig. 13D, E) (Harbin et al., 2023). Together, this data provides compelling evidence that loss of RGS14 could result in metabolic dysfunction, mitochondrial dysregulation, and exacerbate oxidative stress induced by seizure activity.

Neuronal processes require energy in the form of ATP to maintain membrane potentials and ionic gradients, facilitate neurotransmission both pre- and postsynaptically, recycle neurotransmitters, and mediate intracellular signaling, especially in glutamatergic neurons.

Neurons utilize the majority of ATP in the brain compared to other cell types, and the vast majority of neuronal ATP is generated through mitochondrial oxidative phosphorylation after contributions from glycolysis and the TCA cycle (Attwell and Laughlin, 2001). Neurons primarily use glucose as their fuel source for ATP production but can also use other substrates like amino acids (glutamate and glutamine), ketone bodies, and lactate, and although neurons can also use fatty acids as fuel, metabolism of fatty acids in neurons is slower, more oxygen demanding, and increases oxidative stress via elevation of O_2^- (Schonfeld and Reiser, 2013). Astrocytes play a major role in maintaining the availability of oxygen and energy substrates for neurons. Astrocytes provide physical links from synapses to blood vessels and enhance fuel shuttling for neurons during periods of activity while protecting neurons against oxidative stress (Belanger et al., 2011). Astrocytes primarily generate ATP from glycolysis, but much of the brain fatty acid oxidation takes place in astrocytes (Schonfeld and Reiser, 2013). Our WGCNA analysis indicated that two co-expression modules (M5 and M19) were enriched with proteins associated with metabolism (particularly fatty acid oxidation), gap junctions, and potassium ion regulation (Fig. 15) (unpublished data), and cell-type enrichment unsurprisingly identified these modules as being associated with astrocytes. This suggests that metabolism/fatty acid oxidation and other processes in astrocytes may be altered in RGS14 KO hippocampus, which may impair astrocytic response to seizure.

Seizure activity places an intense metabolic demand on the brain as rapidly firing neurons require large amounts of ATP, and neurons are known to enhance anaerobic glycolysis and rely less on aerobic metabolism for ATP production during seizure (Yang et al., 2013). In RGS14 KO mice, different expression patterns of proteins associated with aerobic metabolism in the mitochondria indicates that RGS14 may be involved with regulating the fuel source of ATP generation in the hippocampus during and following seizure activity. Dysregulation of fuel shifting during or following seizure activity may therefore impact subsequent pathology after SE, where

increased utilization of fatty acids as fuel in RGS14 KO mice could enhance oxidative stress (Bazzigaluppi et al., 2017; Schonfeld and Reiser, 2013). Metabolic coupling between neurons and astrocytes is vital during periods of intense neuronal activity as neurons need a constant supply of oxidizable substrates from astrocytes because they do not store any themselves (Barber and Raben, 2019). The abundance of DEPs in RGS14 KO mice related to lipid processes ranging from lipid synthesis (Asah, Acat2), phospholipid regulation (Mtmr1, Dgke), fatty acid oxidation and synthesis (Fasn, Acaa1a), and lipid transport (ApoB, ApoE) (Tables 2, 3) (Harbin et al., 2023) also lends support to abnormalities in lipid dynamics and likely consequences on metabolism and signaling. Several recent studies have demonstrated that ApoE functions as a carrier of fatty acids (especially toxic ones) are transported from neurons to astrocytes during periods of neuronal activity to limit oxidative stress in neurons and enhance the capacity of astrocytic antioxidant defense (Ioannou et al., 2019; Qi et al., 2021). Because ApoE is downregulated by KA in RGS14 KO mice (Table 3), this may perturb neuron-astrocyte lipid shuttling, which would have impacts on mitochondrial function and metabolism (Barber and Raben, 2019). Future studies should evaluate metabolism in isolated neurons, astrocytes, and neuron/astrocyte co-cultures from RGS14 KO mice to determine how RGS14 affects the metabolism of each cell type and metabolic cooperation between the two. Overall, this data supports a novel role for RGS14 in regulating metabolic dynamics in the hippocampus during and following seizure activity.

Even so, the idea that loss of RGS14 specifically in CA2 is responsible for hippocampal proteome changes is limited by the fact that changes in protein expression detected by proteomics only partially reflect those in CA2 PCs since data sets were obtained from whole hippocampi and deletion of RGS14 was not limited to CA2. Although findings may reflect broader changes in signaling in the hippocampus due to loss of RGS14, future studies examining cell-type specific deletion and analysis will be needed to more accurately assess RGS14 roles in CA2 to the observed phenotype. Additionally, alterations in the KO hippocampal proteome are only

suggestive of potential mechanisms that influence increased seizure susceptibility and do not establish causality. Because RGS14 regulates intracellular calcium and G protein signaling in CA2 PCs, synaptic plasticity from CA3 PCs, and possibly other excitatory neuron populations outside of CA2 that influence limbic seizures, we cannot definitively attribute any one cellular process or RGS14 regulation of CA2 as the major factor of susceptibility in RGS14 KO mice. Future studies measuring epileptiform activity in acute hippocampal slices from RGS14 KO mice will be necessary to better define CA2's role in seizure propagation in RGS14 KO mice, where viral introduction of mutant RGS14 constructs that prevent its regulation of certain signaling arms (Squires et al., 2021) could be used to determine functional domains that are responsible for its effect on epileptiform activity. Evaluating seizure pathology from mice with CA2-specific knockdown of RGS14 will also provide greater understanding of RGS14 function in CA2 during pathological events.

4.4. Mechanisms by which RGS14 regulates mitochondrial function and oxidative stress

Because our proteomics supported a novel and exciting role for RGS14 in regulating metabolic processes associated with the mitochondria, we used *in vitro* and *in vivo* approaches to determine if and how RGS14 would be affecting mitochondrial function (Figs. 16-18) (Harbin et al., 2023). We found RGS14 localizes to mitochondria in CA2 PCs and reduces basal and maximal mitochondrial respiration *in vitro*, which corroborates previous findings that global knockdown of RGS14 increased mitochondrial respiration and enhanced COX1 (ETC) and citrate synthase (TCA cycle) activity in brown adipose tissue (Vatner et al., 2023; Vatner et al., 2018). These reports also demonstrated that brown adipose tissue from RGS14 KO mice had elevated NAD⁺/NADH ratios, enhanced mitochondrial biogenesis, and higher cristae density in mitochondria, which further demonstrates enhanced mitochondrial function in RGS14 KO mice. Although the effect of RGS14 on mitochondrial respiration was more modest in HEK cells compared to the results in brown adipose tissue, this may reflect the preference of HEK cells for

glycolysis over respiration (Zhang et al., 2012) or cell-specific components that RGS14 engages with to reduce respiration in more mitochondrial-dependent cell types. Both neurons and brown adipocytes are high in mitochondrial content and must meet intense energy demands for proper organ function (Attwell and Laughlin, 2001; Magistretti and Allaman, 2015; Shinde et al., 2021). Because RGS14 localizes to mitochondria in neurons, we propose RGS14 could regulate mitochondrial function in neurons as it does in brown adipocytes (Vatner et al., 2023; Vatner et al., 2018) and HEK cells (Fig. 16) (Harbin et al., 2023).

RGS14 mitochondrial localization in CA2 PCs is of great interest as CA2 PCs also exhibit higher respiratory activity, more mitochondrial DNA and mitochondrial-related mRNA transcripts, and plasticity-dependent mitochondrial calcium uptake relative to neighboring CA1 and CA3 (Farris et al., 2019). Therefore, RGS14 may be playing a functionally important role in limiting mitochondrial function in this area. Interestingly, RGS12 (another RGS protein of the R12 subfamily with similar domain topology to RGS14) localizes to the mitochondria in primary chondrocytes and mouse cartilage tissue along with the nucleus and cytoplasm (Yuan et al., 2020), similar to the cellular traversing properties of RGS14. Although RGS12 expression (and not knockdown) was shown to enhance mitochondrial function in this report, this data heavily implicates a shared role of RGS proteins in mitochondrial function. Even though we did not directly measure RGS14 effects on mitochondrial respiration in neurons, the fact that RGS14 is highly enriched in CA2 neurons, localizes to mitochondria like a similarly structured RGS protein, and reduces mitochondrial respiration in multiple cell types illustrates that RGS14 is ideally positioned to influence mitochondrial function in CA2 PCs as well. Because neurons rely heavily on mitochondrial oxidative phosphorylation for ATP generation (Shetty et al., 2012), follow-up studies evaluating RGS14's effects on mitochondrial respiration in primary neuronal cultures will be necessary for evaluating neuronal specific effects on mitochondrial function.

However, we were able to gain valuable insight into how loss of RGS14 affects a major property of mitochondria: the production of ROS and associated oxidative stress. 3-NT (elevated in RGS14 KO CA2 (Fig. 17)) is caused by the highly reactive peroxynitrite, which is an ROS generated by the interaction between NO and O_2^- (Ferrer-Sueta et al., 2018), and suggests enhanced oxidative stress (Bandookwala and Sengupta, 2020). Even prior to seizure activity, the increased abundance of 3-NT in RGS14 KO CA2 is striking and suggests RGS14 in untreated animals contributes to mitigating ROS. Our proteomics indicates NOS activity (and therefore NO) could be altered in RGS14 KO hippocampi at baseline, whereas RGS14 may limit the production of O_2^- by its effects on mitochondrial respiration (Turrens, 2003). RGS14 may inhibit ROS production via its inhibition of calcium transients and NMDAR-dependent signaling (Evans et al., 2018b). Calcium influx leads to mitochondrial O_2^- formation in hippocampal neurons (Hongpaisan et al., 2004), while NMDAR agonism generates NO and O_2^- via activation of NOS and NOX, respectively, at the membrane (Di Meo et al., 2016). By limiting glutamatergic signaling at the membrane during seizure activity, there is potential for RGS14 to inhibit NO and/or O_2^- production and subsequent oxidative stress. Follow up studies will determine if RGS14 modulates O_2^- and/or NO in hippocampal neurons (at baseline or following seizure activity) and utilize pharmacological inhibition to elucidate their source(s).

Loss of RGS14 resulted in a marked suppression of SOD2 (the primary mitochondrial O_2^- detoxifying enzyme) in CA2 after KA-SE, which could explain, at least in part, the elevation of 3-NT caused by seizure activity. This is similar to what was recently shown in the brown adipose tissue of RGS14 KO mice, where SOD2 expression was also altered and supports a conserved role for RGS14 in limiting oxidative stress across cell types (Vatner et al., 2023). Interestingly, SOD2 expression was increased in brown adipose tissue, which is similar to our findings in CA1 PCs but opposite of what we saw in CA2 PCs (Fig. 17, 18) (Harbin et al., 2023). Cell-type specific regulation of MAPK signaling by RGS14 in response to injury has been reported (Li et al., 2016;

Zhang et al., 2022), and the data from our report and of others further demonstrates RGS14 specialization of signaling control, which could be related to its effects on mitochondrial function and ROS generation. As a result of enhanced ROS, 3-NT modification is known to alter the structure and activity of proteins susceptible to tyrosine nitrosylation, especially those in the mitochondria which can have deleterious effects on its function (Ferrer-Sueta et al., 2018; Radi et al., 2002). Indeed, SOD2 is inactivated by 3-NT modification (Yamakura et al., 1998), which may contribute to further O_2^- production and oxidative stress (Holley et al., 2011). Related, SOD2 deficient mice develop spontaneous seizures and are more sensitive to KA-induced seizures (Liang and Patel, 2004; Liang et al., 2012). In addition to 3-NT effects on mitochondrial enzymes, NO and O_2^- modify the function of ion channels at the membrane that may influence excitability in RGS14 KO CA2 PCs (Bogeski and Niemeyer, 2014; Radi et al., 2002; Spiers and Steinert, 2021). Therefore, loss of SOD2 and elevated 3-NT in area CA2 of RGS14 KO mice likely reflect a cellular environment with elevated levels of O_2^- and/or NO, which would have a major role in promoting oxidative stress, altering cellular excitability, and contributing to seizure generation in CA2. However, there is little evidence about how neuronal metabolism and oxidative stress in CA2 regulate its excitability and seizure gating, and further studies await to uncover the role of metabolic factors and RGS14's effects on metabolism as it relates to seizure generation and propagation in CA2.

To regulate mitochondrial function, RGS14 would conceivably regulate upstream signals at the plasma membrane/cytosol (via GPCR-, MAPK-, and/or calcium-dependent mechanisms) (Harbin et al., 2021) or engage in similar or novel mechanisms directly in the mitochondria (Benard et al., 2012; Hollinger et al., 2001) (Duchen, 2000; Evans et al., 2018b). As mentioned previously, RGS14 may regulate glutamatergic inductions of NO and/or O_2^- at the membrane, but it is entirely possible that RGS14 engages with other membrane and cytosolic components to regulate intracellular cascades that affect mitochondrial function and generation of ROS there. Membrane-

derived signals are capable of diffusing to the mitochondria or through structural bridges that link the two structures in order to transduce the extracellular response to mitochondria (Montes de Oca Balderas, 2021). Through its GAP activity, RGS14 enhances the inactivation of $G\alpha_{i/o}$ -dependent GPCRs signaling, ultimately enhancing cAMP signals. PKA, the primary target of cAMP, and its anchoring proteins (AKAPs) can localize to the mitochondria and mediate phosphorylation of mitochondrial targets to affect mitochondrial respiration and other functions (Horbinski and Chu, 2005). Interestingly, PKA anchoring and activity in the mitochondria is important for localized translation of SOD2 induction (Ginsberg et al., 2003) and may represent a potential mechanism by which RGS14 modulates SOD2 function in the hippocampus. If RGS14 does regulate SOD2 expression through this mechanism, then it would also indicate that RGS14's effects on cAMP-PKA signaling are different between CA1 and CA2 since SOD2 expression was increased in CA1 but decreased in CA2 KA-treated RGS14 KO mice (Fig. 17, 18) (Harbin et al., 2023). Another mechanism could be through RGS14's interaction with Raf-Ras-MEK-ERK signaling (Harbin et al., 2021). ERK has been shown to localize within the mitochondrial matrix in neurons and influences mitochondrial respiration and apoptotic signaling (Horbinski and Chu, 2005). RGS14's effects on ERK signaling are important for its suppression of synaptic plasticity in CA2 as well as its effects on respiration in brown adipose tissue (Lee et al., 2010; Vatner et al., 2023) and in cardiomyocytes (Li et al., 2016). Similarly, RGS14 was recently shown to inhibit JNK and p38 MAPK (but not ERK) signaling in injured hepatocytes (Zhang et al., 2022), and both of these kinases localize to the mitochondria and modulate apoptotic response to stress (Horbinski and Chu, 2005). Our proteomics demonstrated pathways associated with MAPK signaling to be upregulated in WT mice but unchanged in RGS14 KO mice following KA-SE (Fig. 13) (Harbin et al., 2023), suggesting that the loss of RGS14 dysregulates the hippocampal MAPK response to seizure and could contribute to mitochondrial dysfunction and the observed oxidative stress.

One of the most interesting capabilities of RGS14 is its suppression of intracellular calcium transients through NMDAR (Evans et al., 2018b) and L-type VGCCs (Martin-Montanez et al., 2010). One major function of mitochondria is to regulate calcium homeostasis by buffering intracellular calcium through the mitochondrial calcium uniporter (MCU) and extruding calcium through several exchangers, and mitochondria localize to microdomains of calcium at the plasma membrane or endoplasmic reticulum for more effective buffering. Uptake of calcium by mitochondria have profound effects on its function including the ability to metabolize substrates and produce ATP (Rizzuto et al., 2012). In neurons, mitochondrial calcium uptake can influence neurotransmission and postsynaptic responses, and it has been proposed that mitochondria are transported to areas of elevated synaptic activity to supply localized energy demands (Kann and Kovacs, 2007). In CA2 PCs, inhibition of the MCU was sufficient for promoting synaptic plasticity at the otherwise resistant CA3>CA2 synapses, highlighting the importance of mitochondrial calcium buffering in these neurons (Farris et al., 2019). Seizure activity causes large elevations of cytosolic and mitochondrial calcium concentration in neurons (Kann and Kovacs, 2007), and RGS14 is likely to suppress rises in cytosolic and therefore mitochondrial in CA2 PCs. Because uptake of mitochondrial calcium can stimulate production of O_2^- (Dykens, 1994), enhanced uptake of mitochondrial calcium in RGS14 KO CA2 PCs may represent another means by which RGS14 controls mitochondrial function and related oxidative stress, which is thought to contribute to the development of TLE and associated pathology (Patel, 2004).

An intriguing idea is that RGS14 acts a signaling platform in the mitochondria similar to its role at the plasma membrane. Supporting this, many signaling proteins that RGS14 scaffolds can localize to the mitochondria (Horbinski and Chu, 2005), and we show that RGS14 is abundant in both the inner and outer mitochondrial membranes (Fig. 16) (Harbin et al., 2023). How RGS14 localizes to the organelle is uncertain, but unraveling the mechanisms that control its localization to the mitochondria may provide more insight into its function here. At least one predictive

algorithm for mitochondrial targeting sequences (MTS) suggest that RGS14 may contain an N-terminal MTS (Fukasawa et al., 2015). Alternatively, RGS14 may bind to an effector or chaperone to target the organelle (Schmidt et al., 2010). Additionally, whether RGS14 is constitutively expressed in neuronal mitochondria and if its localization there is modulated by stimulation as it has been shown for other cellular compartments is unknown. Future studies will explore these possibilities. Nevertheless, the mitochondria is garnering attention for its capacity as a signaling hub: sensing a variety of inputs, integrating them within the organelle, and generating an output to affect its function or the function of other organelles. There is substantial overlap between the mitochondria and cell as a whole regarding the inputs, sensing mechanisms, and outputs, and there is an accumulating body of recent literature indicating the presence of GPCRs, G-proteins, and associated effectors and scaffolds that localize to the inner and outer mitochondrial membranes (Picard and Shirihai, 2022). The $G\alpha_{i/o}$ -coupled endocannabinoid 1 (CB1) receptor is expressed in CA1 PCs and localizes to mitochondria, where its activation results in G-protein-dependent inhibition of mitochondrial cAMP accumulation, PKA activity, and complex I activity, and regulates synaptic plasticity and memory in the hippocampus (Benard et al., 2012; Hebert-Chatelain et al., 2016). Purinergic GPCRs (P2YRs) are also expressed in mitochondria and by sensing ADP/ATP can regulate mitochondrial calcium uptake (Picard and Shirihai, 2022). Because endocannabinoid and adenosine signaling are heavily implicated in seizure disorders (Cheung et al., 2019; Weltha et al., 2019), RGS14 may influence GPCR signaling dynamics in the mitochondria as it does at the plasma membrane to affect mitochondrial respiration, calcium uptake, and other functions in response to seizure activity. There is also a possibility that RGS14 modulates the uptake or efflux of mitochondrial calcium as it does at the plasma membrane. Consequentially, RGS14 likely plays an indirect role in redox signaling as well by altering signals to the mitochondria at the membrane or signaling within the mitochondria that affect ROS generation, which may reflect the differential expression of mitochondrial proteins in RGS14 KO mice. Future studies could utilize biochemical assays on isolated mitochondria using functionally

null mutants of RGS14 to determine what components are necessary for its activity in the mitochondria.

Of interest, an interactome analysis identified intramitochondrial membrane GTPase optic atrophy 1 (OPA1) as an abundant binding partner of RGS14 in mouse brain (Evans et al., 2018a). OPA1 is essential for mitochondrial fusion and therefore regulates the quality of mitochondria (Alavi and Fuhrmann, 2013). Interestingly, mitochondrial fusion requires the GTPase domain but does not require GTPase activity, suggesting it mediates mitochondrial fusion through non-canonical means (Cartes-Saavedra et al., 2023). Deficiency in OPA1 results in fragmented but more motile mitochondria while decreasing basal and maximal respiration in neurons (Alavi and Fuhrmann, 2013), which is similar to the effect of RGS14 overexpression (Fig. 16) (Harbin et al., 2023). Interestingly, OPA1 regulates glutamate-induced oxidative stress by regulating the expression of SOD2 (Nguyen et al., 2011). If RGS14 is important for OPA1 function in neurons, then we would expect RGS14 KO mitochondria to have structural abnormalities that would likely impair function similar to what is seen in OPA1 deficient neurons. Therefore, assessing mitochondrial anatomy (number, size, complexity, and fragmentation of mitochondria) in neurons from RGS14 KO mice would provide a better understanding of what processes RGS14 regulates in the mitochondria and how its dysregulation could influence seizure-induced pathology.

4.5. Mechanisms that RGS14 may regulate to promote glial response

Although lasting neuroinflammation is typically associated with worse seizure pathology and outcomes, several studies suggest transient neuroinflammation following seizure is protective in the hippocampus (Eyo et al., 2014; Liu et al., 2020; Wu et al., 2020). Loss of early microglial activation in RGS14 KO mice was a novel finding and suggests a necessary role of RGS14 for prompting an appropriate microglial response to seizure activity (Fig. 20) (Harbin et al., 2023). Interestingly, lack of microgliosis in CA1/CA2 in RGS14 KO mice correlated with RGS14

upregulation in WT CA1/CA2 (Fig. 11) (Harbin et al., 2023), suggesting RGS14 induction in neurons is necessary for regional microglia activation, where it could promote microglia response through a neuronal mechanism. However, glial activation by seizure activity is a complex process, including release of chemoattractive and inflammatory factors from neurons, astrocytes, and microglia (Eyo et al., 2017; Patel et al., 2019). Although some microglial/macrophage populations express RGS14 mRNA (Bennett et al., 2016; Li et al., 2019), we have not observed RGS14 protein expression in microglia or astrocytes in the brain (Evans et al., 2014; Squires et al., 2018a) or RGS14 colocalization with IBA1 in CA1 or CA2 at baseline or following KA-SE. Therefore, we believe it is more likely that RGS14 promotes microglial activation via a neuron-dependent mechanism. However, we cannot rule out a priming effect towards astrocytes and/or microglia, where lack of RGS14 in CA2 and CA1 neurons may affect astrocytic or microglial function prior to injury. This is particularly important for astrocytic function as our proteomics identified a possible dysfunction in astrocytic metabolism and function following KA-SE. Accordingly, we found that, like microglia, astrocytes also fail to become reactive in response to seizure activity in CA1 and CA2 where RGS14 is expressed and induced following seizure (Fig. 22). Thus, deficiency in astrocytic and/or microglial function prior to seizure activity may contribute to the lack of their activation in RGS14 KO when seizures are induced (Eyo et al., 2017; Patel et al., 2019). To delineate the neuronal vs glial contributions in the RGS14 KO phenotype, future studies could examine *ex vivo* activation of microglia and astrocytes isolated from WT and RGS14 KO hippocampi.

A likely candidate for the lack of neuroinflammatory response may be COX-2 and prostaglandin signaling, which was associated with downregulated proteins in RGS14 KO mice (Fig. 12-15) (Harbin et al., 2023). Prostaglandins and their synthesis by COX-2 have emerged as major mediators of neuroinflammation and microgliosis, where neuronal release of prostaglandins like PGE₂ can activate microglia after seizure (Rojas et al., 2019). Upon further examination, we

found prostaglandin reductase 2 (Ptgr2) was downregulated in RGS14 KO hippocampi (Table 2, 3). Ptgr2 metabolizes a PGE2 metabolite, and its downregulation may reflect altered PGE2 levels and subsequent altered neuroinflammation (Chen et al., 2018). Moreso, the acid ceramidase (Asah1), which converts ceramide to sphingosine and free fatty acid, was similarly downregulated in RGS14 KO following KA-SE (Table 2). This enzyme is required for tumor necrosis factor alpha (TNF- α)-dependent increases in COX-2 expression and PGE2 production (Zeidan et al., 2006), further suggesting prostaglandins like PGE2 may be an important factor in microglia response in RGS14 KO mice. Importantly, TNF- α activation of TNF- α receptors is a critical mediator of microglia response during seizure activity, and deletion of these receptors increased neurodegeneration and suppressed microglia activation expression following KA (Bruce et al., 1996), similar to what we observed in RGS14 KO hippocampus. Although promising, further evaluation of RGS14's role in prostaglandin synthesis, signaling, and its mediation of microglia response via TNF- α /COX-2 signaling is needed, which can be assessed by looking at inflammatory cytokine and COX-2 expression following seizure in RGS14 KO mice.

While altered COX pathways could be linked to microglia activation in RGS14 KO mice, another possibility is that microglia in CA1 and CA2 are not attracted to sites of hyperexcitability during seizure activity. While several factors mediate microglial motility, ATP/ADP has been shown to promote microglial chemotaxis following glutamate- and KA-induced stimulation (Eyo et al., 2014). Neuronal hyperactivity results in NMDAR-dependent release of adenosine and ATP, and resting microglia extend processes towards the ATP gradient in a purinergic P2Y₁₂ receptor-dependent process, which can initiate early activation of microglia (Eyo et al., 2017). Because RGS14 is downstream of NMDAR-dependent signaling in CA2 (and CA1 when expressed there), it may be possible that RGS14 is a necessary component that mediates NMDAR-dependent ATP release, and loss of RGS14 could prevent neuronal ATP release and initial response by microglia. Moreso, genetic deletion of the purinergic P2Y₁₂ receptor prevents microglia activation and

worsens behavioral seizures caused by KA, similar to RGS14 KO mice (Eyo et al., 2014). Clearly, microglial response is important for early seizure response, but further experimentation will be necessary to properly examine how RGS14 modulates the microglia and broader neuroinflammatory response in the hippocampus.

Astrocyte reactivity to seizures is typically delayed relative to microglia (Sano et al., 2021), so the lack of astrocyte activation in RGS14 KO hippocampi could therefore be from a dysfunctional release of inflammatory mediators from neurons, microglia, or other cells (Sofroniew, 2020). Because factors that activate microglia and astrocytes are overlapping, it is certainly possible that the aforementioned factors from neurons or the lack of microglial reactivity and their associated release of inflammatory molecules play an equally important part in deficient astrocytic reactivity after KA-SE (Sofroniew, 2014). However, it is interesting that our WGCNA indicated alterations in fatty acid/lipid metabolism, gap junctions, and potassium buffering in astrocytic modules, and these processes may also contribute to the astrocyte dysfunction in RGS14 KO hippocampi. In addition to its effects on metabolism, dysfunction in metabolic coupling of fatty acids between neurons and astrocytes in RGS14 KO mice could arise in altered astrocytic reactivity and inflammation caused by seizure activity (Lee et al., 2021; Virtuoso et al., 2023). Supporting a role for astrocytic gap junctions in glial activation, a recent study demonstrated that deletion of connexins 30 and 43 (two primary connexins that form astrocytic gap junctions) in adult mice promoted hippocampal microglia and astrocytic activation in the absence of injury (Hosli et al., 2022). However, another group found that developmental deletion of both connexins decreased astrocyte reactivity one month after KA-SE (Deshpande et al., 2020). Interestingly, these connexins can act as hemichannels (unconnected to another cell) that release ATP and glutamate into the extracellular space, which could also influence glial activation (Sofroniew, 2014; Xing et al., 2019), although it has been demonstrated that neuronal but not astrocytic release of ATP is required for glutamate-induced microglial chemotaxis in the hippocampus of

WT mice (Eyo et al., 2014). Therefore, astrocytic gap junctions may not be as important for the glial phenotype in RGS14 KO mice, although they may contribute to other epileptic pathology following seizure activity (Mylvaganam et al., 2014). To distinguish the contributions of microglia and astrocytes to the lack of inflammatory response observed in RGS14 KO mice, future studies should profile inflammatory cytokine expression in microglia and astrocytes in RGS14 KO hippocampi prior to seizure activity to determine any differences at baseline that could affect response and then following seizure activity.

4.6. Possible protective roles of RGS14 in CA2 hippocampus and hippocampal TLE pathogenesis

We found RGS14 protein is upregulated markedly in CA2 and CA1 PCs following seizure (Fig. 11) (Harbin et al., 2023), similar to RGS14 upregulation in hepatocytes that is protective after ischemic-reperfusion injury (Zhang et al., 2022). In the hippocampus, RGS14 induction may serve as negative feedback to limit excessive calcium and aberrant signaling caused by seizure (Evans et al., 2018b; Harbin et al., 2021). Complimentary to its influence on signaling, RGS14 induction likely limits seizure-induced oxidative stress and mitochondrial dysfunction in CA2 PCs. While RGS14 was also upregulated in CA1, we did not see 3-NT accumulation and observed the opposite effect on SOD2, which was increased in CA1 compared to WT. This may reflect compensatory mechanisms in CA1 that properly limit O_2^- generation, 3-NT modification, and oxidative stress despite lacking RGS14 induction. Indeed, the translational and transcriptional profiles in areas CA2 and CA1 differ considerably, suggesting different mechanisms (Farris et al., 2019; Gerber et al., 2019). Therefore, RGS14 likely modulates mitochondrial function and oxidative stress differently between CA2 and CA1. Mechanism of RGS14 induction may also underly how RGS14 modulates injury response. Our unpublished findings show no change in the occupancy of the promoter region or regions upstream of the *RGS14* gene, suggesting RGS14 induction involves translation of RGS14 mRNA rather than transcription. Indeed, a recent report found RGS14 mRNA is highly abundant in the dendrites and cell bodies of CA2 and CA1 PCs,

suggesting local translation of mRNA as a mechanism of RGS14 induction (Farris et al., 2019). Future experiments will employ transcriptional and translational inhibition to define the mechanism of RGS14 induction.

Contrary to our hypothesis, we observed no injury in CA2 PCs early after KA-SE, which was also peculiar as CA2 displayed dramatically increased levels of 3-NT that would suggest enhanced oxidative stress and damage (Klein and Ackerman, 2003). This does suggest, however, that RGS14 is dispensable for CA2 resistance likely due to compensatory protection from a number of mechanisms in CA2 PCs such as strong inhibitory drive and high expression of calcium buffering proteins (Dudek et al., 2016). Likewise, the expression of PNNs, which protect against oxidative stress in parvalbumin interneurons and are decreased by seizure activity (Wen et al., 2018), enclose CA2 PCs (Carstens et al., 2016) and may protect against oxidative stress induced injury in RGS14 KO, although it is unknown whether RGS14 affects PNN expression at baseline or after seizure. Additionally, we saw no evidence of injury in CA1 PCs, further indicating RGS14 does not play a direct neuroprotective role in the hippocampus early after seizure injury even though RGS14 is upregulated in these neurons. Supporting this, we saw no evidence of oxidative stress in CA1 as demonstrated by 3-NT expression (data not shown). However, we did observe FJB labeling of CA3 PCs in both WT and RGS14 KO mice, which is typical after KA-SE and indicates both genotypes sustain injury from KA-SE. Our findings suggest loss of RGS14 results in a clear trend towards increased FJB+ cells in CA3 (possibly due to the faster onset of SE and increased duration of seizure activity relative to WT mice), even if not statistically significant likely due to low sample size and high variability. Because KA likely induces CA3 cell injury through excitotoxic mechanisms, enhanced CA3 injury in RGS14 KO would indicate glutamatergic activation and excitability in CA3 PCs (Ben-Ari and Cossart, 2000). Because RGS14 is not expressed in CA3 (Fig. 11), this likely reflects a circuit mechanism where CA3 receives enhanced excitation from CA2, mossy fibers from the DG, or elsewhere, where RGS14 regulates excitatory

tone rather than intracellular signaling in CA3. However, using alternative routes of KA administration (e.g. intrahippocampal) that produce more consistent seizure responses and evaluating neuronal injury at later time points where degeneration becomes more pronounced may better evaluate the protective capacity of RGS14 (Rusina et al., 2021).

Importantly, the capacity of RGS14 to modulate CA2 activity may be clinically relevant as CA2 has been hypothesized to promote epileptogenesis and generate seizure activity in the absence of CA1 and CA3 (Kilias et al., 2022; Whitebirch et al., 2022), which are susceptible to degeneration in TLE relative to the injury resistant CA2 (Steve et al., 2014). CA2 epileptiform activity has been reported in KA and pilocarpine models of TLE (Kilias et al., 2022; Whitebirch et al., 2022) as well as resected tissue from TLE patients (Wittner et al., 2009). Investigation of CA2's contribution to TLE development and its influence on spontaneous seizure generation is only in its early stages, but a recent report performed an extensive evaluation of CA2 function in the PILO-SE model of TLE (Whitebirch et al., 2022). Here, they found that months following PILO-SE, when spontaneous seizures have developed, CA2 function exhibited an overall increased E/I balance as evidenced by increased intrinsic excitability of CA2 and reduced synaptic inhibition onto CA2, which enhanced excitation onto CA1 PCs and increased intrinsic excitability in these neurons. Moreover, acute inhibition of CA2 reduced seizure frequency in mice that developed spontaneous seizures. In a KA-SE model, another group found that CA2 and the DG have coupled epileptiform activity weeks following SE induction (Kilias et al., 2022). In PILO-SE, mossy fiber connections from DG to CA2 were also found to drive excitation over inhibition in CA2 (Whitebirch et al., 2022). In both PILO-SE, KA-SE, and resected TLE tissue, mossy fiber sprouting, a common pathological hallmark of TLE, has been reported to occur in CA2 and is thought to enable the development of epileptiform activity in the hippocampus and spontaneous seizures (Althaus et al., 2016; Freiman et al., 2021; Haussler et al., 2016).

This evidence supports the idea that CA2 is involved in promoting seizure activity in TLE and supports our findings that RGS14 in CA2 PCs would influence excitability of this region and in the hippocampus to modulate behavioral seizures. However, because our analysis only evaluated seizure pathology in the acute phase prior to spontaneous seizure activity, it is currently unknown whether RGS14 is involved in the development of TLE. Spontaneous seizure activity has never been demonstrated in RGS14 KO mice, and, furthermore, RGS14 KO mice live longer than WT counterparts without any apparent pathology (Vatner et al., 2018), suggesting loss of RGS14 is not deleterious for unchallenged mice. However, a tantalizing hypothesis is that RGS14 is a crucial component upon pathological insult. Others have demonstrated that loss of RGS14 is usually beneficial until injury is induced (Li et al., 2016; Zhang et al., 2022), which then causes a more deleterious response in animals lacking RGS14, and our findings here indicate a similar role in hippocampal injury (Harbin et al., 2023). TLE is commonly acquired through traumatic brain injury, hypoxia, SE, or other insults, where initial injury spurs epileptogenesis and eventual spontaneous seizures (Devinsky et al., 2018; Tatum, 2012). We propose that RGS14 is likely to regulate this response and prevent pathogenesis based on our findings, the relevance of RGS14 to injury response, and the increasing implication of CA2 to seizure development.

By regulating CA2 excitability, RGS14 would likely play an important part in controlling hippocampal excitability and propagation of epileptiform activity to CA1 and extrahippocampal structures in the epileptic brain. Because RGS14 is a plasticity inhibiting protein (Lee et al., 2010), it could also be likely that RGS14 limits synaptic potentiation and excitatory drive from sprouting mossy fibers, thereby limiting pathological rewiring of the hippocampus. RGS14's effects on mitochondrial function, metabolism, and oxidative stress may also help limit redox-related changes that might cause cellular dysfunction (Fig. 3-10, Tables 2, 3) (Harbin et al., 2023 and unpublished data). Of great interest is how the lack of microglia and astrocyte activation in the hippocampus affects the development of TLE in RGS14 KO mice (Fig. 20-22) (Harbin et al., 2023

and unpublished data). There is considerable evidence demonstrating a detrimental effect of prolonged neuroinflammation as it relates to hippocampal damage and seizure development (Vezzani et al., 2011). However, the absence of transient glial response to seizure activity may be of pathological consequence as well. Therefore, an important follow-up study to the work conducted here will be the long-term monitoring of RGS14 KO mice for spontaneous seizure activity (latency to spontaneous seizures, frequency of spontaneous seizures, etc.) following SE induction and hippocampal pathology (neuronal loss, neuroinflammation, and mossy fiber sprouting) in the chronic phase of epileptogenesis. Based on our observations here, we would expect that loss of RGS14 would expedite the development of spontaneous seizures by influencing TLE pathology in the hippocampus, likely through CA2-dependent mechanisms but with the possibility of non-CA2 contributions as well.

4.7. Future directions

Although the findings from this work are compelling, they generate more questions than answers but open up many avenues of future experimentation that will be necessary to identify the mechanism(s) by which RGS14 is affecting seizure behavior and pathology. While previous sections of this chapter briefly touch on future directions that stem from each finding, the following will provide a more detailed and cohesive guide for follow-up studies that would expand upon the findings of this dissertation. Many experiments could be imagined, but I will focus broadly on five avenues of investigation that should help unravel the contributions of RGS14 to the main effects observed in the RGS14 KO mice: 1) Measurements of electrical activity in acute hippocampal slices under epileptiform conditions; 2) EEG measurements in and outside of the hippocampus and physiological monitoring of peripheral effects; 3) Evaluation of mitochondria morphology and function in neurons expressing or not expressing RGS14 and identification of domains within RGS14 necessary for localization and effects on mitochondria; 4) Further characterization of RGS14's effects on glia (astrocytes and microglia) at baseline and following seizure and other

promoters of neuroinflammation; 5) The development of spontaneous seizures, pathology, and behavioral impairment associated with TLE.

4.7.1. In vitro measurement of epileptiform activity in acute hippocampal slices

To evaluate RGS14 function in CA2 and its possible contributions to quicker seizure initiation, mice with site-specific deletion of RGS14 in CA2 can be generated using the CreLox system, where WT mice expressing Amigo2-Cre (i.e., Cre expression under the CA2-specific Amigo2 promoter) are injected with AAV-Cre virus containing siRNA targeted towards RGS14 in area CA2 (CA2-RGS14 KO) (Hitti and Siegelbaum, 2014; Kim et al., 2018). After verifying knockdown of RGS14 specifically in CA2, acute hippocampal slices can be obtained from WT, CA2-RGS14 KO, and global RGS14 KO mice. Bath incubation of artificial cerebrospinal fluid (ACSF) with high concentrations of K^+ or low concentrations Mg^{2+} can be used to induce epileptiform activity in hippocampal slices (Raimondo et al., 2017). Direct measurement of electrical activity prior to and during seizure activity could ideally be achieved with a multi electrode array (MEA) that can simultaneously measure local field potentials in each layer of each CA field of the hippocampus (Filatov et al., 2011). These measurements would provide both spatial and temporal localization of epileptiform activity specifically within the hippocampus of mice with RGS14 (WT), mice lacking RGS14 in only CA2 (CA2-RGS14 KO), and mice completely devoid of RGS14 (RGS14 KO). If RGS14 plays a role in seizure initiation in the hippocampus, we would expect quicker generation of epileptiform dynamics, possibly originating in CA2, in the RGS14 KO mice relative to WT mice. If RGS14 does this by specific regulation of CA2 activity, we would likely observe similar results between RGS14 KO and CA2-RGS14 KO hippocampi, but similar temporal-spatial generation of epileptiform activity between WT and CA2-RGS14 KO hippocampi would indicate RGS14 expression outside of the CA2 is more important for seizure initiation. However, if RGS14 does not affect seizure initiation in the hippocampus, we would find no differences in hippocampal epileptiform generation between the three mice, and this would

suggest RGS14 is more important for the propagation of epileptiform activity out of the hippocampus.

4.7.2. In vivo EEG measurements of epileptiform activity and physiological monitoring of respiratory and cardiac function

Similar experiments in vivo could be performed with the three genotypes of mice stated above. These experiments would evaluate how loss of RGS14 globally or specifically in CA2 affects initiation of epileptiform activity within the hippocampus and its propagation to associated structures like the amygdala, where RGS14 is also expressed, and neocortex or motor cortex that is associated with motor seizure activity (Medvedev et al., 2000; Tse et al., 2014). To initiate seizure activity specifically in the hippocampus and reduce mortality, KA could be administered intrahippocampally, and epileptiform activity would be measured using depth electrode recordings in the hippocampus, amygdala, and cortex. Faster generation of epileptiform activity in the hippocampus of RGS14 KO mice would suggest RGS14 regulates seizure generation in the hippocampus, and similar observations in CA2-RGS14 KO mice would imply that RGS14 does so by affecting CA2 activity. If hippocampal epileptiform activity is similar between WT and CA2-RGS14 KO mice, then it is more likely that RGS14 does not affect the initiation of hippocampal epileptiform activity via CA2 regulation. Alternatively, similar observations of hippocampal epileptiform activity between the three genotypes would support the idea that RGS14 does not play a role in limiting the initiation of hippocampal epileptiform activity. During motor seizure activity, we would likely see coincidental epileptiform spiking in the neocortex and/or motor cortex (Medvedev et al., 2000; Tse et al., 2014), and we would expect RGS14 KO mice to have a quicker propagation of epileptiform activity to these regions based on quicker entry into Stage 3 seizure in RGS14 KO mice (Harbin et al., 2023). Additionally, similar latencies of epileptiform propagation to these regions (likely coinciding with decreased latency to Stage 3 seizure activity) between RGS14 KO and CA2-RGS14 KO mice would indicate that RGS14 regulates CA2 specifically to

limit epileptiform propagation out of the hippocampus. Alternatively, a lack of effect in CA2-RGS14 KO mice would suggest RGS14 regulation outside of CA2 is responsible for the observed behavioral effects seen in this dissertation. Because CA2 regulates hippocampal oscillations (Oliva et al., 2023), power spectral analysis could be performed on local field potentials to measure the types and degree of oscillatory activity in the hippocampus during seizure and its oscillatory spread to the amygdala, neocortex, or motor cortex. If RGS14 does control hippocampal synchronization and the spread of oscillatory activity, then we would expect RGS14 KO and likely CA2-RGS14 KO mice to either generate certain types of oscillations (e.g., gamma) quicker or more intensely in the hippocampus and accelerate the spread to associated areas.

We may also see quicker development of epileptiform activity to the amygdala as a result of faster propagation in RGS14 KO or CA2-RGS14 KO mice. Because the effects on latency to mortality were more robust, it would also be advantageous to measure cardiac and respiratory activity in these mice to determine if mortality during SE is caused by cardiac arrest or respiratory depression, respectively. Because the amygdala (and specifically central amygdala where RGS14 is expressed) centrally regulates breathing, the spread of epileptiform activity may correlate with cessation of breathing and mortality (Dlouhy et al., 2015; Nobis et al., 2019; Rhone et al., 2020). Therefore, simultaneous measurements of cardiac/respiratory activity and neuronal activity may provide greater insight into why RGS14 KO mice succumb much quicker than WT mice during SE. Regardless of genotype, we may find a strong correlation between propagation of epileptiform activity to the amygdala and respiratory depression. If RGS14 regulates its effects on SE-induced mortality through a central mechanism, then we would expect to see quicker propagation of seizure activity to the amygdala (or elsewhere) that correlates with quicker entry into respiratory depression in RGS14 KO mice. RGS14 may accomplish this by regulating CA2 activity, where CA2-RGS14 KO mice would behave similarly to RGS14 KO mice (i.e., faster development of coincidental amygdala epileptiform activity and respiratory depression). If

RGS14's effects on mortality are mediated by its expression in the amygdala or elsewhere in the brain, then we would likely see similar results between WT and CA2-RGS14 KO mice and require further evaluation of RGS14's role outside of CA2. However, a lack of respiratory depression or alteration of cardiac activity in RGS14 KO mice would indicate an alternative means by which RGS14 affects mortality during SE.

4.7.3. Evaluation of RGS14's effects on neuronal mitochondria

Deeper characterization of RGS14's function in neuronal mitochondria would likely provide greater understanding of how RGS14 limits oxidative stress and further expand on RGS14's already multifunctional nature in neurons. Using primary hippocampal cultures, we could transduce neurons with full length RGS14 or various truncation mutants (omitting certain domains of the protein) and use immunocytochemistry targeted towards RGS14 and a mitochondrial marker (e.g., COX-IV) to determine what region(s) of RGS14 are necessary for its localization to mitochondria. This experiment would likely lead to the identification of an MTS, which could then be mutated in future experiments to distinguish RGS14's effects at the mitochondria vs. effects upstream of mitochondria that could also alter its function. In the same model system (RGS14 full length vs functional or truncation mutants), we could evaluate oxygen consumption rate of neurons and the effects of RGS14 and the importance of each domain on oxygen consumption. Because our proteomics revealed a potential dysregulation of fatty acid metabolism, a similar experiment could be performed but instead evaluating fuel flexibility of neurons with functional RGS14 or mutant RGS14 to determine if RGS14 shifts energy substrates from primarily glucose to fatty acids or other biomolecules (Qi et al., 2021). Additional studies in this system could include more direct measurements of ROS and oxidative stress using mitoSOX to evaluate superoxide production generated from the mitochondria (Baek et al., 2018) and calcium buffering capacity of mitochondria using calcium fluorescent indicators targeted to the mitochondria, such as mitochondrial-targeted Yellow Cameleon 3.6 (Calvo-Rodriguez et al., 2020). Moreso,

measurement of NO in fixed cells in primary hippocampal neurons using 4-amino-5-methylamino-2',7'-difluorofluorescein diacetate (DAF-FM) (Tjalkens et al., 2011) and evaluating the effects of RGS14 (and mutants) on NO production would be important for determining how RGS14 limits oxidative stress. These experiments could be performed at baseline and during glutamatergic stimulation to simulate repeated neuronal activity. Furthermore, if an MTS is identified and can be mutated to prevent RGS14 mitochondrial localization, then it would be advantageous to compare WT RGS14 to MTS-mutant RGS14 in these experiments to distinguish the effects between RGS14 within mitochondria and RGS14 outside of the mitochondria. Last, using fixed hippocampal tissue from RGS14 KO mice and relevant immunohistochemical markers, several properties of mitochondrial morphology should be evaluated like the number and size of mitochondria, the extent of mitochondrial fusion and fission, and mitochondrial abnormalities (e.g., swelling) at baseline or following seizure activity. Together, this suite of experimentation would greatly improve our understanding of RGS14's role in mitochondrial function.

4.7.4. Characterizing RGS14's role in glial response

Our findings that loss of RGS14 prevented the activation of microglia and astrocytes in regions where RGS14 induction was also observed was surprising but reveals an intriguing idea that RGS14 (and possibly the upregulation) is necessary for glia reactivity after seizure activity. One important question is whether RGS14's effects on glia are specific to seizure activity (glial activation arising from excessive neuronal activity) or translate to other states of neuroinflammation, such as what is observed following infection. To test this idea, WT and RGS14 KO mice could be administered lipopolysaccharide (LPS), a pathogenic component of the bacterial cell wall, which causes robust microglial and astrocyte activation (Skrzypczak-Wiercioch and Salat, 2022). If we observe that microglia and astrocytes from RGS14 KO mice are similarly deficient in their reactivity as they are following SE, then it could reflect inherent dysfunction within glia (and specifically microglia) as microglial toll-like receptors primarily mediate the glial-

activating and neuroinflammatory effects of LPS (Lehnardt et al., 2003). However, similar levels of microgliosis and astrogliosis between WT and RGS14 KO mice following LPS administration would support the idea that RGS14's effects on glial activation are seizure-specific and may suggest a neuronal mechanism of glial activation. Utilizing real-time polymerase chain reaction (RT-PCR) to quantify the expression levels of inflammatory cytokines that increase during glial activation (e.g., TNF- α , interleukin-1 β) either following seizure activity or LPS stimulation would provide further insight into how glia may be dysfunctional in RGS14 KO mice (Vezzani, 2005). Along these lines, evaluating the hippocampal expression pattern of COX-2 and levels of downstream prostaglandins synthesized by COX-2, both of which mediate glial activation and neuroinflammation following seizure activity (Rojas et al., 2019), would better detail the mechanisms by which RGS14 prompts glial response, especially considering that our proteomics revealed altered expression patterns of COX-2/prostaglandin-related proteins in RGS14 KO mice.

However, this would still not satisfy the question of whether RGS14 is mediating its effects on glia activation in either neurons or glia. Two experiments could shed some light on this quandary. First, viral knockdown of RGS14 specifically in neurons using the CreLox system and a neuronal specific promoter (e.g., CaMKII) and then challenging these mutant mice with seizure would identify the neuronal RGS14's contribution to the phenotype. If neuronal knockdown of RGS14 impaired glial response as it does in global RGS14 KO, then it would suggest neuronal RGS14 is necessary for these effects, possibly promoting the expression and release of glial activating factors following seizure. However, if glial activation was observed in mice lacking neuronal RGS14, it would indicate that RGS14 acts in glia or by another mechanism to promote glial response to seizure activity. Although RGS14 expression in glia has not been reported, follow-up studies could utilize microglia- and astrocyte-specific knockdown of RGS14 to determine if RGS14 expression in either cell-type is necessary for glial activation. Second, isolation and culturing of microglia and astrocytes from RGS14 KO mice would allow us to determine if there is

inherent dysfunction within RGS14 KO glia without the direct effects of neuron. Activation of isolated RGS14 KO microglia or astrocytes in vitro would suggest that there is no intrinsic dysfunction within each glial cell and support a neuronal-specific mechanism by which RGS14 promotes glial response. However, if glia from RGS14 KO mice are unable to activate, further studies assessing microglia and astrocytic function would be necessary. Microglial function could be assessed using chemotaxis and phagocytosis assays in response to glial activating factors like ATP (Eyo et al., 2017). Astrocyte function could also be evaluated in isolated or astrocyte-neuron co-cultures to evaluate metabolic cooperation. Assessing expression and activity levels of important metabolic enzymes like glutamine synthetase and the transfer of energy substrates between the two cell types would expand on the proteomics results that indicate potential dysregulation of astrocytic capabilities, and fuel flex testing astrocyte and neuron-astrocyte cultures would shed light on neurometabolic cooperativity in RGS14 KO mice (Qi et al., 2021). Taken together, these potential experiments would provide groundwork for a better understanding of RGS14's role in glia response.

4.7.5. Monitoring the development of TLE and associated pathology after SE

The last and most obvious follow-up to this work is the likely consequence of extreme seizure activity: the development of spontaneous seizures and other TLE-like phenomena. Following SE, we could use video-EEG monitoring of behavioral and electrical seizure activity, respectively, to determine if RGS14 KO mice have altered sensitivity to the development of spontaneous seizures. We could measure parameters such as the latency to first spontaneous seizure and the frequency, duration, and intensity of spontaneous seizures once they emerge. This could be done in both RGS14 KO mice and CA2-RGS14 KO mice, as area CA2 is important for sustaining spontaneous seizure activity in rodent models of TLE. It would also be helpful to evaluate TLE pathology that exists in the phase of spontaneous seizure development, including sustained gliosis, neurodegeneration in the hippocampus and in other regions, and mossy fiber

sprouting in the hippocampus, particularly to area CA2 which receives sprouting connections following SE (Haussler et al., 2016). Because RGS14 suppresses postsynaptic synaptic plasticity in area CA2 (Lee et al., 2010), it is possible that loss of RGS14 enhances mossy fiber connections within area CA2 and could contribute to hippocampal network rewiring that likely underlies spontaneous seizure formation. As an indicator neuronal damage and brain dysfunction, RGS14 KO mice could be evaluated for cognitive impairment using spatial (Morris water maze) and object recognition (novel object) memory tasks, both of which rely on proper functioning of the hippocampus (Zemla and Basu, 2017). Additional behavioral assays could include assessment of depressive-like behaviors using the forced-swim test and anxiety-like behaviors like novelty suppressed feeding (Belovicova et al., 2017). The faster or more frequent development of spontaneous seizure activity, exacerbated pathology, and enhanced behavioral impairment in RGS14 KO or CA2-RGS14 KO mice would provide compelling evidence that RGS14 is an important component of limiting the development of TLE and its consequences and justify RGS14 as a novel therapeutic target to prevent the development of TLE in humans.

4.8. Conclusions and working model of CA2 regulation by RGS14 during seizure activity

Our findings suggest that RGS14 dampens behavioral seizures, limits hippocampal pathology, and regulates CA2 PC function by engaging mitochondria oxidative stress pathways in addition to other established regulatory roles as illustrated in our proposed working model (Fig. 23). Consistent with this idea, RGS14 protein was upregulated in area CA2 after KA-induced SE. Mice lacking RGS14 had faster onset of SE and mortality, striking alterations in metabolic and mitochondrial protein expression, enhanced oxidative stress, and region-dependent suppression of glial activation. Although mechanistic insights into RGS14 roles in seizure response are limited in our study, we show that RGS14 localized to mitochondria in CA2 hippocampus and regulated mitochondrial respiration as one possible and newly appreciated mechanism for RGS14 protective actions.

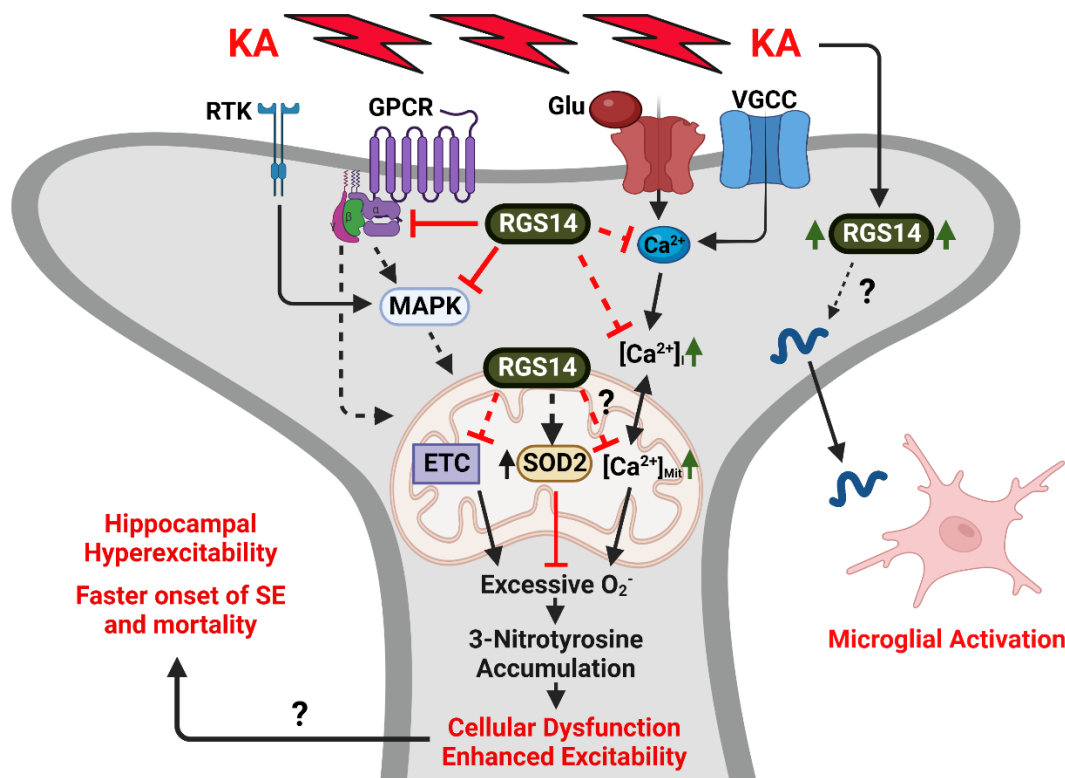


Figure 23. Proposed working model for RGS14 regulation of CA2 pyramidal neurons following seizure. (Harbin et al., 2023) Diagram of a CA2 dendritic spine illustrating known and speculative roles for RGS14 in intracellular regulation. RGS14 at the plasma membrane and in the cytosol can negatively regulate both GPCR- and MAPK-dependent signaling, while buffering calcium transients from NMDA receptors and VGCC through an unknown mechanism. In addition to its localization at the membrane and in cytosolic spaces, RGS14 localizes to mitochondria in CA2 pyramidal cells. By its effect on signaling and calcium buffering at the membrane/cytosol, its localization to the mitochondria, or through an unknown mechanism, RGS14 is capable of influencing metabolic/mitochondrial protein expression, including SOD2. Although speculative, RGS14 may buffer mitochondrial calcium in a similar fashion to buffering membrane calcium transients of dendritic spine. Regulatory capacity by RGS14 culminates to provide balance of ROS (O_2^-) and mitochondrial function. RGS14 expression is induced by seizure activity, and loss

RGS14 induction is coincidental with local glial response. Loss of RGS14 regulation culminates to enhanced oxidative stress, aberrant signaling, and cellular dysfunction of CA2, which may contribute to susceptibility to seizure activity and pathology. Created in BioRender.

Additionally, our observed changes in protein sets/pathways provide compelling evidence of altered responses in RGS14 KO mice that are ripe for future study. As mentioned above, it is unclear whether these early pathological alterations contribute to the development of spontaneous seizures and other TLE pathology. Because of the numerous effects of RGS14 in the CA2 region and CA2's recent implication in TLE, long term monitoring of RGS14 KO mice for TLE development using video/EEG for spontaneous seizure development, behavioral assays for cognitive impairment, and histological assessment for TLE pathology will be an important follow-up to our findings. Future studies will also explore how RGS14 engages the mitochondria and metabolic processes in the hippocampus. Additionally, RGS14's peculiar role of neuroinflammatory regulation will also need to be further investigated with special interest on glial activation caused by seizure-inducing stimuli vs general inflammatory stimuli. Together, our findings highlight a novel and important regulatory role of RGS14 in area CA2, seizure development, and related pathology with implications for TLE pathogenesis.

References

- Abbott NJ, Ronnback L and Hansson E (2006) Astrocyte-endothelial interactions at the blood-brain barrier. *Nat Rev Neurosci* **7**(1): 41-53.
- Alavi MV and Fuhrmann N (2013) Dominant optic atrophy, OPA1, and mitochondrial quality control: understanding mitochondrial network dynamics. *Mol Neurodegener* **8**: 32.
- Alberini CM (2009) Transcription factors in long-term memory and synaptic plasticity. *Physiol Rev* **89**(1): 121-145.
- Alexander GM, Brown LY, Farris S, Lustberg D, Pantazis C, Gloss B, Plummer NW, Jensen P and Dudek SM (2018) CA2 neuronal activity controls hippocampal low gamma and ripple oscillations. *Elife* **7**.
- Alexander GM, Farris S, Pirone JR, Zheng C, Colgin LL and Dudek SM (2016) Social and novel contexts modify hippocampal CA2 representations of space. *Nat Commun* **7**: 10300.
- Alexander GM, Riddick NV, McCann KE, Lustberg D, Moy SS and Dudek SM (2019) Modulation of CA2 neuronal activity increases behavioral responses to fear conditioning in female mice. *Neurobiol Learn Mem* **163**: 107044.
- Alqinyah M and Hooks SB (2018) Regulating the regulators: Epigenetic, transcriptional, and post-translational regulation of RGS proteins. *Cell Signal* **42**: 77-87.
- Althaus AL, Zhang H and Parent JM (2016) Axonal plasticity of age-defined dentate granule cells in a rat model of mesial temporal lobe epilepsy. *Neurobiol Dis* **86**: 187-196.
- Attwell D and Laughlin SB (2001) An energy budget for signaling in the grey matter of the brain. *J Cereb Blood Flow Metab* **21**(10): 1133-1145.
- Baek SH, Cho Y, Lee J, Choi BY, Choi Y, Park JS, Kim H, Sul J, Kim E, Park JH and Jo DG (2018) Intracellular and Mitochondrial Reactive Oxygen Species Measurement in Primary Cultured Neurons. *Bio Protoc* **8**(11): e2871.
- Bandookwala M and Sengupta P (2020) 3-Nitrotyrosine: a versatile oxidative stress biomarker for major neurodegenerative diseases. *Int J Neurosci* **130**(10): 1047-1062.
- Barber CN and Raben DM (2019) Lipid Metabolism Crosstalk in the Brain: Glia and Neurons. *Front Cell Neurosci* **13**: 212.
- Basu J and Siegelbaum SA (2015) The Corticohippocampal Circuit, Synaptic Plasticity, and Memory. *Cold Spring Harb Perspect Biol* **7**(11).
- Bazzigaluppi P, Ebrahim Amini A, Weisspapir I, Stefanovic B and Carlen PL (2017) Hungry Neurons: Metabolic Insights on Seizure Dynamics. *Int J Mol Sci* **18**(11).
- Beamer E, Kuchukulla M, Boison D and Engel T (2021) ATP and adenosine-Two players in the control of seizures and epilepsy development. *Prog Neurobiol* **204**: 102105.
- Belanger M, Allaman I and Magistretti PJ (2011) Brain energy metabolism: focus on astrocyte-neuron metabolic cooperation. *Cell Metab* **14**(6): 724-738.
- Belovicova K, Bogi E, Csatlosova K and Dubovicky M (2017) Animal tests for anxiety-like and depression-like behavior in rats. *Interdiscip Toxicol* **10**(1): 40-43.
- Ben-Ari Y and Cossart R (2000) Kainate, a double agent that generates seizures: two decades of progress. *Trends Neurosci* **23**(11): 580-587.
- Ben-Ari Y, Tremblay E and Ottersen OP (1980) Injections of kainic acid into the amygdaloid complex of the rat: an electrographic, clinical and histological study in relation to the pathology of epilepsy. *Neuroscience* **5**(3): 515-528.
- Ben-Johny M and Yue DT (2014) Calmodulin regulation (calmodulation) of voltage-gated calcium channels. *J Gen Physiol* **143**(6): 679-692.
- Benard G, Massa F, Puente N, Lourenco J, Bellocchio L, Soria-Gomez E, Matias I, Delamarre A, Metna-Laurent M, Cannich A, Hebert-Chatelain E, Mulle C, Ortega-Gutierrez S, Martin-Fontecha M, Klugmann M, Guggenhuber S, Lutz B, Gertsch J, Chaouloff F, Lopez-

- Rodriguez ML, Grandes P, Rossignol R and Marsicano G (2012) Mitochondrial CB(1) receptors regulate neuronal energy metabolism. *Nat Neurosci* **15**(4): 558-564.
- Bennett ML, Bennett FC, Liddelow SA, Ajami B, Zamanian JL, Fernhoff NB, Mulinyawe SB, Bohlen CJ, Adil A, Tucker A, Weissman IL, Chang EF, Li G, Grant GA, Hayden Gephart MG and Barres BA (2016) New tools for studying microglia in the mouse and human CNS. *Proc Natl Acad Sci U S A* **113**(12): E1738-1746.
- Bennett MV, Contreras JE, Bukauskas FF and Saez JC (2003) New roles for astrocytes: gap junction hemichannels have something to communicate. *Trends Neurosci* **26**(11): 610-617.
- Betke KM, Wells CA and Hamm HE (2012) GPCR mediated regulation of synaptic transmission. *Prog Neurobiol* **96**(3): 304-321.
- Blumcke I, Thom M, Aronica E, Armstrong DD, Bartolomei F, Bernasconi A, Bernasconi N, Bien CG, Cendes F, Coras R, Cross JH, Jacques TS, Kahane P, Mathern GW, Miyata H, Moshe SL, Oz B, Ozkara C, Perucca E, Sisodiya S, Wiebe S and Spreafico R (2013) International consensus classification of hippocampal sclerosis in temporal lobe epilepsy: a Task Force report from the ILAE Commission on Diagnostic Methods. *Epilepsia* **54**(7): 1315-1329.
- Boehringer R, Polygalov D, Huang AJY, Middleton SJ, Robert V, Wintzer ME, Piskorowski RA, Chevaleyre V and McHugh TJ (2017) Chronic Loss of CA2 Transmission Leads to Hippocampal Hyperexcitability. *Neuron* **94**(3): 642-655 e649.
- Bogeski I and Niemeyer BA (2014) Redox regulation of ion channels. *Antioxid Redox Signal* **21**(6): 859-862.
- Bos JL, Rehmann H and Wittinghofer A (2007) GEFs and GAPs: critical elements in the control of small G proteins. *Cell* **129**(5): 865-877.
- Botcher NA, Falck JE, Thomson AM and Mercer A (2014) Distribution of interneurons in the CA2 region of the rat hippocampus. *Front Neuroanat* **8**: 104.
- Branch MR and Hepler JR (2017) Endogenous RGS14 is a cytoplasmic-nuclear shuttling protein that localizes to juxtannuclear membranes and chromatin-rich regions of the nucleus. *PLoS One* **12**(9): e0184497.
- Brennan AM, Suh SW, Won SJ, Narasimhan P, Kauppinen TM, Lee H, Edling Y, Chan PH and Swanson RA (2009) NADPH oxidase is the primary source of superoxide induced by NMDA receptor activation. *Nat Neurosci* **12**(7): 857-863.
- Brown DA and Sihra TS (2008) Presynaptic signaling by heterotrimeric G-proteins. *Handb Exp Pharmacol*(184): 207-260.
- Bruce AJ, Boling W, Kindy MS, Peschon J, Kraemer PJ, Carpenter MK, Holtzman FW and Mattson MP (1996) Altered neuronal and microglial responses to excitotoxic and ischemic brain injury in mice lacking TNF receptors. *Nat Med* **2**(7): 788-794.
- Buckmaster P (2012) Mossy Fiber Sprouting in the Dentate Gyrus, in *Jasper's Basic Mechanisms of the Epilepsies* (Noebels J, Avoli, M, Rogawski, MA, Olsen, RW, Delgado-Escueta, AV ed), National Center for Biotechnology Information (US), Bethesda (MD).
- Butler LS, Silva AJ, Abeliovich A, Watanabe Y, Tonegawa S and McNamara JO (1995) Limbic epilepsy in transgenic mice carrying a Ca²⁺/calmodulin-dependent kinase II alpha-subunit mutation. *Proc Natl Acad Sci U S A* **92**(15): 6852-6855.
- Buzsaki G (2015) Hippocampal sharp wave-ripple: A cognitive biomarker for episodic memory and planning. *Hippocampus* **25**(10): 1073-1188.
- Calvo-Rodriguez M, Hou SS, Snyder AC, Kharitonova EK, Russ AN, Das S, Fan Z, Muzikansky A, Garcia-Alloza M, Serrano-Pozo A, Hudry E and Bacskai BJ (2020) Increased mitochondrial calcium levels associated with neuronal death in a mouse model of Alzheimer's disease. *Nat Commun* **11**(1): 2146.

- Campolo N, Issoglio FM, Estrin DA, Bartesaghi S and Radi R (2020) 3-Nitrotyrosine and related derivatives in proteins: precursors, radical intermediates and impact in function. *Essays Biochem* **64**(1): 111-133.
- Carstens KE, Phillips ML, Pozzo-Miller L, Weinberg RJ and Dudek SM (2016) Perineuronal Nets Suppress Plasticity of Excitatory Synapses on CA2 Pyramidal Neurons. *J Neurosci* **36**(23): 6312-6320.
- Cartes-Saavedra B, Lagos D, Macuada J, Arancibia D, Burte F, Sjoberg-Herrera MK, Andres ME, Horvath R, Yu-Wai-Man P, Hajnoczky G and Eisner V (2023) OPA1 disease-causing mutants have domain-specific effects on mitochondrial ultrastructure and fusion. *Proc Natl Acad Sci U S A* **120**(12): e2207471120.
- Chen C and Bazan NG (2005) Endogenous PGE2 regulates membrane excitability and synaptic transmission in hippocampal CA1 pyramidal neurons. *J Neurophysiol* **93**(2): 929-941.
- Chen H and Lambert NA (2000) Endogenous regulators of G protein signaling proteins regulate presynaptic inhibition at rat hippocampal synapses. *Proc Natl Acad Sci U S A* **97**(23): 12810-12815.
- Chen IJ, Hee SW, Liao CH, Lin SY, Su L, Shun CT and Chuang LM (2018) Targeting the 15-keto-PGE2-PTGR2 axis modulates systemic inflammation and survival in experimental sepsis. *Free Radic Biol Med* **115**: 113-126.
- Cheung KAK, Peiris H, Wallace G, Holland OJ and Mitchell MD (2019) The Interplay between the Endocannabinoid System, Epilepsy and Cannabinoids. *Int J Mol Sci* **20**(23).
- Chevaleyre V and Siegelbaum SA (2010) Strong CA2 pyramidal neuron synapses define a powerful disinaptic cortico-hippocampal loop. *Neuron* **66**(4): 560-572.
- Cho H, Kim DU and Kehrl JH (2005) RGS14 is a centrosomal and nuclear cytoplasmic shuttling protein that traffics to promyelocytic leukemia nuclear bodies following heat shock. *J Biol Chem* **280**(1): 805-814.
- Clastadonte J, Haydo, PG (2012) Astrocytes and Epilepsy, in *Jasper's Basic Mechanisms of the Epilepsies* (Noebels J, Avoli, M, Rogawski, MA, Olsen, RW, Delgado-Escueta, AV ed), National Center for Biotechnology Information (US), Bethesda (MD).
- Colgin LL, Denninger T, Fyhn M, Hafting T, Bonnevie T, Jensen O, Moser MB and Moser EI (2009) Frequency of gamma oscillations routes flow of information in the hippocampus. *Nature* **462**(7271): 353-357.
- Cui Z, Gerfen CR and Young WS, 3rd (2013) Hypothalamic and other connections with dorsal CA2 area of the mouse hippocampus. *J Comp Neurol* **521**(8): 1844-1866.
- Cunha RA (2005) Neuroprotection by adenosine in the brain: From A(1) receptor activation to A(2A) receptor blockade. *Purinergic Signal* **1**(2): 111-134.
- Curia G, Longo D, Biagini G, Jones RS and Avoli M (2008) The pilocarpine model of temporal lobe epilepsy. *J Neurosci Methods* **172**(2): 143-157.
- Deshpande T, Li T, Henning L, Wu Z, Muller J, Seifert G, Steinhauser C and Bedner P (2020) Constitutive deletion of astrocytic connexins aggravates kainate-induced epilepsy. *Glia* **68**(10): 2136-2147.
- Devinsky O, Vezzani A, O'Brien TJ, Jette N, Scheffer IE, de Curtis M and Perucca P (2018) Epilepsy. *Nat Rev Dis Primers* **4**: 18024.
- Di Meo S, Reed TT, Venditti P and Victor VM (2016) Role of ROS and RNS Sources in Physiological and Pathological Conditions. *Oxid Med Cell Longev* **2016**: 1245049.
- Dlouhy BJ, Gehlbach BK, Kreple CJ, Kawasaki H, Oya H, Buzza C, Granner MA, Welsh MJ, Howard MA, Wemmie JA and Richerson GB (2015) Breathing Inhibited When Seizures Spread to the Amygdala and upon Amygdala Stimulation. *J Neurosci* **35**(28): 10281-10289.
- Donegan ML, Stefanini F, Meira T, Gordon JA, Fusi S and Siegelbaum SA (2020) Coding of social novelty in the hippocampal CA2 region and its disruption and rescue in a 22q11.2 microdeletion mouse model. *Nat Neurosci* **23**(11): 1365-1375.

- Duchen MR (2000) Mitochondria and calcium: from cell signalling to cell death. *J Physiol* **529 Pt 1**(Pt 1): 57-68.
- Dudek SM, Alexander GM and Farris S (2016) Rediscovering area CA2: unique properties and functions. *Nat Rev Neurosci* **17**(2): 89-102.
- Dunn HA and Ferguson SS (2015) PDZ Protein Regulation of G Protein-Coupled Receptor Trafficking and Signaling Pathways. *Mol Pharmacol* **88**(4): 624-639.
- Dykens JA (1994) Isolated cerebral and cerebellar mitochondria produce free radicals when exposed to elevated CA²⁺ and Na⁺: implications for neurodegeneration. *J Neurochem* **63**(2): 584-591.
- Engel J, Jr. (2001) Mesial temporal lobe epilepsy: what have we learned? *Neuroscientist* **7**(4): 340-352.
- Evans PR, Gerber KJ, Dammer EB, Duong DM, Goswami D, Lustberg DJ, Zou J, Yang JJ, Dudek SM, Griffin PR, Seyfried NT and Hepler JR (2018a) Interactome Analysis Reveals Regulator of G Protein Signaling 14 (RGS14) is a Novel Calcium/Calmodulin (Ca²⁺)/CaM and CaM Kinase II (CaMKII) Binding Partner. *J Proteome Res* **17**(4): 1700-1711.
- Evans PR, Lee SE, Smith Y and Hepler JR (2014) Postnatal developmental expression of regulator of G protein signaling 14 (RGS14) in the mouse brain. *J Comp Neurol* **522**(1): 186-203.
- Evans PR, Parra-Bueno P, Smirnov MS, Lustberg DJ, Dudek SM, Hepler JR and Yasuda R (2018b) RGS14 Restricts Plasticity in Hippocampal CA2 by Limiting Postsynaptic Calcium Signaling. *eNeuro* **5**(3).
- Eyo UB, Murugan M and Wu LJ (2017) Microglia-Neuron Communication in Epilepsy. *Glia* **65**(1): 5-18.
- Eyo UB, Peng J, Swiatkowski P, Mukherjee A, Bispo A and Wu LJ (2014) Neuronal hyperactivity recruits microglial processes via neuronal NMDA receptors and microglial P2Y₁₂ receptors after status epilepticus. *J Neurosci* **34**(32): 10528-10540.
- Farris S, Ward JM, Carstens KE, Samadi M, Wang Y and Dudek SM (2019) Hippocampal Subregions Express Distinct Dendritic Transcriptomes that Reveal Differences in Mitochondrial Function in CA2. *Cell Rep* **29**(2): 522-539 e526.
- Fernandez-Moya SM, Bauer KE and Kiebler MA (2014) Meet the players: local translation at the synapse. *Front Mol Neurosci* **7**: 84.
- Ferrer-Sueta G, Campolo N, Trujillo M, Bartesaghi S, Carballal S, Romero N, Alvarez B and Radi R (2018) Biochemistry of Peroxynitrite and Protein Tyrosine Nitration. *Chem Rev* **118**(3): 1338-1408.
- Filatov G, Krishnan GP, Rulkov NF and Bazhenov M (2011) Dynamics of epileptiform activity in mouse hippocampal slices. *J Biol Phys* **37**(3): 347-360.
- Folbergrova J and Kunz WS (2012) Mitochondrial dysfunction in epilepsy. *Mitochondrion* **12**(1): 35-40.
- Foster SL, Lustberg DJ, Harbin NH, Bramlett SN, Hepler JR and Weinshenker D (2021) RGS14 modulates locomotor behavior and ERK signaling induced by environmental novelty and cocaine within discrete limbic structures. *Psychopharmacology (Berl)* **238**(10): 2755-2773.
- Freiman TM, Haussler U, Zentner J, Doostkam S, Beck J, Scheiwe C, Brandt A, Haas CA and Puhahn-Schmeiser B (2021) Mossy fiber sprouting into the hippocampal region CA2 in patients with temporal lobe epilepsy. *Hippocampus* **31**(6): 580-592.
- Friedman A, Heinemann, U (2012) Role of Blood-Brain Barrier Dysfunction in Epileptogenesis, in *Jasper's Basic Mechanisms of the Epilepsies* (Noebels J, Avoli, M, Rogawski, MA, Olsen, RW, Delgado-Escueta, AV ed), National Center for Biotechnology Information (US), Bethesda (MD).
- Friedman PA, Sneddon WB, Mamonova T, Montanez-Miranda C, Ramineni S, Harbin NH, Squires KE, Geffer JV, Magyar CE, Emlet DR and Hepler JR (2022) RGS14 regulates

- PTH- and FGF23-sensitive NPT2A-mediated renal phosphate uptake via binding to the NHERF1 scaffolding protein. *J Biol Chem* **298**(5): 101836.
- Fukasawa Y, Tsuji J, Fu SC, Tomii K, Horton P and Imai K (2015) MitoFates: improved prediction of mitochondrial targeting sequences and their cleavage sites. *Mol Cell Proteomics* **14**(4): 1113-1126.
- Gassmann M and Bettler B (2012) Regulation of neuronal GABA(B) receptor functions by subunit composition. *Nat Rev Neurosci* **13**(6): 380-394.
- Gerber KJ, Dammer EB, Duong DM, Deng Q, Dudek SM, Seyfried NT and Hepler JR (2019) Specific Proteomes of Hippocampal Regions CA2 and CA1 Reveal Proteins Linked to the Unique Physiology of Area CA2. *J Proteome Res* **18**(6): 2571-2584.
- Gerber KJ, Squires KE and Hepler JR (2016) Roles for Regulator of G Protein Signaling Proteins in Synaptic Signaling and Plasticity. *Mol Pharmacol* **89**(2): 273-286.
- Gerber KJ, Squires KE and Hepler JR (2018) 14-3-3gamma binds regulator of G protein signaling 14 (RGS14) at distinct sites to inhibit the RGS14:Galpha(i)-AIF(4)(-) signaling complex and RGS14 nuclear localization. *J Biol Chem* **293**(38): 14616-14631.
- Gilda JE and Gomes AV (2015) Western blotting using in-gel protein labeling as a normalization control: stain-free technology. *Methods Mol Biol* **1295**: 381-391.
- Ginsberg MD, Feliciello A, Jones JK, Avvedimento EV and Gottesman ME (2003) PKA-dependent binding of mRNA to the mitochondrial AKAP121 protein. *J Mol Biol* **327**(4): 885-897.
- Goebel-Goody SM, Baum M, Paspalas CD, Fernandez SM, Carty NC, Kurup P and Lombroso PJ (2012) Therapeutic implications for striatal-enriched protein tyrosine phosphatase (STEP) in neuropsychiatric disorders. *Pharmacol Rev* **64**(1): 65-87.
- Goetzl EJ (2007) Diverse pathways for nuclear signaling by G protein-coupled receptors and their ligands. *FASEB J* **21**(3): 638-642.
- Gold SJ, Ni YG, Dohlman HG and Nestler EJ (1997) Regulators of G-protein signaling (RGS) proteins: region-specific expression of nine subtypes in rat brain. *J Neurosci* **17**(20): 8024-8037.
- Greene D, Richardson S and Turro E (2017) ontologyX: a suite of R packages for working with ontological data. *Bioinformatics* **33**(7): 1104-1106.
- Gu X, Ma Y, Liu Y and Wan Q (2021) Measurement of mitochondrial respiration in adherent cells by Seahorse XF96 Cell Mito Stress Test. *STAR Protoc* **2**(1): 100245.
- Gynther M, Petsalo A, Hansen SH, Bunch L and Pickering DS (2015) Blood-brain barrier permeability and brain uptake mechanism of kainic acid and dihydrokainic acid. *Neurochem Res* **40**(3): 542-549.
- Harbin NH, Bramlett SN, Montanez-Miranda C, Terzioglu G and Hepler JR (2021) RGS14 Regulation of Post-Synaptic Signaling and Spine Plasticity in Brain. *Int J Mol Sci* **22**(13).
- Harbin NH, Lustberg DJ, Hurst C, Pare J, Crotty KM, Waters AL, Yeligar SM, Smith Y, Seyfried NT, Weinshenker D and Hepler JR (2023) RGS14 limits seizure-induced mitochondrial oxidative stress and pathology in hippocampus. *Neurobiol Dis* **181**: 106128.
- Hata AN and Breyer RM (2004) Pharmacology and signaling of prostaglandin receptors: multiple roles in inflammation and immune modulation. *Pharmacol Ther* **103**(2): 147-166.
- Hatanpaa KJ, Raisanen JM, Herndon E, Burns DK, Foong C, Habib AA and White CL, 3rd (2014) Hippocampal sclerosis in dementia, epilepsy, and ischemic injury: differential vulnerability of hippocampal subfields. *J Neuropathol Exp Neurol* **73**(2): 136-142.
- Haussler U, Rinas K, Kiliyas A, Egert U and Haas CA (2016) Mossy fiber sprouting and pyramidal cell dispersion in the hippocampal CA2 region in a mouse model of temporal lobe epilepsy. *Hippocampus* **26**(5): 577-588.
- Hebert-Chatelain E, Desprez T, Serrat R, Bellocchio L, Soria-Gomez E, Busquets-Garcia A, Pagano Zottola AC, Delamarre A, Cannich A, Vincent P, Varilh M, Robin LM, Terral G, Garcia-Fernandez MD, Colavita M, Mazier W, Drago F, Puente N, Reguero L, Elezgarai I, Dupuy JW, Cota D, Lopez-Rodriguez ML, Barreda-Gomez G, Massa F, Grandes P,

- Benard G and Marsicano G (2016) A cannabinoid link between mitochondria and memory. *Nature* **539**(7630): 555-559.
- Herring BE and Nicoll RA (2016) Long-Term Potentiation: From CaMKII to AMPA Receptor Trafficking. *Annu Rev Physiol* **78**: 351-365.
- Higley MJ and Sabatini BL (2012) Calcium signaling in dendritic spines. *Cold Spring Harb Perspect Biol* **4**(4): a005686.
- Hiragi T, Ikegaya Y and Koyama R (2018) Microglia after Seizures and in Epilepsy. *Cells* **7**(4).
- Hitti FL and Siegelbaum SA (2014) The hippocampal CA2 region is essential for social memory. *Nature* **508**(7494): 88-92.
- Holley AK, Bakthavatchalu V, Velez-Roman JM and St Clair DK (2011) Manganese superoxide dismutase: guardian of the powerhouse. *Int J Mol Sci* **12**(10): 7114-7162.
- Hollinger S, Taylor JB, Goldman EH and Hepler JR (2001) RGS14 is a bifunctional regulator of Galphai/o activity that exists in multiple populations in brain. *J Neurochem* **79**(5): 941-949.
- Hongpaisan J, Winters CA and Andrews SB (2004) Strong calcium entry activates mitochondrial superoxide generation, upregulating kinase signaling in hippocampal neurons. *J Neurosci* **24**(48): 10878-10887.
- Horbinski C and Chu CT (2005) Kinase signaling cascades in the mitochondrion: a matter of life or death. *Free Radic Biol Med* **38**(1): 2-11.
- Hosli L, Binini N, Ferrari KD, Thieren L, Looser ZJ, Zuend M, Zanker HS, Berry S, Holub M, Mobius W, Ruhwedel T, Nave KA, Giaume C, Weber B and Saab AS (2022) Decoupling astrocytes in adult mice impairs synaptic plasticity and spatial learning. *Cell Rep* **38**(10): 110484.
- Hu JH, Malloy C and Hoffman DA (2020) P38 Regulates Kainic Acid-Induced Seizure and Neuronal Firing via Kv4.2 Phosphorylation. *Int J Mol Sci* **21**(16).
- Iglesias JE, Augustinack JC, Nguyen K, Player CM, Player A, Wright M, Roy N, Frosch MP, McKee AC, Wald LL, Fischl B, Van Leemput K and Alzheimer's Disease Neuroimaging I (2015) A computational atlas of the hippocampal formation using ex vivo, ultra-high resolution MRI: Application to adaptive segmentation of in vivo MRI. *Neuroimage* **115**: 117-137.
- Ioannou MS, Jackson J, Sheu SH, Chang CL, Weigel AV, Liu H, Pasolli HA, Xu CS, Pang S, Matthies D, Hess HF, Lippincott-Schwartz J and Liu Z (2019) Neuron-Astrocyte Metabolic Coupling Protects against Activity-Induced Fatty Acid Toxicity. *Cell* **177**(6): 1522-1535 e1514.
- Jeon SH, Kim YS, Bae CD and Park JB (2000) Activation of JNK and p38 in rat hippocampus after kainic acid induced seizure. *Exp Mol Med* **32**(4): 227-230.
- Jiang J, Quan Y, Ganesh T, Pouliot WA, Dudek FE and Dingledine R (2013) Inhibition of the prostaglandin receptor EP2 following status epilepticus reduces delayed mortality and brain inflammation. *Proc Natl Acad Sci U S A* **110**(9): 3591-3596.
- Johanson SO, Crouch MF and Hendry IA (1996) Signal transduction from membrane to nucleus: the special case for neurons. *Neurochem Res* **21**(7): 779-785.
- Johnson ECB, Carter EK, Dammer EB, Duong DM, Gerasimov ES, Liu Y, Liu J, Betarbet R, Ping L, Yin L, Serrano GE, Beach TG, Peng J, De Jager PL, Haroutunian V, Zhang B, Gaiteri C, Bennett DA, Gearing M, Wingo TS, Wingo AP, Lah JJ, Levey AI and Seyfried NT (2022) Large-scale deep multi-layer analysis of Alzheimer's disease brain reveals strong proteomic disease-related changes not observed at the RNA level. *Nat Neurosci* **25**(2): 213-225.
- Johnson ECB, Dammer EB, Duong DM, Ping L, Zhou M, Yin L, Higginbotham LA, Guajardo A, White B, Troncoso JC, Thambisetty M, Montine TJ, Lee EB, Trojanowski JQ, Beach TG, Reiman EM, Haroutunian V, Wang M, Schadt E, Zhang B, Dickson DW, Ertekin-Taner N, Golde TE, Petyuk VA, De Jager PL, Bennett DA, Wingo TS, Rangaraju S, Hajjar I, Shulman JM, Lah JJ, Levey AI and Seyfried NT (2020) Large-scale proteomic analysis of

- Alzheimer's disease brain and cerebrospinal fluid reveals early changes in energy metabolism associated with microglia and astrocyte activation. *Nat Med* **26**(5): 769-780.
- Kandratavicius L, Balista PA, Lopes-Aguiar C, Ruggiero RN, Umeoka EH, Garcia-Cairasco N, Bueno-Junior LS and Leite JP (2014) Animal models of epilepsy: use and limitations. *Neuropsychiatr Dis Treat* **10**: 1693-1705.
- Kann O and Kovacs R (2007) Mitochondria and neuronal activity. *Am J Physiol Cell Physiol* **292**(2): C641-657.
- Kay K, Sosa M, Chung JE, Karlsson MP, Larkin MC and Frank LM (2016) A hippocampal network for spatial coding during immobility and sleep. *Nature* **531**(7593): 185-190.
- Khan SM, Sleno R, Gora S, Zylbergold P, Laverdure JP, Labbe JC, Miller GJ and Hebert TE (2013) The expanding roles of Gbetagamma subunits in G protein-coupled receptor signaling and drug action. *Pharmacol Rev* **65**(2): 545-577.
- Kilias A, Tulke S, Barheier N, Ruther P and Haussler U (2022) Integration of the CA2 region in the hippocampal network during epileptogenesis. *Hippocampus*.
- Kim H, Kim M, Im SK and Fang S (2018) Mouse Cre-LoxP system: general principles to determine tissue-specific roles of target genes. *Lab Anim Res* **34**(4): 147-159.
- Klein JA and Ackerman SL (2003) Oxidative stress, cell cycle, and neurodegeneration. *J Clin Invest* **111**(6): 785-793.
- Kovac S, Domijan AM, Walker MC and Abramov AY (2014) Seizure activity results in calcium- and mitochondria-independent ROS production via NADPH and xanthine oxidase activation. *Cell Death Dis* **5**(10): e1442.
- Kreitzer AC and Malenka RC (2005) Dopamine modulation of state-dependent endocannabinoid release and long-term depression in the striatum. *J Neurosci* **25**(45): 10537-10545.
- Krohn F, Novello M, van der Giessen RS, De Zeeuw CI, Pel JJM and Bosman LWJ (2023) The integrated brain network that controls respiration. *Elife* **12**.
- Labouebe G, Lomazzi M, Cruz HG, Creton C, Lujan R, Li M, Yanagawa Y, Obata K, Watanabe M, Wickman K, Boyer SB, Slesinger PA and Luscher C (2007) RGS2 modulates coupling between GABAB receptors and GIRK channels in dopamine neurons of the ventral tegmental area. *Nat Neurosci* **10**(12): 1559-1568.
- Lagerstrom MC and Schioth HB (2008) Structural diversity of G protein-coupled receptors and significance for drug discovery. *Nat Rev Drug Discov* **7**(4): 339-357.
- Langfelder P and Horvath S (2007) Eigengene networks for studying the relationships between co-expression modules. *BMC Syst Biol* **1**: 54.
- Larminie C, Murdock P, Walhin JP, Duckworth M, Blumer KJ, Scheideler MA and Garnier M (2004) Selective expression of regulators of G-protein signaling (RGS) in the human central nervous system. *Brain Res Mol Brain Res* **122**(1): 24-34.
- Lee JA, Hall B, Allsop J, Alqarni R and Allen SP (2021) Lipid metabolism in astrocytic structure and function. *Semin Cell Dev Biol* **112**: 123-136.
- Lee SE, Simons SB, Heldt SA, Zhao M, Schroeder JP, Vellano CP, Cowan DP, Ramineni S, Yates CK, Feng Y, Smith Y, Sweatt JD, Weinschenker D, Ressler KJ, Dudek SM and Hepler JR (2010) RGS14 is a natural suppressor of both synaptic plasticity in CA2 neurons and hippocampal-based learning and memory. *Proc Natl Acad Sci U S A* **107**(39): 16994-16998.
- Lehnardt S, Massillon L, Follett P, Jensen FE, Ratan R, Rosenberg PA, Volpe JJ and Vartanian T (2003) Activation of innate immunity in the CNS triggers neurodegeneration through a Toll-like receptor 4-dependent pathway. *Proc Natl Acad Sci U S A* **100**(14): 8514-8519.
- Lehr AB, Kumar A, Tetzlaff C, Hafting T, Fyhn M and Stober TM (2021) CA2 beyond social memory: Evidence for a fundamental role in hippocampal information processing. *Neurosci Biobehav Rev* **126**: 398-412.
- Lerma J and Marques JM (2013) Kainate receptors in health and disease. *Neuron* **80**(2): 292-311.

- Leroy F, Park J, Asok A, Brann DH, Meira T, Boyle LM, Buss EW, Kandel ER and Siegelbaum SA (2018) A circuit from hippocampal CA2 to lateral septum disinhibits social aggression. *Nature* **564**(7735): 213-218.
- Levesque M and Avoli M (2013) The kainic acid model of temporal lobe epilepsy. *Neurosci Biobehav Rev* **37**(10 Pt 2): 2887-2899.
- Levesque M, Langlois JM, Lema P, Courtemanche R, Bilodeau GA and Carmant L (2009) Synchronized gamma oscillations (30-50 Hz) in the amygdalo-hippocampal network in relation with seizure propagation and severity. *Neurobiol Dis* **35**(2): 209-218.
- Li Q, Cheng Z, Zhou L, Darmanis S, Neff NF, Okamoto J, Gulati G, Bennett ML, Sun LO, Clarke LE, Marschallinger J, Yu G, Quake SR, Wyss-Coray T and Barres BA (2019) Developmental Heterogeneity of Microglia and Brain Myeloid Cells Revealed by Deep Single-Cell RNA Sequencing. *Neuron* **101**(2): 207-223 e210.
- Li R and Buchanan GF (2019) Scurrying to Understand Sudden Expected Death in Epilepsy: Insights From Animal Models. *Epilepsy Curr* **19**(6): 390-396.
- Li Y, Tang XH, Li XH, Dai HJ, Miao RJ, Cai JJ, Huang ZJ, Chen AF, Xing XW, Lu Y and Yuan H (2016) Regulator of G protein signalling 14 attenuates cardiac remodelling through the MEK-ERK1/2 signalling pathway. *Basic Res Cardiol* **111**(4): 47.
- Liang LP, Ho YS and Patel M (2000) Mitochondrial superoxide production in kainate-induced hippocampal damage. *Neuroscience* **101**(3): 563-570.
- Liang LP and Patel M (2004) Mitochondrial oxidative stress and increased seizure susceptibility in Sod2(-/+) mice. *Free Radic Biol Med* **36**(5): 542-554.
- Liang LP, Waldbaum S, Rowley S, Huang TT, Day BJ and Patel M (2012) Mitochondrial oxidative stress and epilepsy in SOD2 deficient mice: attenuation by a lipophilic metalloporphyrin. *Neurobiol Dis* **45**(3): 1068-1076.
- Lisman J, Yasuda R and Raghavachari S (2012) Mechanisms of CaMKII action in long-term potentiation. *Nat Rev Neurosci* **13**(3): 169-182.
- Liu M, Jiang L, Wen M, Ke Y, Tong X, Huang W and Chen R (2020) Microglia depletion exacerbates acute seizures and hippocampal neuronal degeneration in mouse models of epilepsy. *Am J Physiol Cell Physiol* **319**(3): C605-C610.
- Liu XB and Murray KD (2012) Neuronal excitability and calcium/calmodulin-dependent protein kinase type II: location, location, location. *Epilepsia* **53 Suppl 1**: 45-52.
- Magistretti PJ and Allaman I (2015) A cellular perspective on brain energy metabolism and functional imaging. *Neuron* **86**(4): 883-901.
- Martin-Montanez E, Acevedo MJ, Lopez-Tellez JF, Duncan RS, Mateos AG, Pavia J, Koulen P and Khan ZU (2010) Regulator of G-protein signaling 14 protein modulates Ca(2)+ influx through Cav1 channels. *Neuroreport* **21**(16): 1034-1039.
- Masmudi-Martin M, Navarro-Lobato I, Lopez-Aranda MF, Delgado G, Martin-Montanez E, Quiros-Ortega ME, Carretero-Rey M, Narvaez L, Garcia-Garrido MF, Posadas S, Lopez-Tellez JF, Blanco E, Jimenez-Recuerda I, Granados-Duran P, Paez-Rueda J, Lopez JC and Khan ZU (2019) RGS14(414) treatment induces memory enhancement and rescues episodic memory deficits. *FASEB J* **33**(11): 11804-11820.
- Masuh I, Balaji S, Muntean BS, Skamangas NK, Chavali S, Tesmer JJG, Babu MM and Martemyanov KA (2020) A Global Map of G Protein Signaling Regulation by RGS Proteins. *Cell* **183**(2): 503-521 e519.
- McCann KE, Lustberg DJ, Shaughnessy EK, Carstens KE, Farris S, Alexander GM, Radzicki D, Zhao M and Dudek SM (2021) Novel role for mineralocorticoid receptors in control of a neuronal phenotype. *Mol Psychiatry* **26**(1): 350-364.
- McIntyre DC and Gilby KL (2008) Mapping seizure pathways in the temporal lobe. *Epilepsia* **49 Suppl 3**: 23-30.
- McKenzie AT, Moyon S, Wang M, Katsyv I, Song WM, Zhou X, Dammer EB, Duong DM, Aaker J, Zhao Y, Beckmann N, Wang P, Zhu J, Lah JJ, Seyfried NT, Levey AI, Katsel P,

- Haroutunian V, Schadt EE, Popko B, Casaccia P and Zhang B (2017) Multiscale network modeling of oligodendrocytes reveals molecular components of myelin dysregulation in Alzheimer's disease. *Mol Neurodegener* **12**(1): 82.
- Medvedev A, Mackenzie L, Hiscock JJ and Willoughby JO (2000) Kainic acid induces distinct types of epileptiform discharge with differential involvement of hippocampus and neocortex. *Brain Res Bull* **52**(2): 89-98.
- Mercer A, Trigg HL and Thomson AM (2007) Characterization of neurons in the CA2 subfield of the adult rat hippocampus. *J Neurosci* **27**(27): 7329-7338.
- Middleton SJ and McHugh TJ (2020) CA2: A Highly Connected Intrahippocampal Relay. *Annu Rev Neurosci* **43**: 55-72.
- Missler M, Sudhof TC and Biederer T (2012) Synaptic cell adhesion. *Cold Spring Harb Perspect Biol* **4**(4): a005694.
- Mittal V and Linder ME (2006) Biochemical characterization of RGS14: RGS14 activity towards G-protein alpha subunits is independent of its binding to Rap2A. *Biochem J* **394**(Pt 1): 309-315.
- Modi B, Pimpinella D, Paziienti A, Zacchi P, Cherubini E and Griguoli M (2019) Possible Implication of the CA2 Hippocampal Circuit in Social Cognition Deficits Observed in the Neuroligin 3 Knock-Out Mouse, a Non-Syndromic Animal Model of Autism. *Front Psychiatry* **10**: 513.
- Mohapel P, Dufresne C, Kelly ME and McIntyre DC (1996) Differential sensitivity of various temporal lobe structures in the rat to kindling and status epilepticus induction. *Epilepsy Res* **23**(3): 179-187.
- Montanez-Miranda C, Bramlett SN and Hepler JR (2022) RGS14 expression in CA2 hippocampus, amygdala, and basal ganglia: Implications for human brain physiology and disease. *Hippocampus*.
- Montes de Oca Balderas P (2021) Mitochondria-plasma membrane interactions and communication. *J Biol Chem* **297**(4): 101164.
- Morris NL, Harris FL, Brown LAS and Yeligar SM (2021) Alcohol induces mitochondrial derangements in alveolar macrophages by upregulating NADPH oxidase 4. *Alcohol* **90**: 27-38.
- Mylvaganam S, Ramani M, Krawczyk M and Carlen PL (2014) Roles of gap junctions, connexins, and pannexins in epilepsy. *Front Physiol* **5**: 172.
- Newton AC, Bootman MD and Scott JD (2016) Second Messengers. *Cold Spring Harb Perspect Biol* **8**(8).
- Nguyen D, Alavi MV, Kim KY, Kang T, Scott RT, Noh YH, Lindsey JD, Wissinger B, Ellisman MH, Weinreb RN, Perkins GA and Ju WK (2011) A new vicious cycle involving glutamate excitotoxicity, oxidative stress and mitochondrial dynamics. *Cell Death Dis* **2**(12): e240.
- Nguyen LH, Leiser SC, Song D, Brunner D, Roberds SL, Wong M and Bordey A (2022) Inhibition of MEK-ERK signaling reduces seizures in two mouse models of tuberous sclerosis complex. *Epilepsy Res* **181**: 106890.
- Niquet J, Lopez-Meraz, ML, Wasterlain, CG (2012) Programmed Necrosis After Status Epilepticus, in *Jasper's Basic Mechanisms of the Epilepsies* (Noebels J, Avoli, M, Rogawski, MA, Olsen, RW, Delgado-Escueta, AV ed), National Center for Biotechnology Information (US), Bethesda (MD).
- Niswender CM and Conn PJ (2010) Metabotropic glutamate receptors: physiology, pharmacology, and disease. *Annu Rev Pharmacol Toxicol* **50**: 295-322.
- Nobis WP, Gonzalez Otarula KA, Templer JW, Gerard EE, VanHaerents S, Lane G, Zhou G, Rosenow JM, Zelano C and Schuele S (2019) The effect of seizure spread to the amygdala on respiration and onset of ictal central apnea. *J Neurosurg* **132**(5): 1313-1323.
- Novak A, Vizjak K and Rakusa M (2022) Cognitive Impairment in People with Epilepsy. *J Clin Med* **11**(1).

- Oldham WM and Hamm HE (2008) Heterotrimeric G protein activation by G-protein-coupled receptors. *Nat Rev Mol Cell Biol* **9**(1): 60-71.
- Oliva A, Fernandez-Ruiz A, Buzsaki G and Berenyi A (2016) Role of Hippocampal CA2 Region in Triggering Sharp-Wave Ripples. *Neuron* **91**(6): 1342-1355.
- Oliva A, Fernandez-Ruiz A and Karaba LA (2023) CA2 orchestrates hippocampal network dynamics. *Hippocampus* **33**(3): 241-251.
- Patel DC, Tewari BP, Chaunsali L and Sontheimer H (2019) Neuron-glia interactions in the pathophysiology of epilepsy. *Nat Rev Neurosci* **20**(5): 282-297.
- Patel M (2004) Mitochondrial dysfunction and oxidative stress: cause and consequence of epileptic seizures. *Free Radic Biol Med* **37**(12): 1951-1962.
- Picard M and Shirihai OS (2022) Mitochondrial signal transduction. *Cell Metab* **34**(11): 1620-1653.
- Pimpinella D, Mastroilli V, Giorgi C, Coemans S, Lecca S, Lalive AL, Ostermann H, Fuchs EC, Monyer H, Mele A, Cherubini E and Griguoli M (2021) Septal cholinergic input to CA2 hippocampal region controls social novelty discrimination via nicotinic receptor-mediated disinhibition. *Elife* **10**.
- Piskorowski RA and Chevaleyre V (2013) Delta-opioid receptors mediate unique plasticity onto parvalbumin-expressing interneurons in area CA2 of the hippocampus. *J Neurosci* **33**(36): 14567-14578.
- Purves D, Augustine, GJ, Fitzpatrick, D et al. (2008) *Neuroscience*. 4th ed. Sunderland (MA): Sinauer Associates.
- Puttachary S, Sharma S, Stark S and Thippeswamy T (2015) Seizure-induced oxidative stress in temporal lobe epilepsy. *Biomed Res Int* **2015**: 745613.
- Qi G, Mi Y, Shi X, Gu H, Brinton RD and Yin F (2021) ApoE4 Impairs Neuron-Astrocyte Coupling of Fatty Acid Metabolism. *Cell Rep* **34**(1): 108572.
- Racine RJ (1972) Modification of seizure activity by electrical stimulation. II. Motor seizure. *Electroencephalogr Clin Neurophysiol* **32**(3): 281-294.
- Radi R, Cassina A, Hodara R, Quijano C and Castro L (2002) Peroxynitrite reactions and formation in mitochondria. *Free Radic Biol Med* **33**(11): 1451-1464.
- Raimondo JV, Heinemann U, de Curtis M, Goodkin HP, Dulla CG, Janigro D, Ikeda A, Lin CK, Jiruska P, Galanopoulou AS and Bernard C (2017) Methodological standards for in vitro models of epilepsy and epileptic seizures. A TASK1-WG4 report of the AES/ILAE Translational Task Force of the ILAE. *Epilepsia* **58 Suppl 4**(Suppl 4): 40-52.
- Reimand J, Isserlin R, Voisin V, Kucera M, Tannus-Lopes C, Rostamianfar A, Wadi L, Meyer M, Wong J, Xu C, Merico D and Bader GD (2019) Pathway enrichment analysis and visualization of omics data using g:Profiler, GSEA, Cytoscape and EnrichmentMap. *Nat Protoc* **14**(2): 482-517.
- Rhone AE, Kovach CK, Harmata GI, Sullivan AW, Tranel D, Ciliberto MA, Howard MA, Richerson GB, Steinschneider M, Wemmie JA and Dlouhy BJ (2020) A human amygdala site that inhibits respiration and elicits apnea in pediatric epilepsy. *JCI Insight* **5**(6).
- Rizzuto R, De Stefani D, Raffaello A and Mammucari C (2012) Mitochondria as sensors and regulators of calcium signalling. *Nat Rev Mol Cell Biol* **13**(9): 566-578.
- Rojas A, Chen D, Ganesh T, Varvel NH and Dingledine R (2019) The COX-2/prostanoid signaling cascades in seizure disorders. *Expert Opin Ther Targets* **23**(1): 1-13.
- Rojas A and Dingledine R (2013) Ionotropic glutamate receptors: regulation by G-protein-coupled receptors. *Mol Pharmacol* **83**(4): 746-752.
- Rojas A, Gueorguieva P, Lelutiu N, Quan Y, Shaw R and Dingledine R (2014) The prostaglandin EP1 receptor potentiates kainate receptor activation via a protein kinase C pathway and exacerbates status epilepticus. *Neurobiol Dis* **70**: 74-89.
- Rusina E, Bernard C and Williamson A (2021) The Kainic Acid Models of Temporal Lobe Epilepsy. *eNeuro* **8**(2).

- Samadi M, Hales CA, Lustberg DJ, Farris S, Ross MR, Zhao M, Hepler JR, Harbin NH, Robinson ESJ, Banks PJ, Bashir ZI and Dudek SM (2023) Mechanisms of mGluR-dependent plasticity in hippocampal area CA2. *Hippocampus*.
- Sano F, Shigetomi E, Shinozaki Y, Tsuzukiya H, Saito K, Mikoshiba K, Horiuchi H, Cheung DL, Nabekura J, Sugita K, Aihara M and Koizumi S (2021) Reactive astrocyte-driven epileptogenesis is induced by microglia initially activated following status epilepticus. *JCI Insight* **6**(9).
- Saugstad JA, Marino MJ, Folk JA, Hepler JR and Conn PJ (1998) RGS4 inhibits signaling by group I metabotropic glutamate receptors. *J Neurosci* **18**(3): 905-913.
- Schinkel AH (1999) P-Glycoprotein, a gatekeeper in the blood-brain barrier. *Adv Drug Deliv Rev* **36**(2-3): 179-194.
- Schmidt O, Pfanner N and Meisinger C (2010) Mitochondrial protein import: from proteomics to functional mechanisms. *Nat Rev Mol Cell Biol* **11**(9): 655-667.
- Schmued LC, Albertson C and Slikker W, Jr. (1997) Fluoro-Jade: a novel fluorochrome for the sensitive and reliable histochemical localization of neuronal degeneration. *Brain Res* **751**(1): 37-46.
- Schonfeld P and Reiser G (2013) Why does brain metabolism not favor burning of fatty acids to provide energy? Reflections on disadvantages of the use of free fatty acids as fuel for brain. *J Cereb Blood Flow Metab* **33**(10): 1493-1499.
- Sethakorn N, Yau DM and Dulin NO (2010) Non-canonical functions of RGS proteins. *Cell Signal* **22**(9): 1274-1281.
- Seyfried NT, Dammer EB, Swarup V, Nandakumar D, Duong DM, Yin L, Deng Q, Nguyen T, Hales CM, Wingo T, Glass J, Gearing M, Thambisetty M, Troncoso JC, Geschwind DH, Lah JJ and Levey AI (2017) A Multi-network Approach Identifies Protein-Specific Co-expression in Asymptomatic and Symptomatic Alzheimer's Disease. *Cell Syst* **4**(1): 60-72 e64.
- Sharma K, Schmitt S, Bergner CG, Tyanova S, Kannaiyan N, Manrique-Hoyos N, Kongi K, Cantuti L, Hanisch UK, Philips MA, Rossner MJ, Mann M and Simons M (2015) Cell type- and brain region-resolved mouse brain proteome. *Nat Neurosci* **18**(12): 1819-1831.
- Shetty PK, Galeffi F and Turner DA (2012) Cellular Links between Neuronal Activity and Energy Homeostasis. *Front Pharmacol* **3**: 43.
- Shin EJ, Jeong JH, Chung YH, Kim WK, Ko KH, Bach JH, Hong JS, Yoneda Y and Kim HC (2011) Role of oxidative stress in epileptic seizures. *Neurochem Int* **59**(2): 122-137.
- Shinde AB, Song A and Wang QA (2021) Brown Adipose Tissue Heterogeneity, Energy Metabolism, and Beyond. *Front Endocrinol (Lausanne)* **12**: 651763.
- Shu FJ, Ramineni S, Amyot W and Hepler JR (2007) Selective interactions between Gi alpha1 and Gi alpha3 and the GoLoco/GPR domain of RGS14 influence its dynamic subcellular localization. *Cell Signal* **19**(1): 163-176.
- Shu FJ, Ramineni S and Hepler JR (2010) RGS14 is a multifunctional scaffold that integrates G protein and Ras/Raf MAPkinase signalling pathways. *Cell Signal* **22**(3): 366-376.
- Sigel E and Steinmann ME (2012) Structure, function, and modulation of GABA(A) receptors. *J Biol Chem* **287**(48): 40224-40231.
- Simons SB, Escobedo Y, Yasuda R and Dudek SM (2009) Regional differences in hippocampal calcium handling provide a cellular mechanism for limiting plasticity. *Proc Natl Acad Sci U S A* **106**(33): 14080-14084.
- Skrzypczak-Wiercioch A and Salat K (2022) Lipopolysaccharide-Induced Model of Neuroinflammation: Mechanisms of Action, Research Application and Future Directions for Its Use. *Molecules* **27**(17).
- Sofroniew MV (2014) Astrogliosis. *Cold Spring Harb Perspect Biol* **7**(2): a020420.
- Sofroniew MV (2020) Astrocyte Reactivity: Subtypes, States, and Functions in CNS Innate Immunity. *Trends Immunol* **41**(9): 758-770.

- Sofroniew MV and Vinters HV (2010) Astrocytes: biology and pathology. *Acta Neuropathol* **119**(1): 7-35.
- Spanoghe J, Larsen LE, Craey E, Manzella S, Van Dycke A, Boon P and Raedt R (2020) The Signaling Pathways Involved in the Anticonvulsive Effects of the Adenosine A(1) Receptor. *Int J Mol Sci* **22**(1).
- Spiers JG and Steinert JR (2021) Nitroergic modulation of ion channel function in regulating neuronal excitability. *Channels (Austin)* **15**(1): 666-679.
- Squires KE, Gerber KJ, Pare JF, Branch MR, Smith Y and Hepler JR (2018a) Regulator of G protein signaling 14 (RGS14) is expressed pre- and postsynaptically in neurons of hippocampus, basal ganglia, and amygdala of monkey and human brain. *Brain Struct Funct* **223**(1): 233-253.
- Squires KE, Gerber KJ, Tillman MC, Lustberg DJ, Montanez-Miranda C, Zhao M, Ramineni S, Scharer CD, Saha RN, Shu FJ, Schroeder JP, Ortlund EA, Weinschenker D, Dudek SM and Hepler JR (2021) Human genetic variants disrupt RGS14 nuclear shuttling and regulation of LTP in hippocampal neurons. *J Biol Chem* **296**: 100024.
- Squires KE, Montanez-Miranda C, Pandya RR, Torres MP and Hepler JR (2018b) Genetic Analysis of Rare Human Variants of Regulators of G Protein Signaling Proteins and Their Role in Human Physiology and Disease. *Pharmacol Rev* **70**(3): 446-474.
- Steve TA, Jirsch JD and Gross DW (2014) Quantification of subfield pathology in hippocampal sclerosis: a systematic review and meta-analysis. *Epilepsy Res* **108**(8): 1279-1285.
- Stewart A and Fisher RA (2015) Introduction: G Protein-coupled Receptors and RGS Proteins. *Prog Mol Biol Transl Sci* **133**: 1-11.
- Suzuki N, Hajicek N and Kozasa T (2009) Regulation and physiological functions of G12/13-mediated signaling pathways. *Neurosignals* **17**(1): 55-70.
- Tai TY, Warner LN, Jones TD, Jung S, Concepcion FA, Skyrud DW, Fender J, Liu Y, Williams AD, Neumaier JF, D'Ambrosio R and Poolos NP (2017) Antiepileptic action of c-Jun N-terminal kinase (JNK) inhibition in an animal model of temporal lobe epilepsy. *Neuroscience* **349**: 35-47.
- Tatum WO (2012) Mesial temporal lobe epilepsy. *J Clin Neurophysiol* **29**(5): 356-365.
- Tellez-Zenteno JF and Hernandez-Ronquillo L (2012) A review of the epidemiology of temporal lobe epilepsy. *Epilepsy Res Treat* **2012**: 630853.
- Tesmer JJ, Berman DM, Gilman AG and Sprang SR (1997) Structure of RGS4 bound to AIF4--activated G(i alpha1): stabilization of the transition state for GTP hydrolysis. *Cell* **89**(2): 251-261.
- Thom M (2014) Review: Hippocampal sclerosis in epilepsy: a neuropathology review. *Neuropathol Appl Neurobiol* **40**(5): 520-543.
- Tjalkens RB, Carbone DL and Wu G (2011) Detection of nitric oxide formation in primary neural cells and tissues. *Methods Mol Biol* **758**: 267-277.
- Traver S, Bidot C, Spassky N, Baltauss T, De Tand MF, Thomas JL, Zalc B, Janoueix-Lerosey I and Gunzburg JD (2000) RGS14 is a novel Rap effector that preferentially regulates the GTPase activity of galphao. *Biochem J* **350 Pt 1**(Pt 1): 19-29.
- Traver S, Spingard A, Gaudriault G and De Gunzburg J (2004) The RGS (regulator of G-protein signalling) and GoLoco domains of RGS14 co-operate to regulate Gi-mediated signalling. *Biochem J* **379**(Pt 3): 627-632.
- Traynelis SF, Wollmuth LP, McBain CJ, Menniti FS, Vance KM, Ogden KK, Hansen KB, Yuan H, Myers SJ and Dingledine R (2010) Glutamate receptor ion channels: structure, regulation, and function. *Pharmacol Rev* **62**(3): 405-496.
- Tse K, Puttachary S, Beamer E, Sills GJ and Thippeswamy T (2014) Advantages of repeated low dose against single high dose of kainate in C57BL/6J mouse model of status epilepticus: behavioral and electroencephalographic studies. *PLoS One* **9**(5): e96622.

- Tulke S, Haas CA and Haussler U (2019) Expression of brain-derived neurotrophic factor and structural plasticity in the dentate gyrus and CA2 region correlate with epileptiform activity. *Epilepsia* **60**(6): 1234-1247.
- Turrens JF (2003) Mitochondrial formation of reactive oxygen species. *J Physiol* **552**(Pt 2): 335-344.
- Varemo L, Nielsen J and Nookaew I (2013) Enriching the gene set analysis of genome-wide data by incorporating directionality of gene expression and combining statistical hypotheses and methods. *Nucleic Acids Res* **41**(8): 4378-4391.
- Vatner DE, Oydanich M, Zhang J, Campbell SC and Vatner SF (2023) Exercise enhancement by RGS14 disruption is mediated by brown adipose tissue. *Aging Cell*: e13791.
- Vatner DE, Zhang J, Oydanich M, Guers J, Katsyuba E, Yan L, Sinclair D, Auwerx J and Vatner SF (2018) Enhanced longevity and metabolism by brown adipose tissue with disruption of the regulator of G protein signaling 14. *Aging Cell* **17**(4): e12751.
- Vellano CP, Brown NE, Blumer JB and Hepler JR (2013) Assembly and function of the regulator of G protein signaling 14 (RGS14).H-Ras signaling complex in live cells are regulated by Galphai1 and Galphai-linked G protein-coupled receptors. *J Biol Chem* **288**(5): 3620-3631.
- Vellano CP, Maher EM, Hepler JR and Blumer JB (2011) G protein-coupled receptors and resistance to inhibitors of cholinesterase-8A (Ric-8A) both regulate the regulator of g protein signaling 14 RGS14.Galphai1 complex in live cells. *J Biol Chem* **286**(44): 38659-38669.
- Vezzani A (2005) Inflammation and epilepsy. *Epilepsy Curr* **5**(1): 1-6.
- Vezzani A, French J, Bartfai T and Baram TZ (2011) The role of inflammation in epilepsy. *Nat Rev Neurol* **7**(1): 31-40.
- Virtuoso A, De Luca C, Korai SA, Papa M and Cirillo G (2023) Neuroinflammation and glial activation in the central nervous system: a metabolic perspective. *Neural Regen Res* **18**(5): 1025-1026.
- Vismer MS, Forcelli PA, Skopin MD, Gale K and Koubeissi MZ (2015) The piriform, perirhinal, and entorhinal cortex in seizure generation. *Front Neural Circuits* **9**: 27.
- Volterra A and Meldolesi J (2005) Astrocytes, from brain glue to communication elements: the revolution continues. *Nat Rev Neurosci* **6**(8): 626-640.
- Waldbaum S and Patel M (2010) Mitochondria, oxidative stress, and temporal lobe epilepsy. *Epilepsy Res* **88**(1): 23-45.
- Wang Q, Yu S, Simonyi A, Sun GY and Sun AY (2005) Kainic acid-mediated excitotoxicity as a model for neurodegeneration. *Mol Neurobiol* **31**(1-3): 3-16.
- Weltha L, Reemmer J and Boison D (2019) The role of adenosine in epilepsy. *Brain Res Bull* **151**: 46-54.
- Wen TH, Binder DK, Ethell IM and Razak KA (2018) The Perineuronal 'Safety' Net? Perineuronal Net Abnormalities in Neurological Disorders. *Front Mol Neurosci* **11**: 270.
- Whitebirch AC, LaFrancois JJ, Jain S, Leary P, Santoro B, Siegelbaum SA and Scharfman HE (2022) Enhanced excitability of the hippocampal CA2 region and its contribution to seizure activity in a mouse model of temporal lobe epilepsy. *Neuron* **110**(19): 3121-3138 e3128.
- Willard FS, Willard MD, Kimple AJ, Soundararajan M, Oestreich EA, Li X, Sowa NA, Kimple RJ, Doyle DA, Der CJ, Zylka MJ, Snider WD and Siderovski DP (2009) Regulator of G-protein signaling 14 (RGS14) is a selective H-Ras effector. *PLoS One* **4**(3): e4884.
- Wittner L, Huberfeld G, Clemenceau S, Eross L, Dezamis E, Entz L, Ulbert I, Baulac M, Freund TF, Magloczky Z and Miles R (2009) The epileptic human hippocampal cornu ammonis 2 region generates spontaneous interictal-like activity in vitro. *Brain* **132**(Pt 11): 3032-3046.
- Wu W, Li Y, Wei Y, Bosco DB, Xie M, Zhao MG, Richardson JR and Wu LJ (2020) Microglial depletion aggravates the severity of acute and chronic seizures in mice. *Brain Behav Immun* **89**: 245-255.

- Wu Y, Dissing-Olesen L, MacVicar BA and Stevens B (2015) Microglia: Dynamic Mediators of Synapse Development and Plasticity. *Trends Immunol* **36**(10): 605-613.
- Xia Z and Storm DR (2005) The role of calmodulin as a signal integrator for synaptic plasticity. *Nat Rev Neurosci* **6**(4): 267-276.
- Xing L, Yang T, Cui S and Chen G (2019) Connexin Hemichannels in Astrocytes: Role in CNS Disorders. *Front Mol Neurosci* **12**: 23.
- Yamakura F, Taka H, Fujimura T and Murayama K (1998) Inactivation of human manganese-superoxide dismutase by peroxynitrite is caused by exclusive nitration of tyrosine 34 to 3-nitrotyrosine. *J Biol Chem* **273**(23): 14085-14089.
- Yang H, Wu J, Guo R, Peng Y, Zheng W, Liu D and Song Z (2013) Glycolysis in energy metabolism during seizures. *Neural Regen Res* **8**(14): 1316-1326.
- Yap EL and Greenberg ME (2018) Activity-Regulated Transcription: Bridging the Gap between Neural Activity and Behavior. *Neuron* **100**(2): 330-348.
- Ye X and Carew TJ (2010) Small G protein signaling in neuronal plasticity and memory formation: the specific role of ras family proteins. *Neuron* **68**(3): 340-361.
- Yuan G, Yang S, Liu M and Yang S (2020) RGS12 is required for the maintenance of mitochondrial function during skeletal development. *Cell Discov* **6**: 59.
- Zamponi GW and Currie KP (2013) Regulation of Ca(V)₂ calcium channels by G protein coupled receptors. *Biochim Biophys Acta* **1828**(7): 1629-1643.
- Zeidan YH, Pettus BJ, Elojeimy S, Taha T, Obeid LM, Kawamori T, Norris JS and Hannun YA (2006) Acid ceramidase but not acid sphingomyelinase is required for tumor necrosis factor- α -induced PGE₂ production. *J Biol Chem* **281**(34): 24695-24703.
- Zemla R and Basu J (2017) Hippocampal function in rodents. *Curr Opin Neurobiol* **43**: 187-197.
- Zhang J, Nuebel E, Wisidagama DR, Setoguchi K, Hong JS, Van Horn CM, Imam SS, Vergnes L, Malone CS, Koehler CM and Teitell MA (2012) Measuring energy metabolism in cultured cells, including human pluripotent stem cells and differentiated cells. *Nat Protoc* **7**(6): 1068-1085.
- Zhang JK, Ding MJ, Liu H, Shi JH, Wang ZH, Wen PH, Zhang Y, Yan B, Guo DF, Zhang XD, Tao RL, Yan ZP, Zhang Y, Liu Z, Guo WZ and Zhang SJ (2022) Regulator of G-protein signaling 14 protects the liver from ischemia-reperfusion injury by suppressing TGF- β -activated kinase 1 activation. *Hepatology* **75**(2): 338-352.
- Zhang Y, Chen K, Sloan SA, Bennett ML, Scholze AR, O'Keefe S, Phatnani HP, Guarnieri P, Caneda C, Ruderisch N, Deng S, Liddelow SA, Zhang C, Daneman R, Maniatis T, Barres BA and Wu JQ (2014) An RNA-sequencing transcriptome and splicing database of glia, neurons, and vascular cells of the cerebral cortex. *J Neurosci* **34**(36): 11929-11947.
- Zhao M, Choi YS, Obrietan K and Dudek SM (2007) Synaptic plasticity (and the lack thereof) in hippocampal CA2 neurons. *J Neurosci* **27**(44): 12025-12032.
- Zhao P, Nunn C, Ramineni S, Hepler JR and Chidiac P (2013) The Ras-binding domain region of RGS14 regulates its functional interactions with heterotrimeric G proteins. *J Cell Biochem* **114**(6): 1414-1423.